

Acceleratori per neutroni

A. Pisent

INFN-Laboratori Nazionali di Legnaro

The lecturer

- Liceo classico 1981 (60/60)
- Degree in Physics at Padova University in 1986 with thesis in theoretical Accelerator Physics (110/110 cum laude)
- Post doc at Karlsruhe University and as Los Alamos (University of California); CERN fellow.
- Since 1990 at INFN Legnaro National Laboratory
- Responsible for
 - beam dynamics of Linac3 low energy part (built by LNL)
 - Beam dynamics of PIAVE superconducting RFQ
 - Construction of TRASCO RFQ (high intensity proton) and MUNES neutron source.
 - Design and construction of ESS drift tube linac
 - Design and construction of IFMIF EVEDA RFQ (high intensity deuterons)
- Professore a contratto of Accelerator Physics at Padova University (undergraduate and PHD) for many years.

General plan

- Seminar 1: neutron sources, general principles, reactors vs accelerators, different kind of accelerators, n-flux time structure
- Seminar 2 specific issues for the high intensity linac of an intense neutron source. Beam dynamics, RF optimization, superconducting vs normalconducting. Example: the European Spallation Source (ESS)
- Seminar 3: High intensity injectors: the preparation of a high quality beam, the RFQ. Example: IFMIF (International Fusion Material Irradiation Facility)

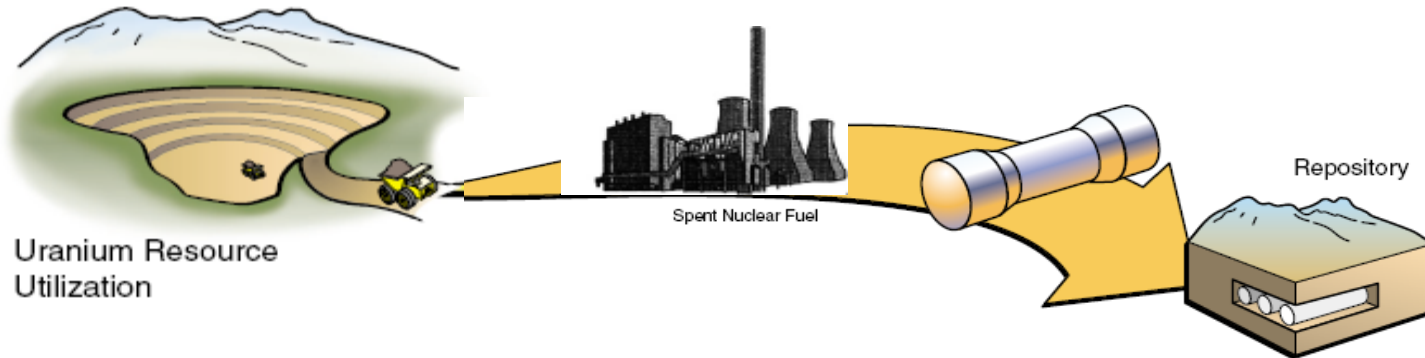
Neutrons and Neutron Sources

- The neutron was discovered in 1932 by Chadwick
- Coherent neutron diffraction (Bragg scattering by crystal lattice planes) was first demonstrated in 1936 by Mitchel & Powers and Halban & Preiswerk as an exercise in wave mechanics
- The possibility of using the scattering of neutrons as a probe of materials developed with the availability of copious quantities of slow neutrons from reactors after 1945. Fermi's group used Bragg scattering to measure nuclear cross-sections
- Many applications using neutrons as probe of matter (next lecture)
- In my third lesson two particular applications using continuous high intensity n fluxes:
 - test of material for next fusion reactors (IFMIF)
 - Neutrons for BNCT (Boron Neutron Capture Therapy)

Nuclear Wastes Transmutation

The current nuclear reactors

Current nuclear systems are “once through”



Problems of current reactors :

- Low **burn-up efficiency** (inefficient use of U resources)
- production of large volumes of **radioactive nuclear waste** with long life-time
- Need of large **investments** and long construction **times**
- **Proliferation issues** (use of fissile material for military or terroristic purposes)

In the short term: **problem of nuclear waste disposal**

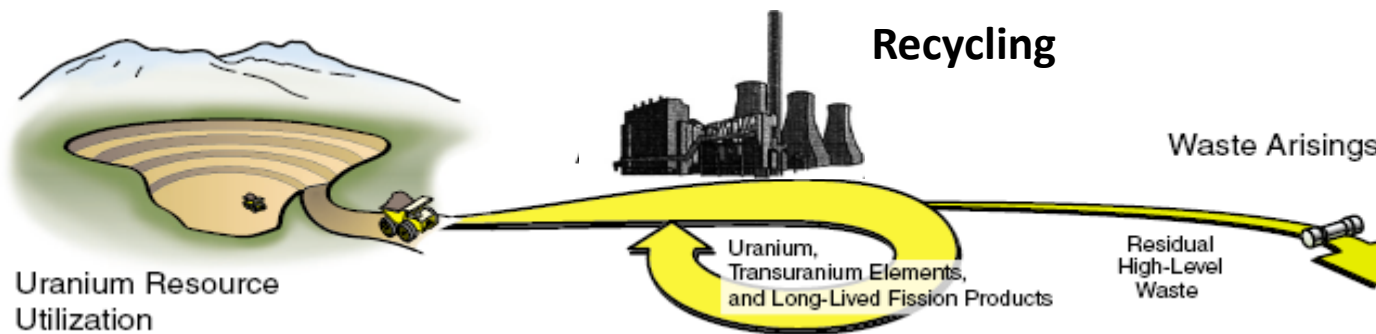
In the long period (> 50 years): **availability** of Uranium

courtesy N. Colonna – INFN Bari

New generation reactors

New generation reactors should address the main issues of current nuclear reactors (production of high-level nuclear waste, inefficient use of Uranium resources, proliferation, etc...).

The main principle of new generation reactors is the **recycling** of the spent fuel, so to fulfill a **closed fuel cycle**.



Advanced nuclear systems currently being studied:

- **Generation IV** (critical), for energy and hydrogen production;
- **Accelerator Driven Systems** (subcritical), mostly aimed at nuclear waste transmutation (LLFF e MA).

courtesy N. Colonna – INFN Bari

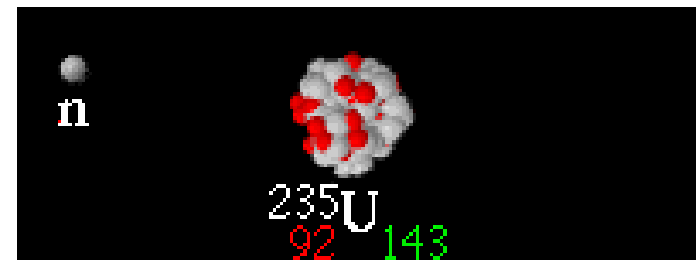
Neutrons: nuclear fission

- Fission:

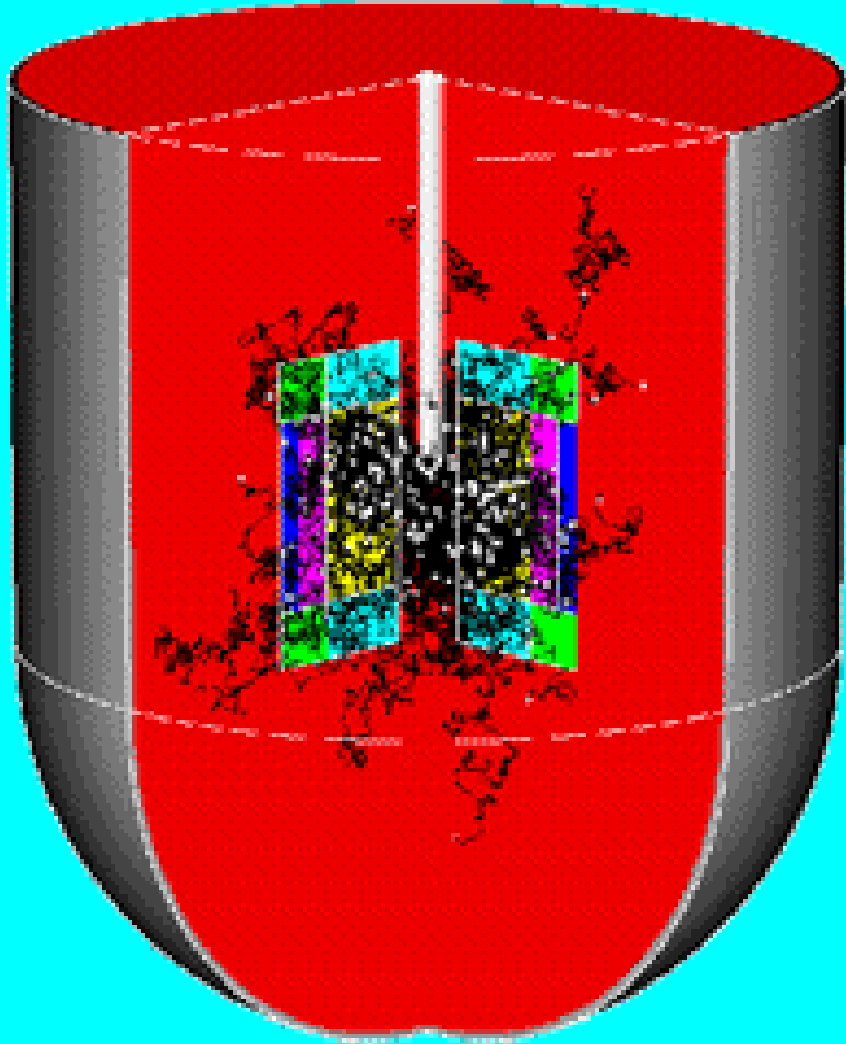


moderated by

200 MeV/n
D₂O (H₂O) to thermal or lost

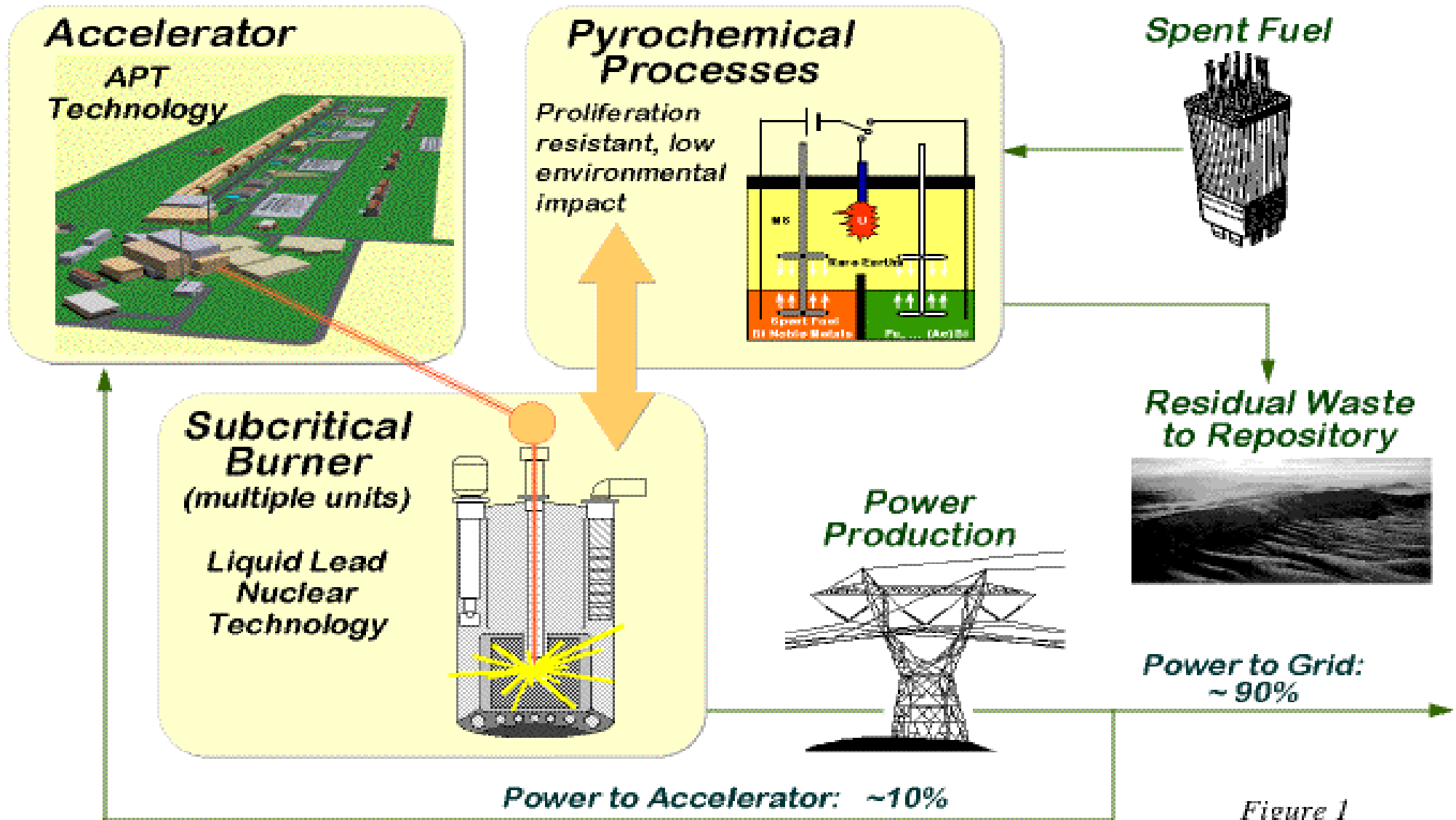


$$k = \frac{\text{n. neutrons available for new fissions}}{\text{n. absorbed + lost neutrons}}$$



- $k < 1$ subcritical reactor (intrinsically safe)
- The reaction is fed by the neutrons produced by the accelerator/converter
- The feed back for reactor dynamics stability is not based on delayed neutrons
- In this way it is possible to process with fast neutrons the spent fuel

ATW Consists of Three Major Functional Blocks



Nuclear waste transmutation

Transmutation (or nuclear incineration) of radioactive waste



Neutron induced reactions that transform **long-lived** radioactive isotopes into **stable** or **short-lived** isotopes.

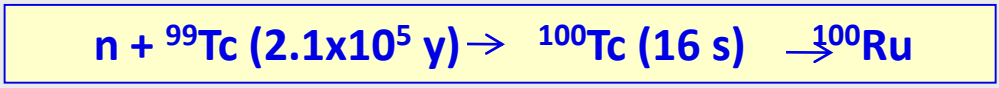
Transmutation reactions

Fission Fragments (LLFF)

^{151}Sm , ^{99}Tc , ^{121}I , ^{79}Se ...



neutron capture (n, γ)



From ETWG Report, 2001

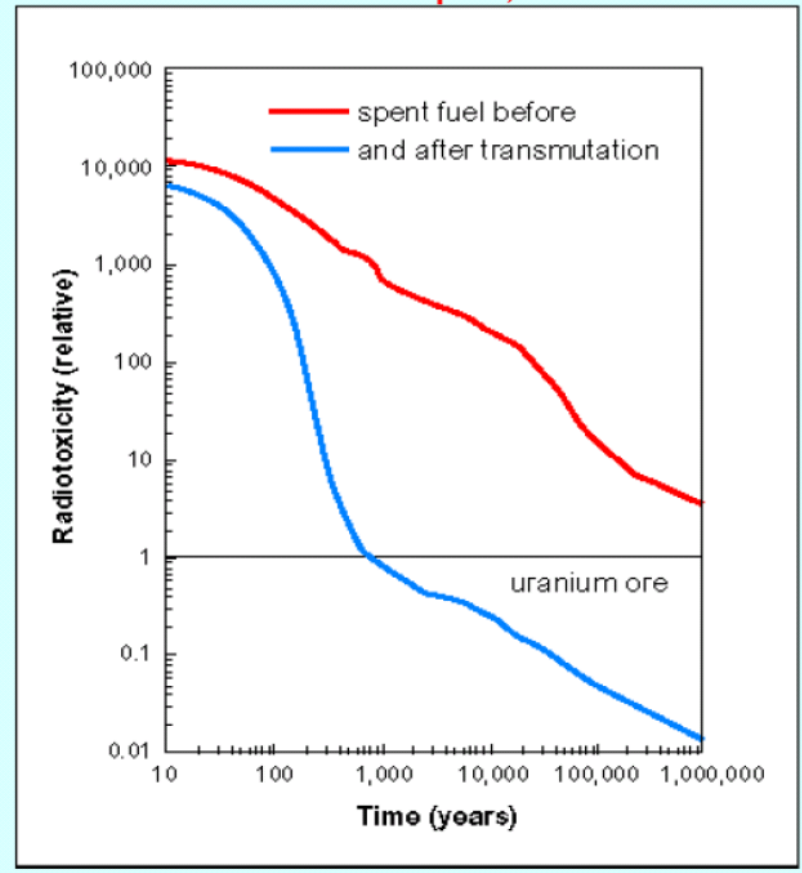
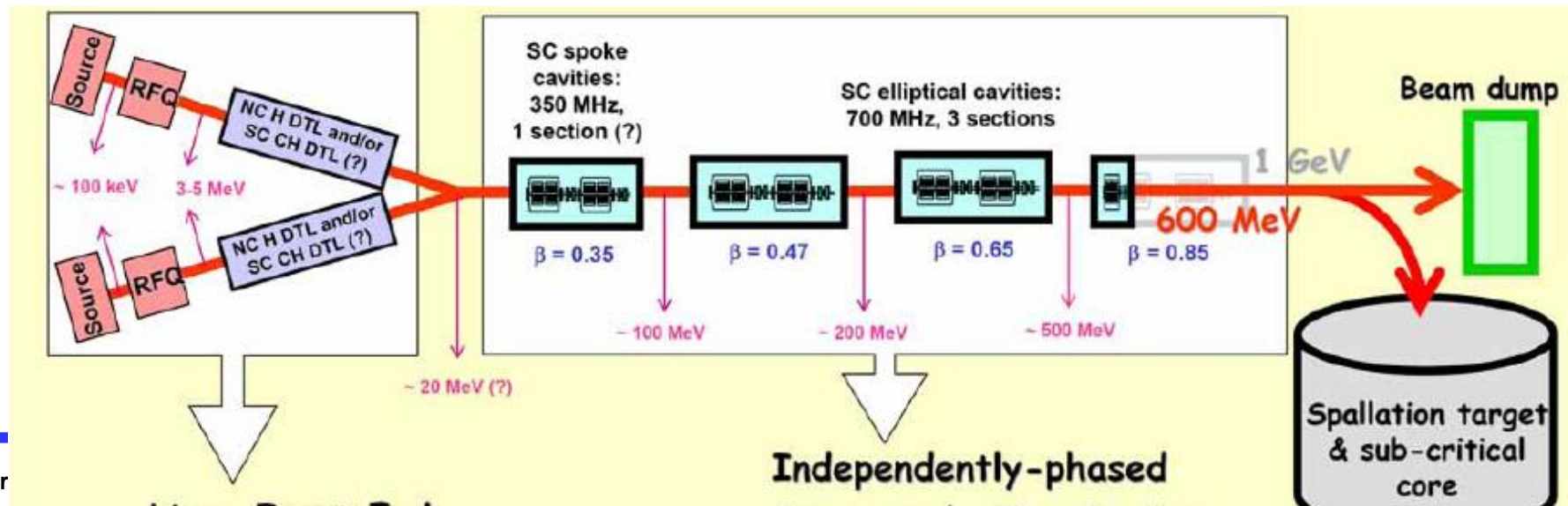


Fig. 1 – Ingestion radio-toxicity of 1 ton of spent nuclear fuel. With a separation efficiency of 99.9% of the long-lived by-products from the waste, followed by transmutation, reference radio-toxicity levels can be reached within 700 years

High intensity linac: specific requirements

- Reliable and economic operation
- Low power consumption
- Low beam losses
 - Hands on maintenance of the accelerator
 - Large beam bore
 - Good quality beam prepared from the low energy accelerators
- Superconducting accelerating structures
- High transmission RFQs
- For fission reactor applications few interruptions longer > 1 s per year.



Accelerator efficiency η for EA application

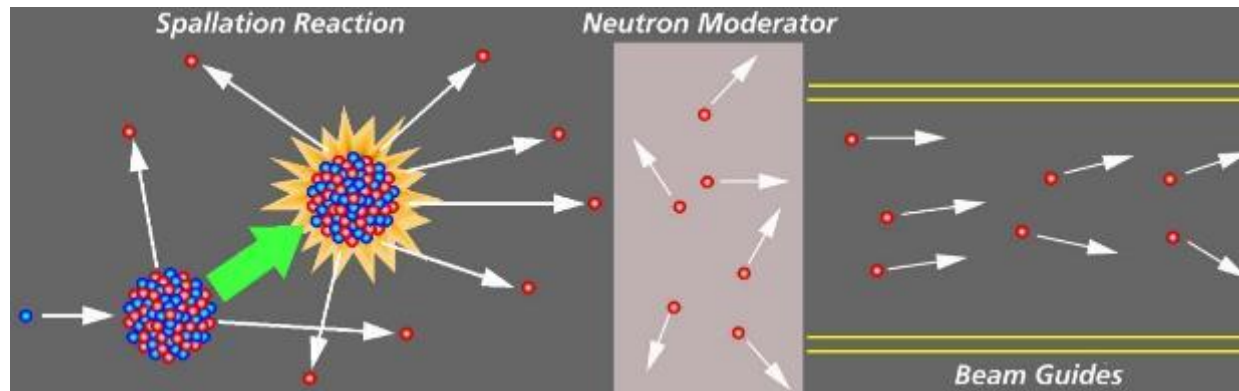
$$P_{produced} = \left[\eta \eta_{conversion} \frac{G_0}{1-k} - 1 \right] P_{accelerator}$$

with

- $P_{produced}$ power delivered to the electrical network
- $\eta = P_{beam} / P_{accelerator}$
- $\eta_{conversion}$ heat-electricity conversion efficiency
- $G_0 = 2.5$ gain
- k neutron multiplication factor
- $P_{accelerator}$ power consumption of the accelerator

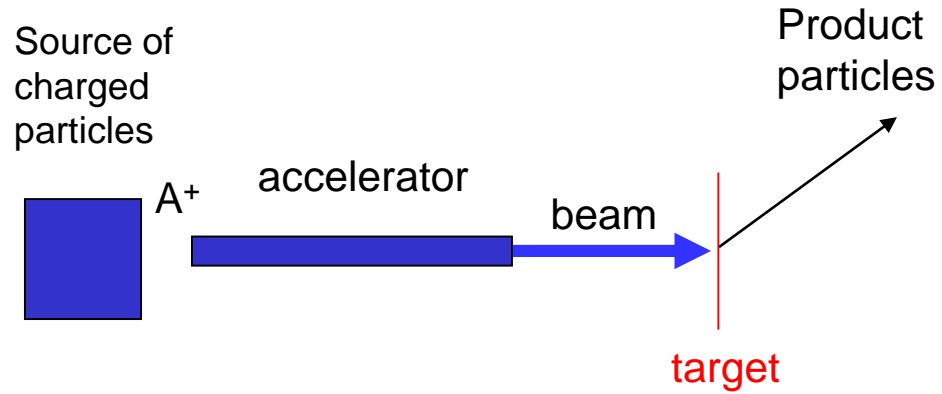
How Are Neutron Beams Produced?

- Neutrons are one of the fundamental building blocks of matter that can be released through:
 - The fission process by splitting atoms in a nuclear reactor
 - The spallation process by bombarding heavy metal atoms with energetic protons

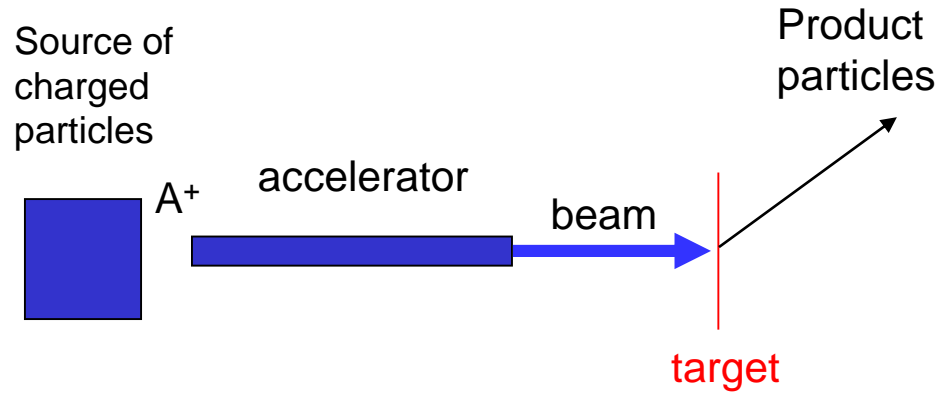


- Both kind of neutrons were present in the previous example
- The moderated neutrons, once released, can be transmitted through beam guides into the laboratory and used for a wide variety of research and development projects

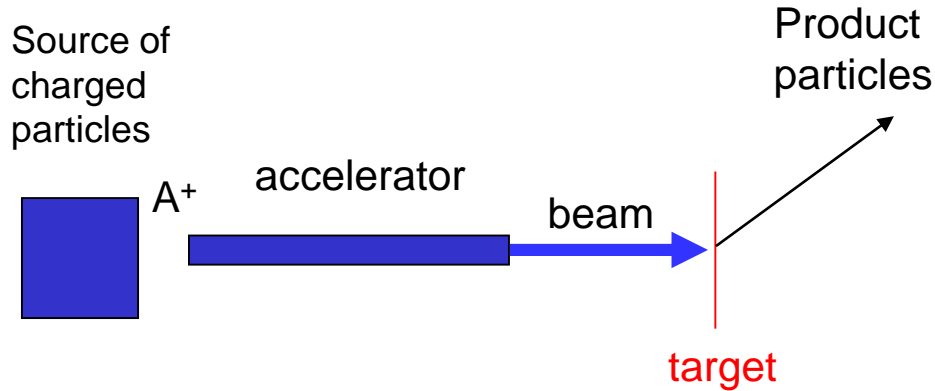
Scheme of experiment with accelerated particles



Scheme of experiment with accelerated particles



Scheme of experiment with accelerated particles



- If the target is thin (i.e. if multiple scattering has low probability) neutron production rate is

$$\frac{dN_e}{dt} = \sigma \left[\frac{N_d}{S} \frac{dN_i}{dt} \right]$$

Cross section

Beam current

Target thickness

$$\frac{N_d}{S} = \frac{N_{Avogadro}}{A} \text{density [g/cm}^2\text{]}$$

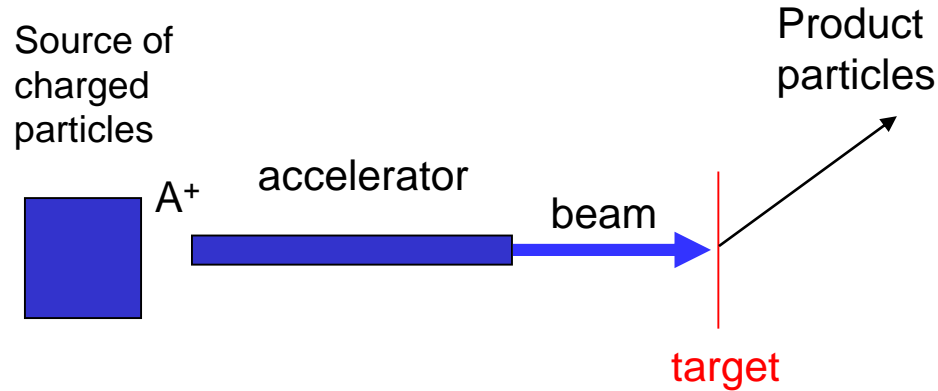
$$N_{Avogadro} = 6 \cdot 10^{23} [\text{g}^{-1}]$$

$$\frac{dN_i}{dt} = \frac{I_{beam}}{e}$$

$$e = 1.6 \cdot 10^{-19} \text{C}$$

Scheme of experiment with accelerated particles

Low intensity

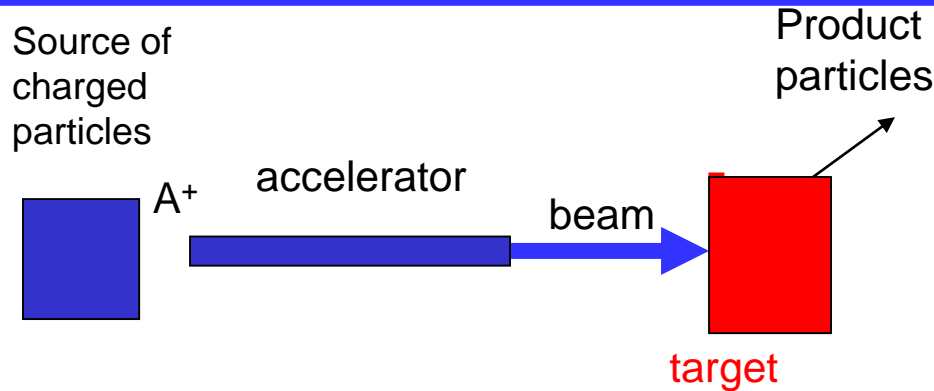


- If the target is thin (i.e. if multiple scattering has low probability) neutron production rate is

$$\frac{dN_e}{dt} = \sigma \left[\frac{N_d}{S} \frac{dN_i}{dt} \right]$$



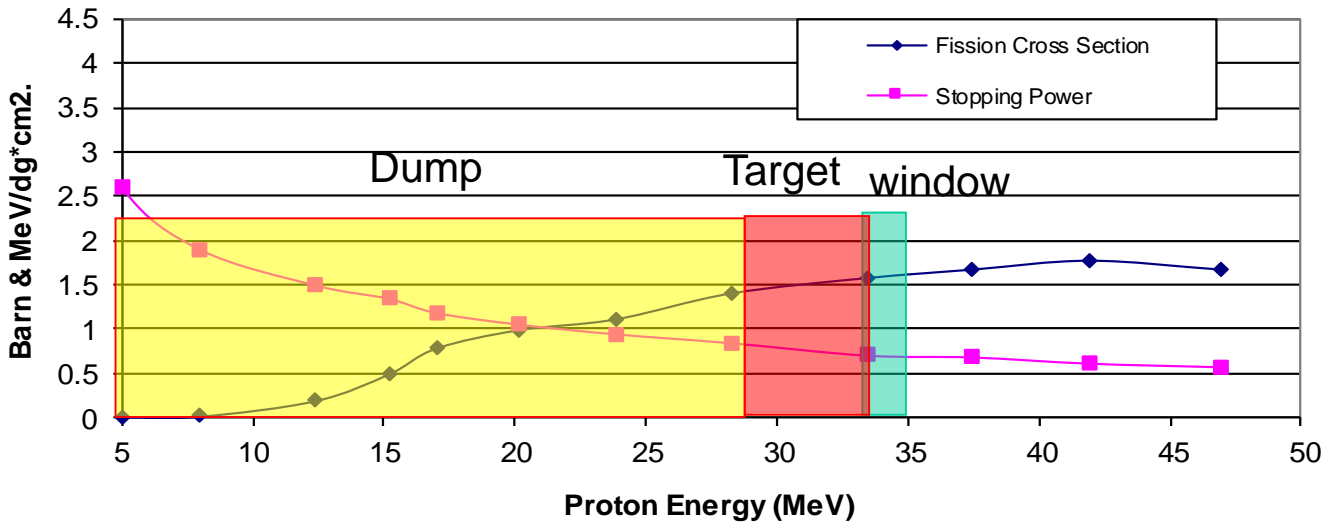
High intensity



- To increase the production of particles (for given conditions or fixed σ) one needs
 - **High power** beam
 - **Thick target.** The beam power is (almost) completely dissipated in the target mainly with electromagnetic scattering into the electrons in the material.

Scheme of experiment with accelerated particles

Stopping Power & Fission Cross Section for p-> UCx

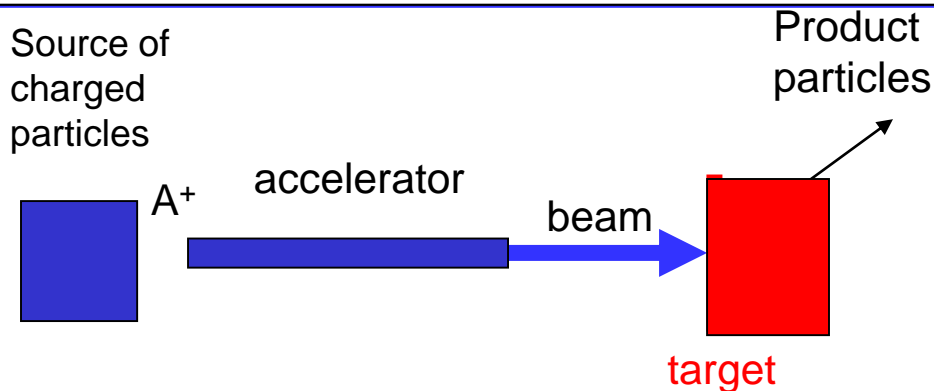


$$\frac{dN_e}{dt} \approx \left[\frac{1}{S} \int_{w_{in}}^{w_{out}} N_d \sigma(w) dw \right] \left[\frac{dN_i}{dt} \right]$$

Cross section

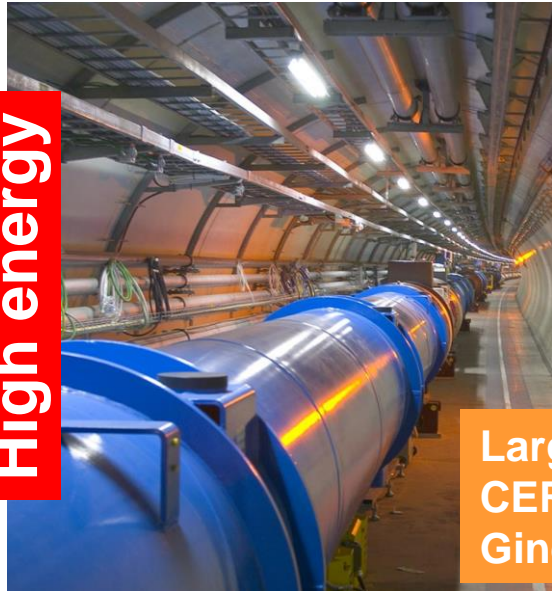
Beam current

High intensity



- To increase the production of particles (for given conditions or fixed σ) one needs
 - **High power** beam
 - **Thick target.** The beam power is (almost) completely dissipated in the target mainly with electromagnetic scattering into the electrons in the material.

High intensity particle accelerators

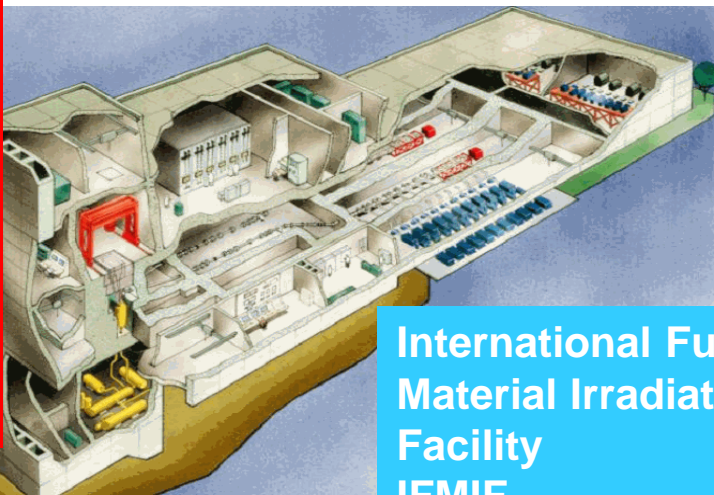


Large Hadron Collider
CERN
Ginevra

High energy

- Thin target **high energy**
 - High energy 7 000 000 MeV
 - Clean experimental conditions (thin target)
 - Event rate compatible with the acquisition system 10^9 s^{-1}
 - Moderate efficiency in power conversion to beam

High intensity



International Fusion
Material Irradiation
Facility
IFMIF

- Thick target **high intensity**
 - Moderate particle energy (40 MeV)
 - Large event rate 10^{15} s^{-1}
 - Perturbed experimental conditions (multiple events during particle deceleration in the target)
 - High efficiency in power conversion to beam

4B CAMPIONATO TEDESCO VETTURE DA TURISMO

Mercedes-Benz CLK
Pilota: Bernd Schneider

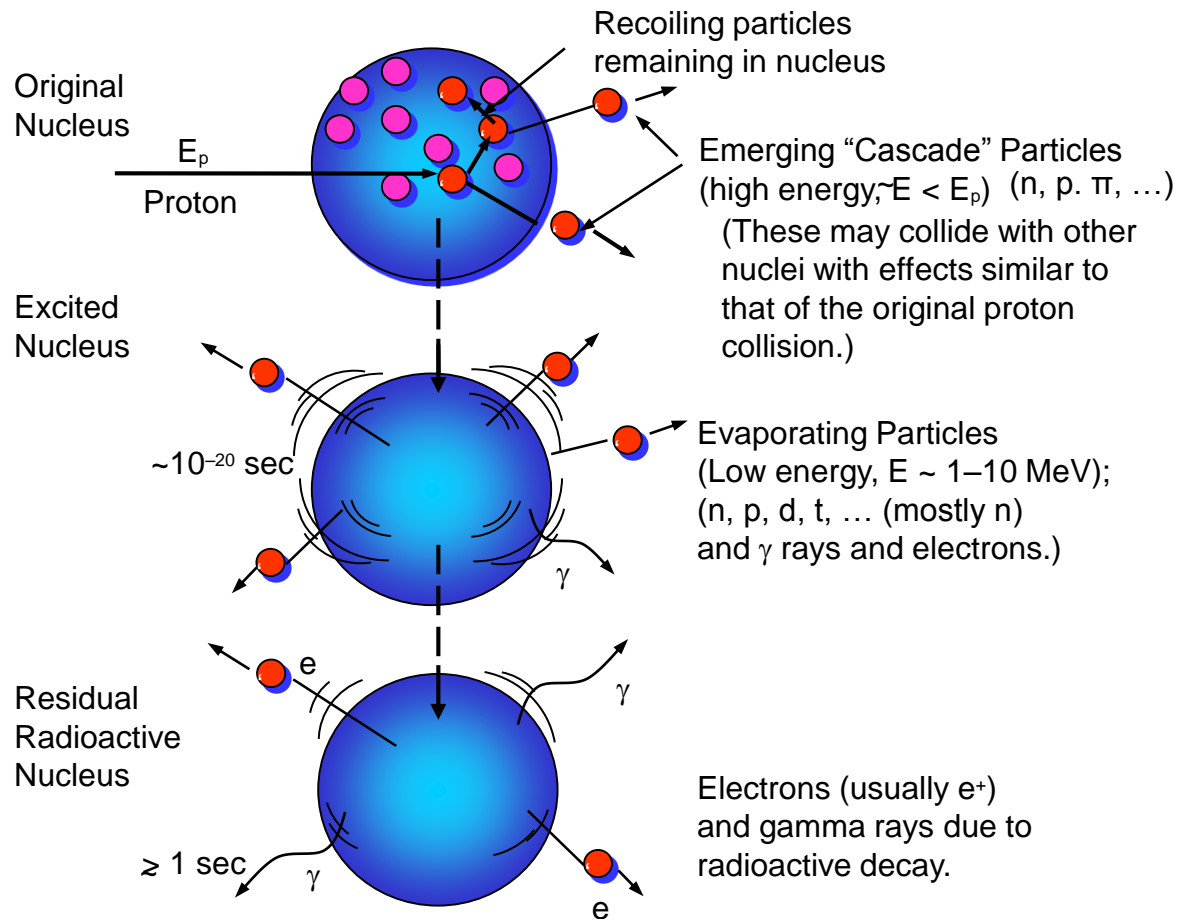
		Cilindrata:	3 999 cmc
		Potenza:	338 kW / 460 CV
		Cilindri:	8
<small>a) Opel c) Opel d) Abt-Audi</small>		Peso:	1 110 kg
		Velocità:	285 km/h

A1 Mercedes Actros BlueTec

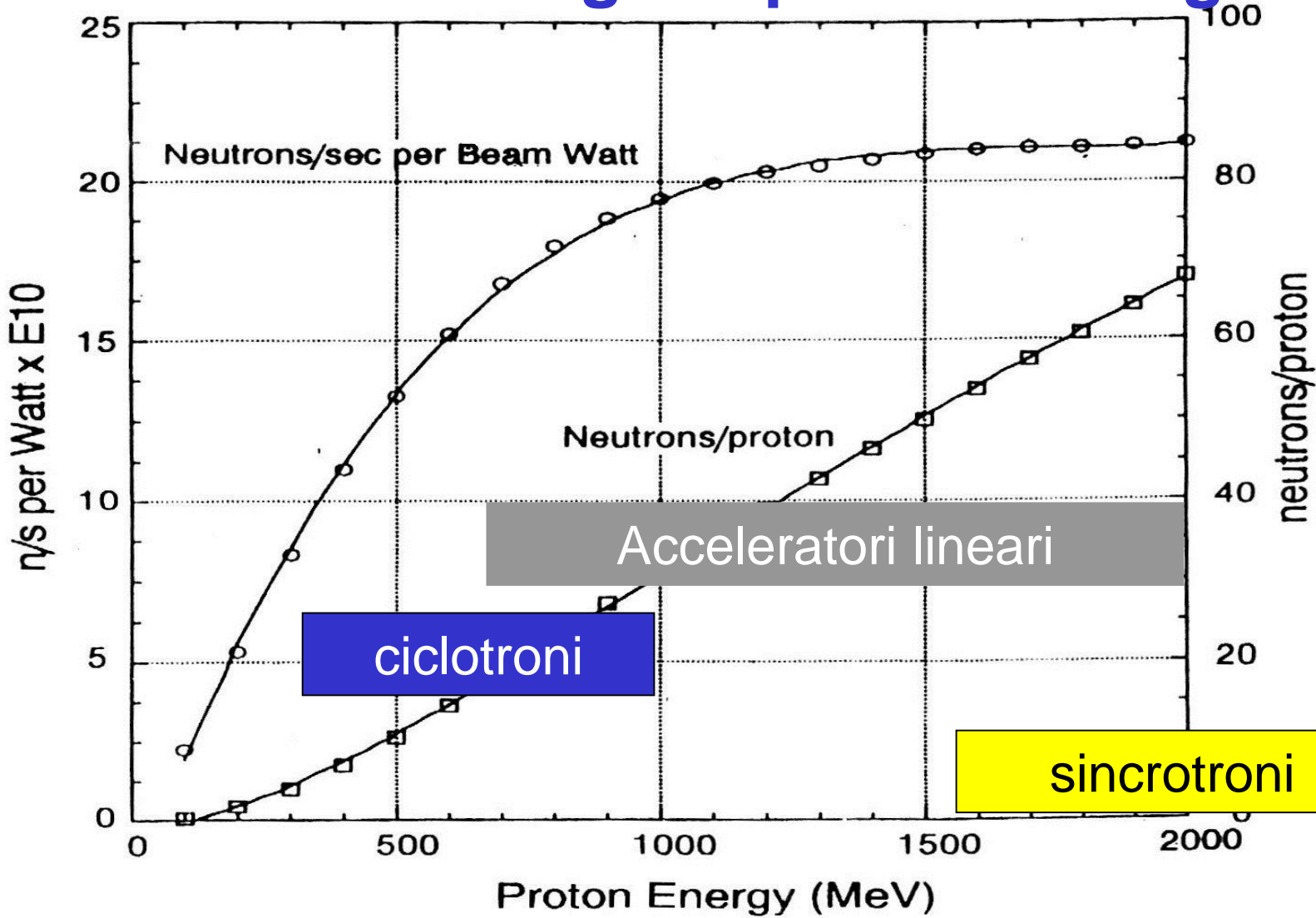
	max. km/h	130		cilindrata/cmc	15928
	peso/kg	26000		cilindri	8
	potenza/CV	598		giri/min.	1800

TOP QUARTETTO

Spallation-Evaporation Production of Neutrons



Produzione di neutroni per spallazione da un bersaglio spesso di tungsteno



Record attuali

LAMF 800 GeV 1 mA

PSI 2 mA 600 MeV

ISIS
RAL 3 GeV 0.1 mA

Types of Neutron Sources

- Pulsed spallation source e.g., ISIS, LANSCE
 - 200 μA , 0.8 GeV, 160 kW
 - 2×10^{13} n/cm²/s average flux
 - 8×10^{15} n/cm²/s peak flux

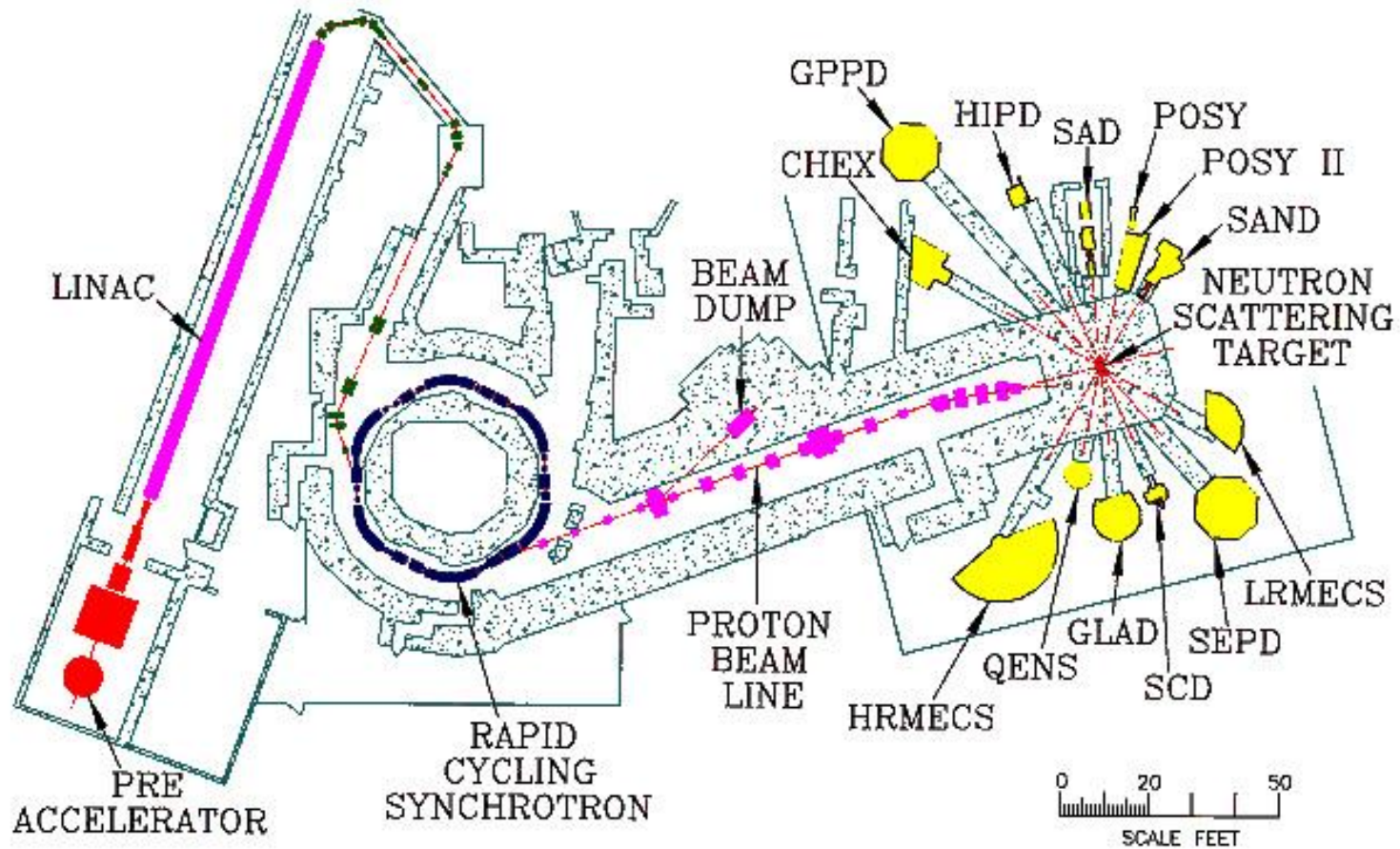
Advantages:

- high peak flux
- advantageous time structure for many applications
- accelerator based – politics simpler than reactors
- technology rapidly evolving

Disadvantages:

- low time averaged flux
- not all applications exploit time structure
- rapidly evolving technology

IPNS Facilities Map



2000-05272 uc/arb

Types of Neutron Sources

- CW spallation source e.g., PSI
0.85 mA, 590 MeV, 0.9 MW
 1×10^{14} n/cm²/s average flux

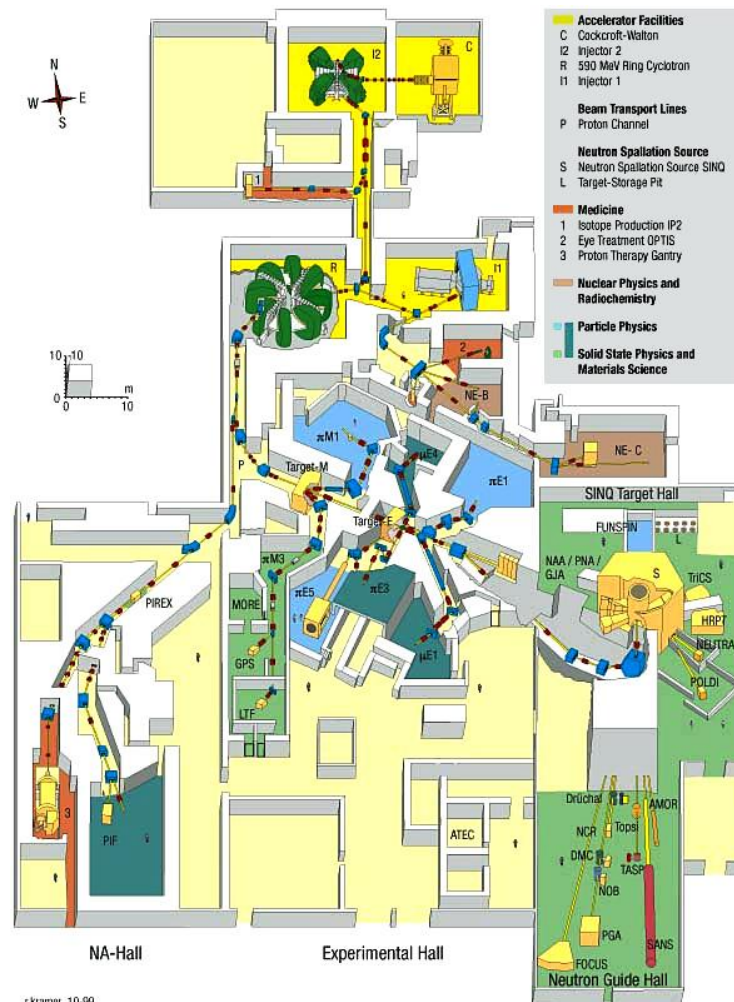
Advantages:

- high time averaged flux
- uses reactor type instrumentation (mature technology)

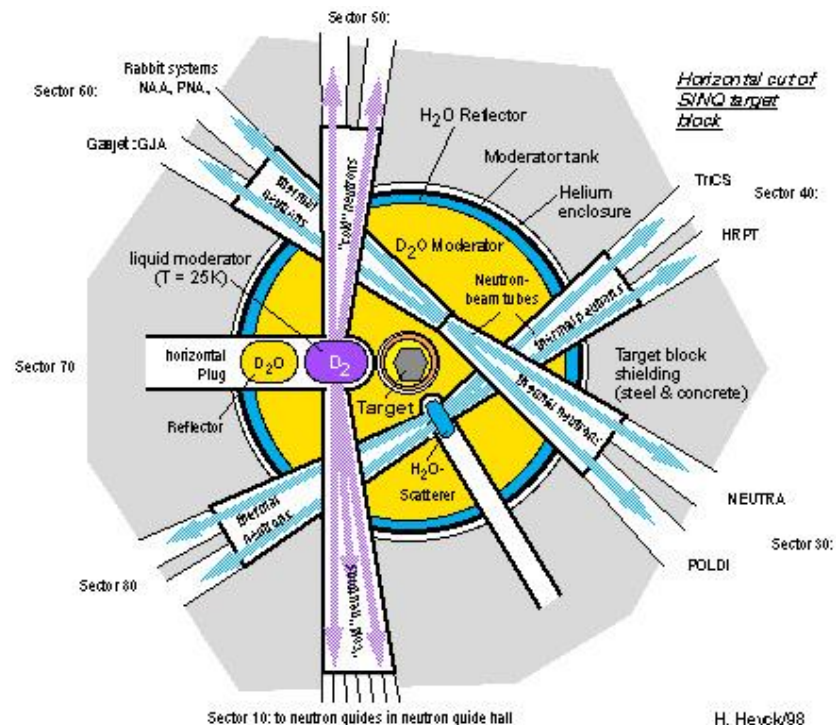
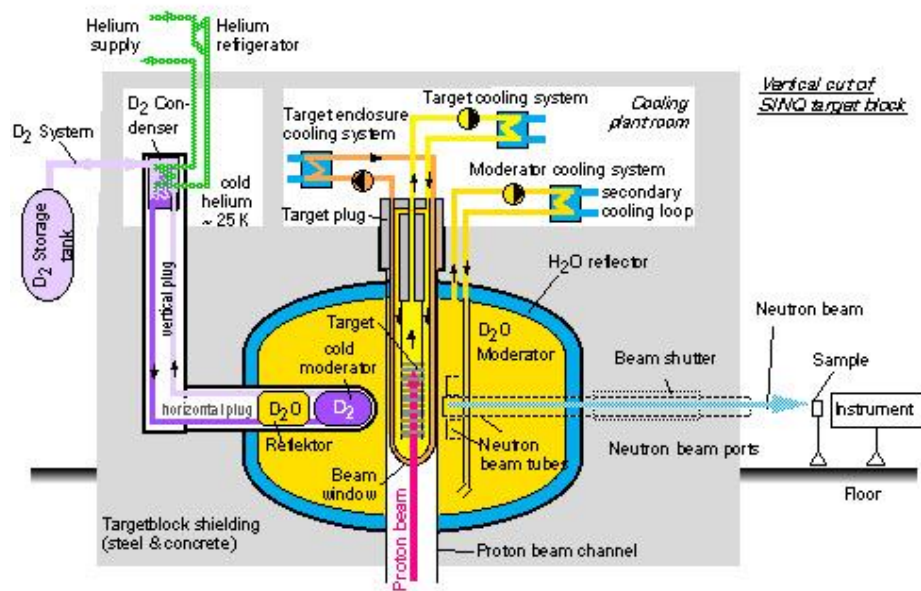
Disadvantages:

- no time structure
- high background

PSI Proton Accelerators and Experimental Facilities

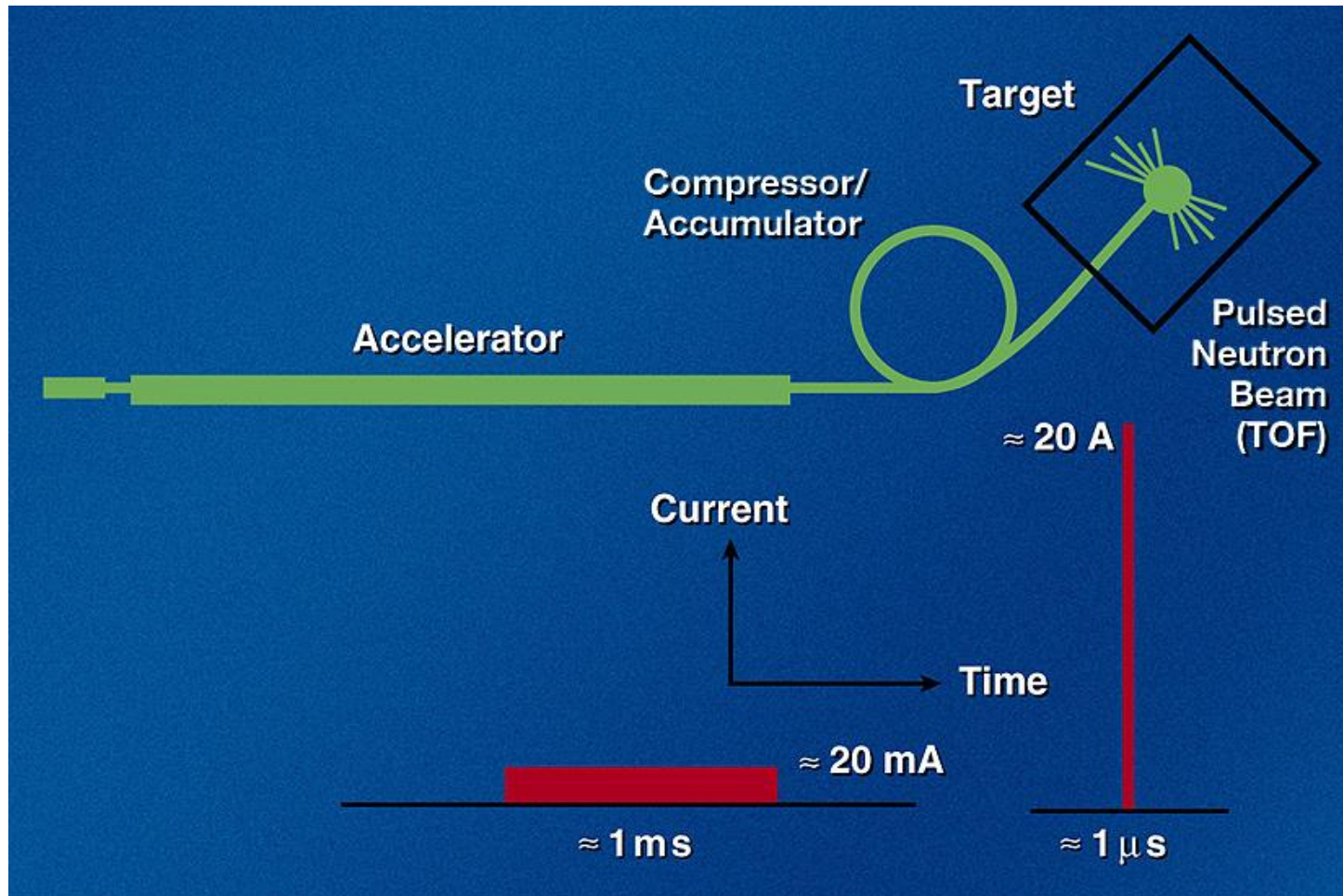


Principle of the Spallation Neutron Source SINQ

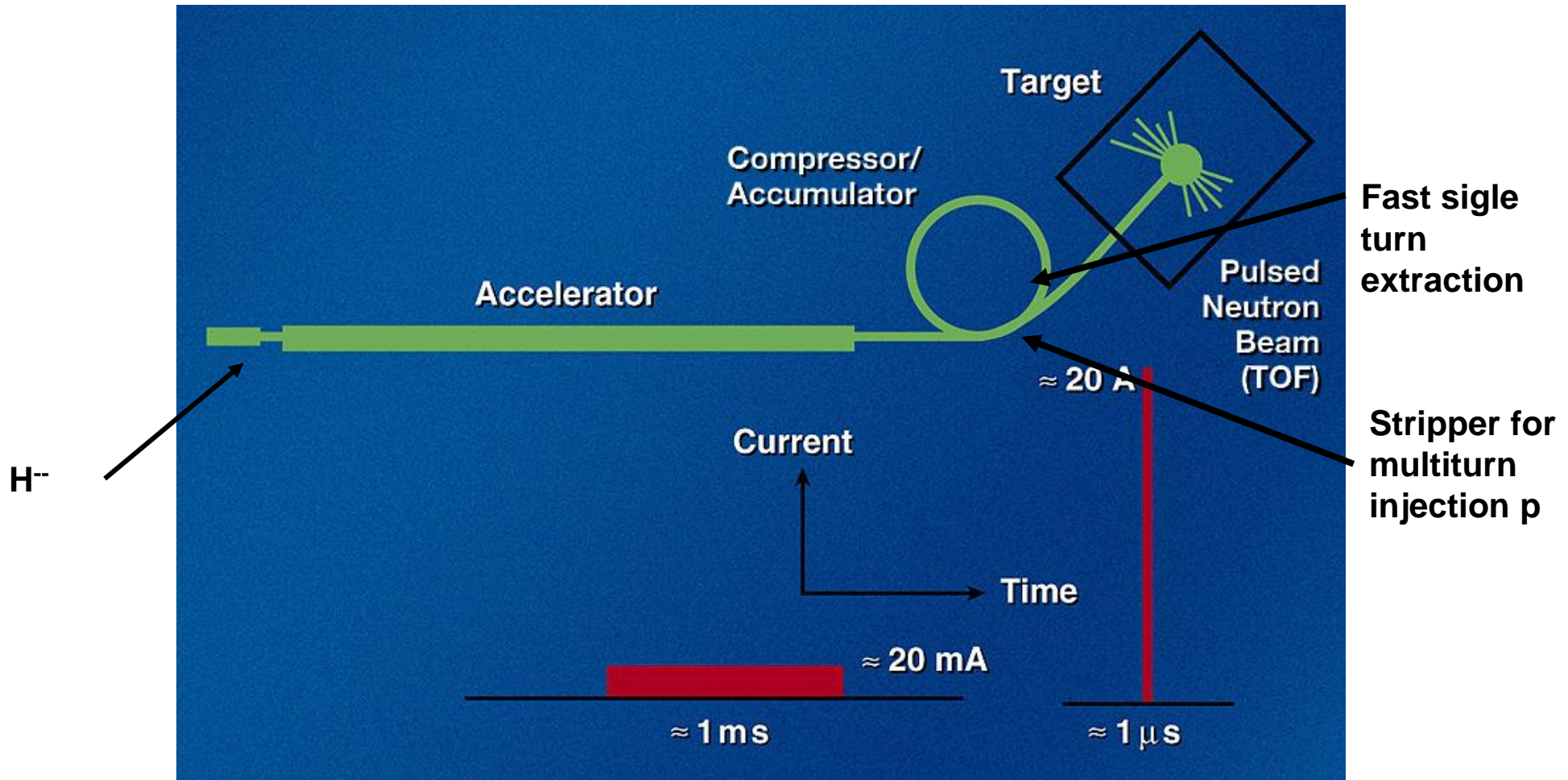


H. Heyck/98

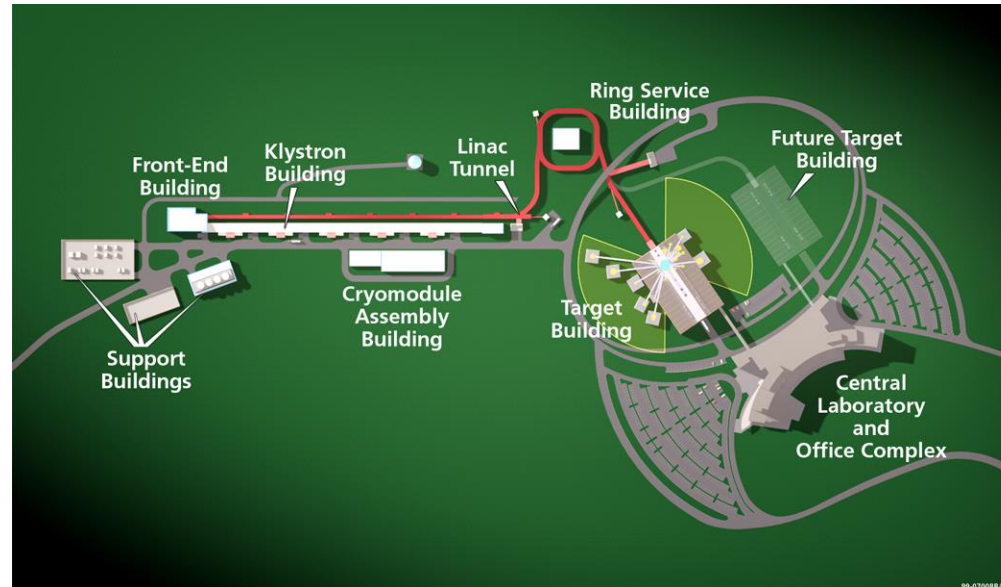
Anatomy of a Pulsed Spallation Source



Anatomy of a Pulsed Spallation Source



The Spallation Neutron Source



- At 2 MW it will be $\sim 12x$ ISIS with a time averaged flux \sim NIST
- The peak thermal neutron flux will be $\sim 125x$ NIST
- SNS is the world's leading facility for neutron scattering

Summary Parameters for the SNS

• Proton beam power on target	2.0 MW
• Average proton beam current on target	2.0 mA
• Pulse repetition rate	60 Hz
• Peak linac H- current	52 mA
• Chopper beam-on duty factor	68 %
• Linac length, with 5 empty cryomodule slots	331 m
• DTL output energy	87 MeV
• Number of DTL 402.5-MHz 2.5-MW klystrons	7
• CCL output energy	185 MeV
• Number of CCL 805-MHz 2.5-MW klystrons	8
• SRF linac output beam energy	~1.0 GeV
• Number of SRF cavities	97
• Number of linac 805-MHz 0.5-MW klystrons	97

Summary Parameters for the SNS (cont.)

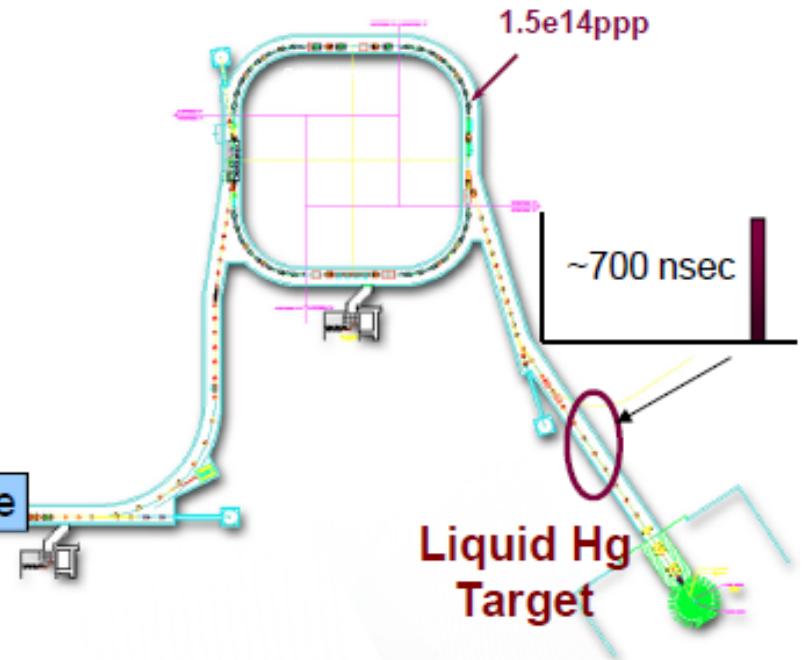
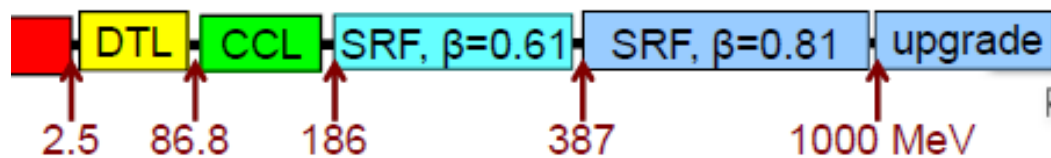
• Linac beam duty factor		6.0 %
• HEBT length		170 m
• Accumulator ring circumference		248.0 m
• Ring orbit rotation time		945 ns
• Number of injected turns	1060	
• Ring fill time		1.0 ms
• Ring beam extraction gap		250 ns
• RTBT length		151 m
• Protons per pulse on target		2.08E+14
• Proton pulse width on target		695 ns
• Target material	Hg	
• Number of ambient/composite/cold mod.		1/1/2
• Number of neutron beam shutters	18	
• Initial number of instruments		10

The SNS Accelerator

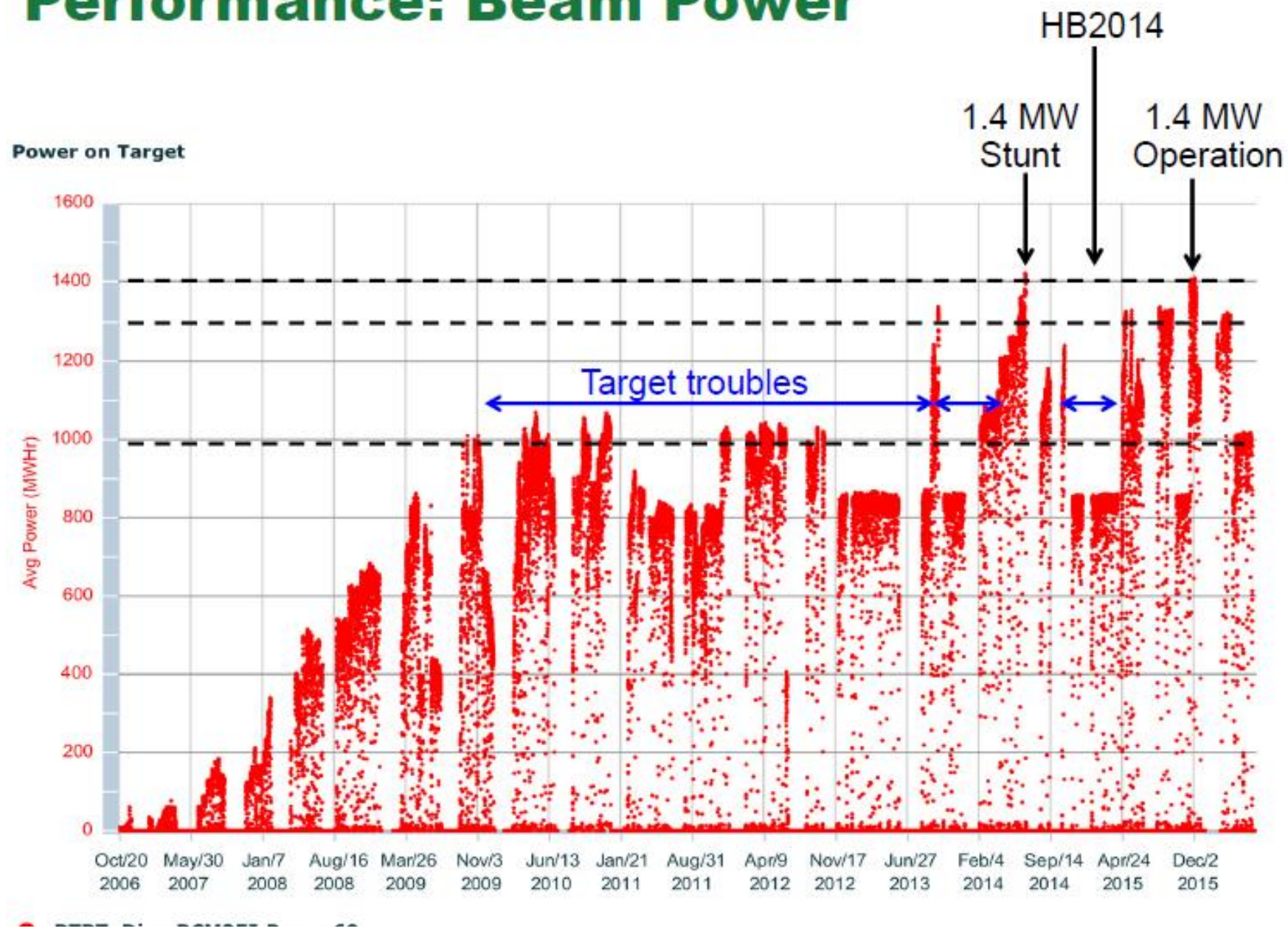
Top Level Goals:

1. 1.4 MW (designed for up to 2 MW)
2. 90% Reliability
3. < 1 W/m beam loss (~ 100 mrem/hr @ 30 cm)

Most design decisions were motivated by these goals.

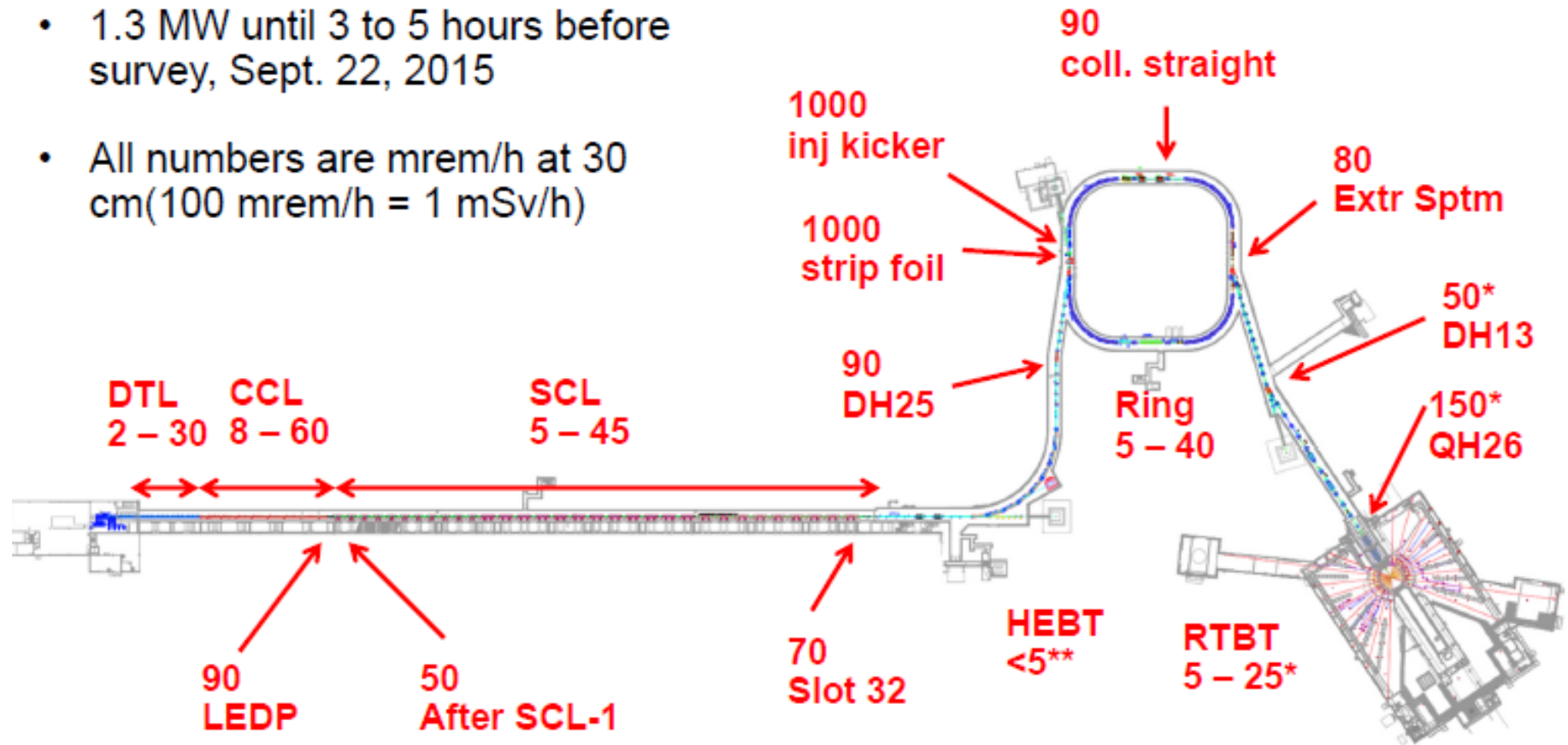


Performance: Beam Power



Performance: Activation levels

- 1.3 MW until 3 to 5 hours before survey, Sept. 22, 2015
- All numbers are mrem/h at 30 cm (100 mrem/h = 1 mSv/h)

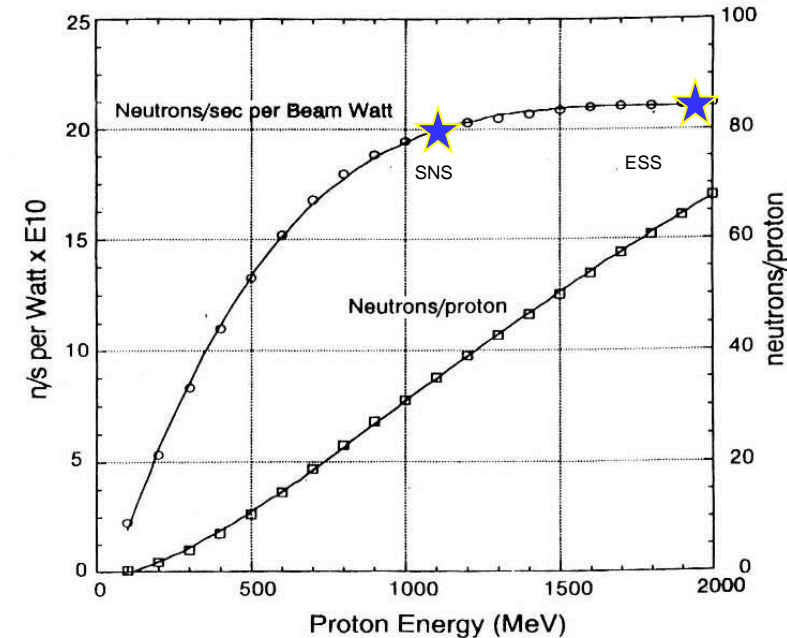


Except for a few hot spots, the dose rates are relatively low (< 1 W/m).

- * 3 days after 1.3 MW
- ** No survey near this time, indicated does rates are typical

Neutron sources

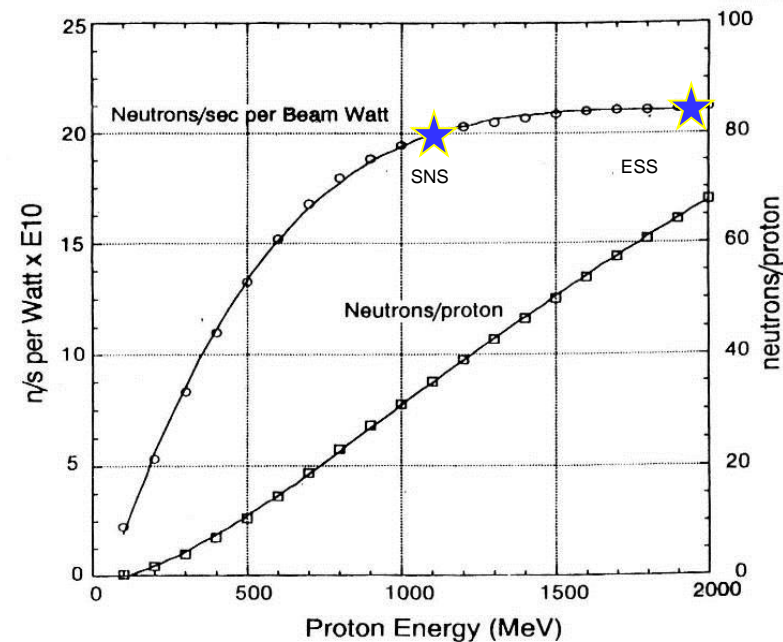
- Most used neutron sources are
 - Research reactors (critical reactors with a large external flux)
 - Spallation sources (p accelerators above 600 MeV)



Spallation production
(W solid target)

Neutron sources

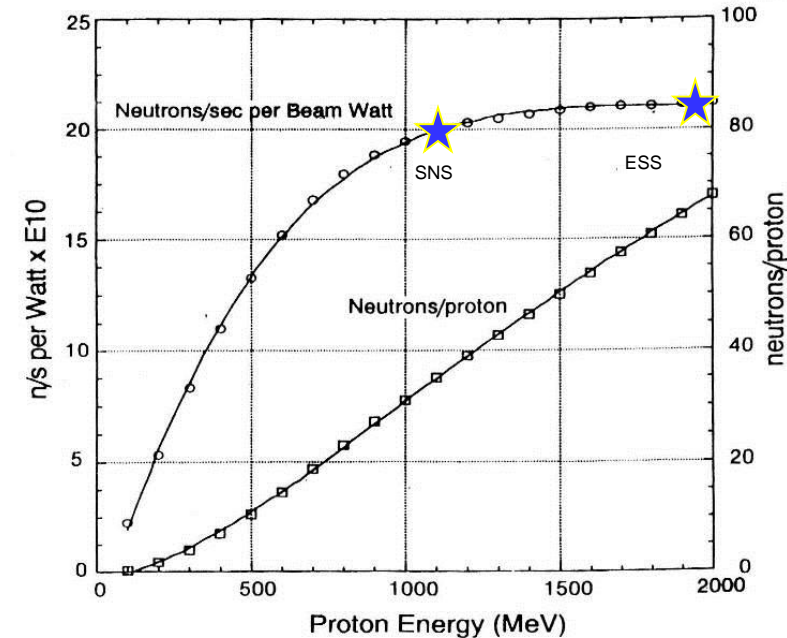
- Most used neutron sources are
 - Research reactors (critical reactors with a large external flux)
 - Energy to be dissipated (in the core) about 200 MeV per neutron produced (neutron production $3.2 \cdot 10^{10}$ n/(s*W))
 - Spallation sources (p accelerators above 600 MeV)
 - neutron production $2 \cdot 10^{11}$ n/(s*W), i.e. energy to be dissipated (in the production target) about 30 MeV per neutron produced



Spallation production
(W solid target)

Neutron sources

- Most used neutron sources are
 - Research reactors (critical reactors with a large external flux)
 - Energy to be dissipated (in the core) about 200 MeV per neutron produced (neutron production $3.2 \cdot 10^{10}$ n/(s*W))
 - Spallation sources (p accelerators above 600 MeV)
 - neutron production $2 \cdot 10^{11}$ n/(s*W), i.e. energy to be dissipated (in the production target) about 30 MeV per neutron produced
 - Low energy accelerator sources (d linac 40 MeV, p linacs 3-5 MeV)
 - Energy to be dissipated (in the production target) About 600 MeV/n for d at 40 MeV (10^{10} n/(s*W)), and 9 GeV/n for 5 MeV p on beryllium (10^8 n/(s*W))

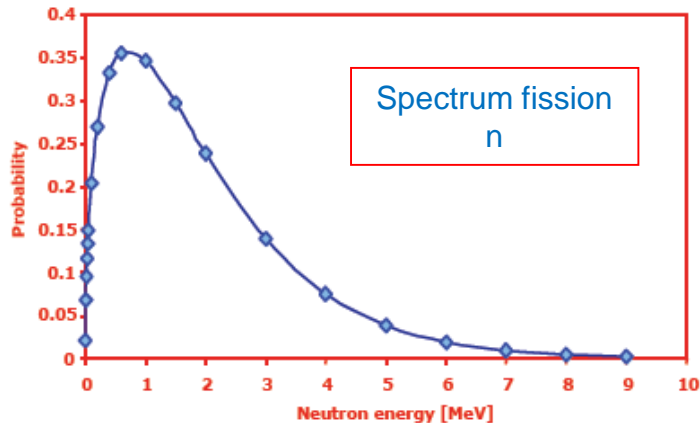


Spallation production
(W solid target)

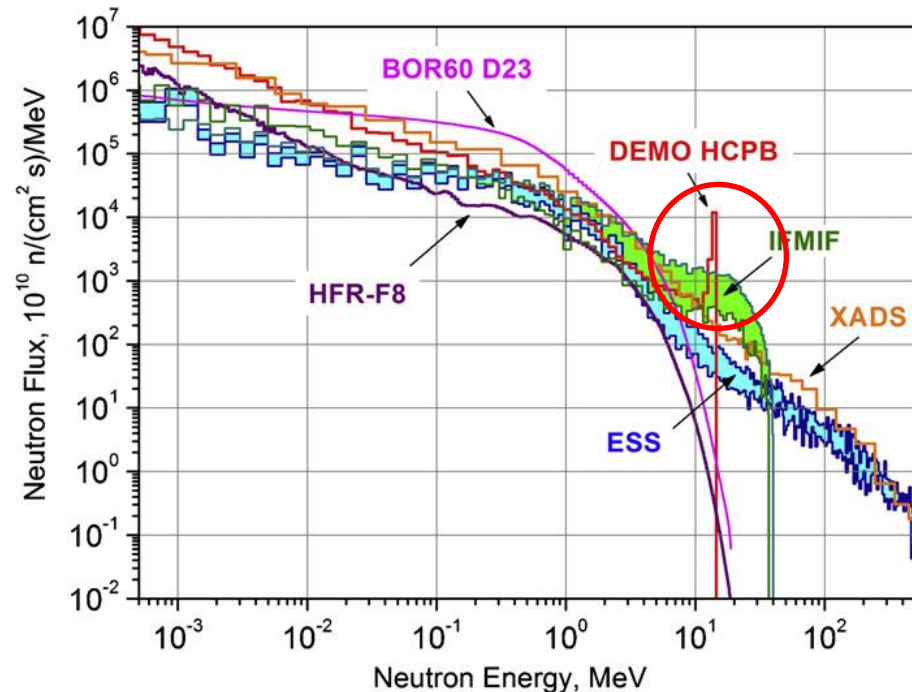
A specific source is needed to simulate DEMO

- The accumulation of gas in the materials lattice is intimately related with the neutron energy
- $^{54}\text{Fe}(n,\alpha)^{51}\text{Cr}$
- (incident n threshold at **2.9 MeV**)
- and
- $^{54}\text{Fe}(n,p)^{54}\text{Mn}$
- (incident n threshold at **0.9 MeV**)

- **Swelling** and **embrittlement** of materials takes place



Neutron flux compared with DEMO's in available and planned neutron sources

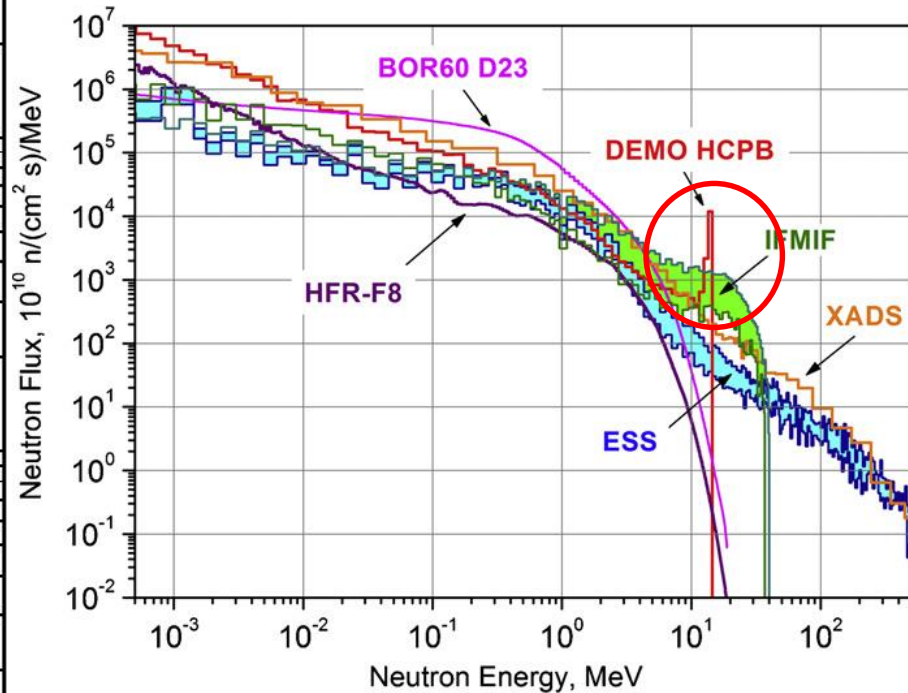
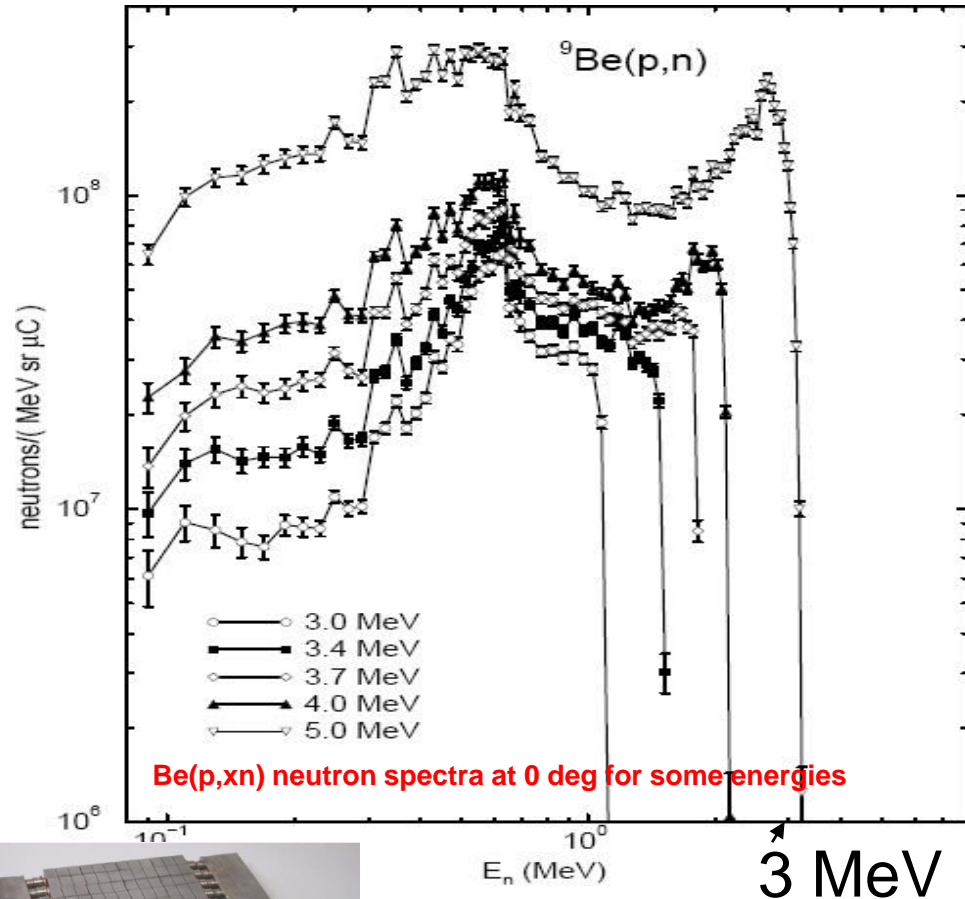


Steven J. Zinkle, A. Moeslang, *Evaluation of irradiation facility options for fusion materials research and development*, Nuclear Engineering & Design, pre-printed (2013)

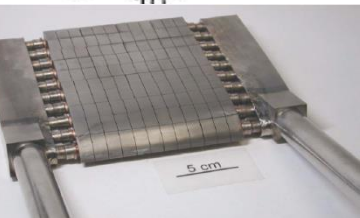
A specific source is needed for BNCT

- For Boron Neutron Capture Therapy is necessary to avoid high energy tails (non specific damage to tissues)

Neutron flux compared with DEMO's in available and planned neutron sources



Steven J. Zinkle, A. Moeslang, *Evaluation of irradiation facility options for fusion materials research and development*, Nuclear Engineering & Design, pre-printed (2013)



5 MeV protons with Be target
MUNES

Alternative neutron sources (1/3)

- Electron linacs

As an example ARIEL project at TRIUMF (0.5 MW, 50 MeV 10 mA cw for $5 \cdot 10^{13}$ fission/s, i.e. neutron production 10^8 n/(s*W))

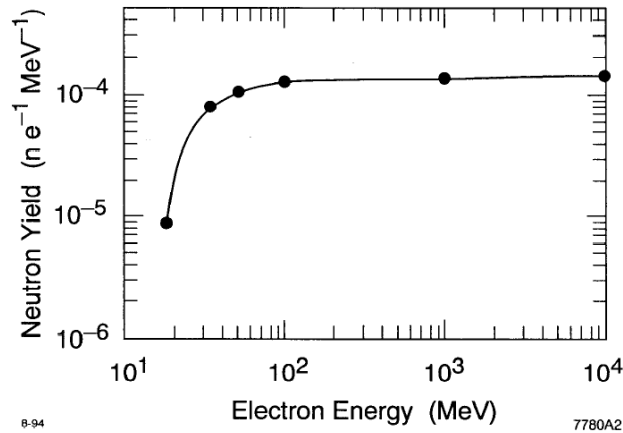
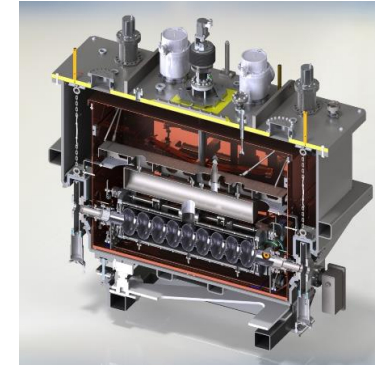
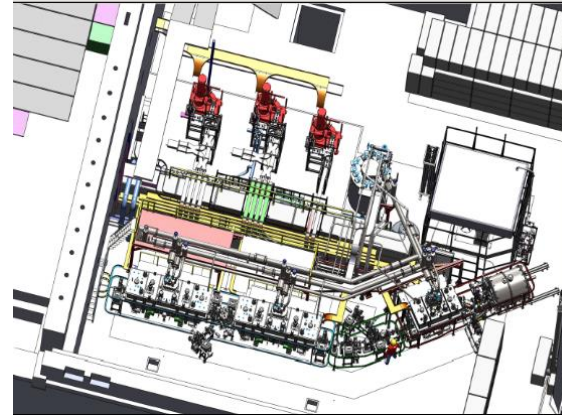



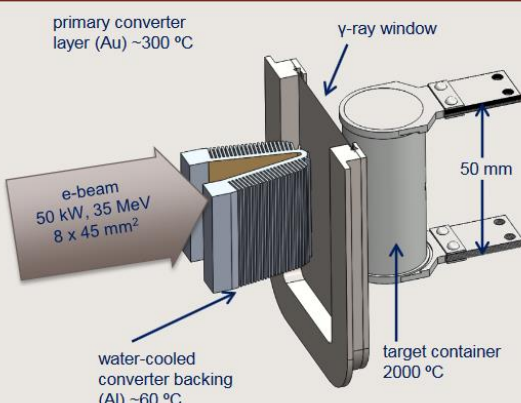
Figure 2. Neutron yields produced in 20 r.l.-thick iron targets as a function of electron energy.

TRIUMF

ARIEL electron-to-γ converter


explosion bonded Au/Al test sample





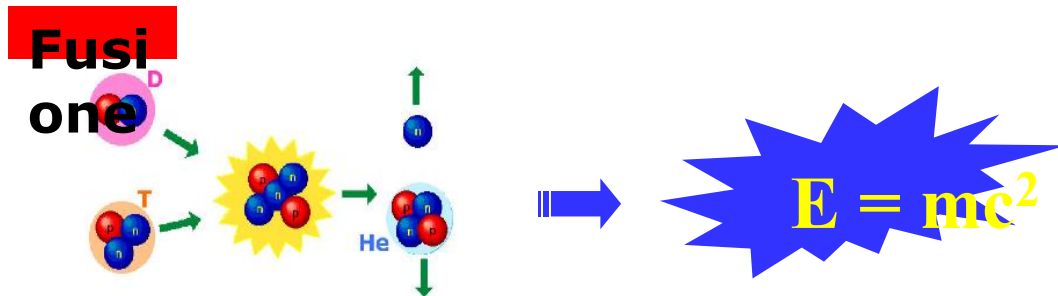
Courtesy of A. Gottberg

electro-plated Au/Al test sample

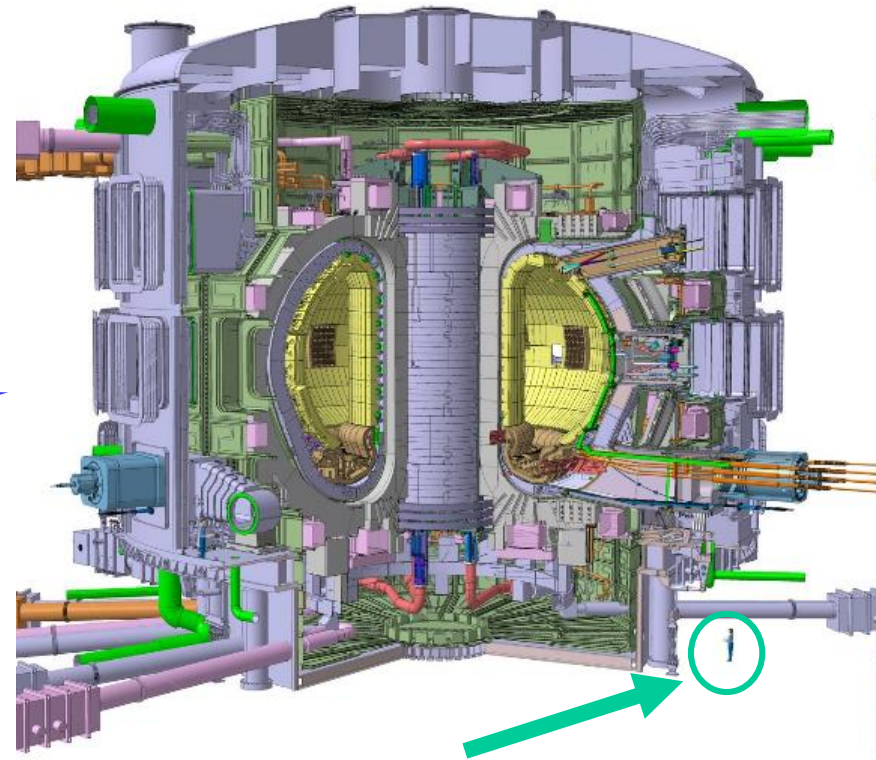


Alternative neutron sources (2/3)

- The tokamak is of course a powerful neutron source.



- About 20 MeV per neutron,
- $10^{11} \text{ n}/(\text{s} \cdot \text{W})$. Huge technological issues to get an advantageous energy balance
- Future Fusion plants GW $\Rightarrow 10^{20} \text{ n/s}$

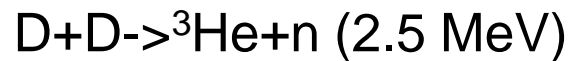


ITER

International Thermonuclear Experimental Reactor

Alternative neutron sources (3/3)

- Sealed D T electrostatic sources



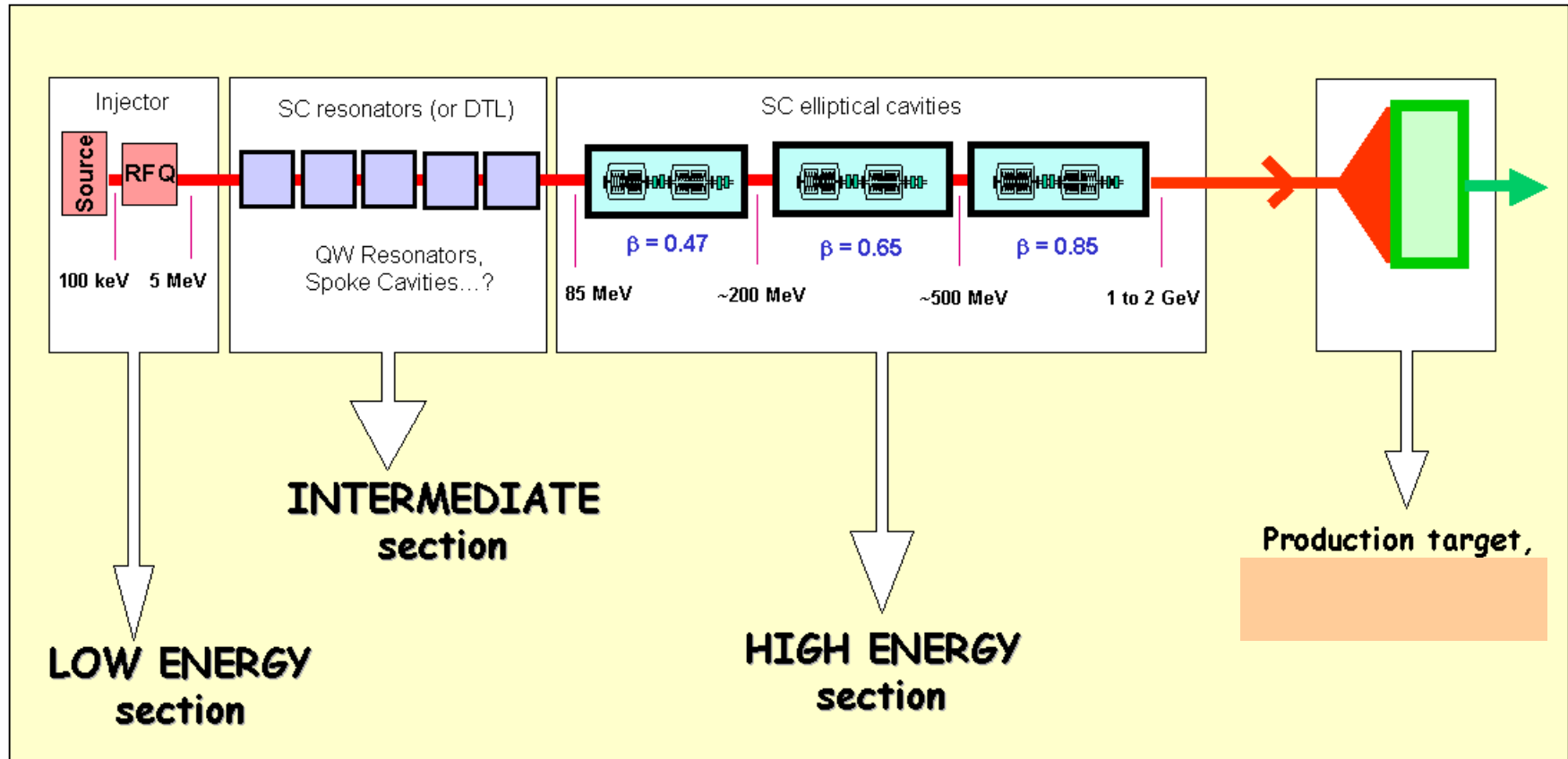
, typical sealed D-T tube, 10^6 n/pulse
in 10 us 100 Hz

- Limited by the power on the target and the current d current , and by the tritium availability. 10^{10} - 10^{11} n/(s*W).



Nuclear physicist at the [Idaho National Laboratory](#) sets up an experiment using an electronic neutron generator. (Wikipedia)

DRIVER ACCELERATOR structure

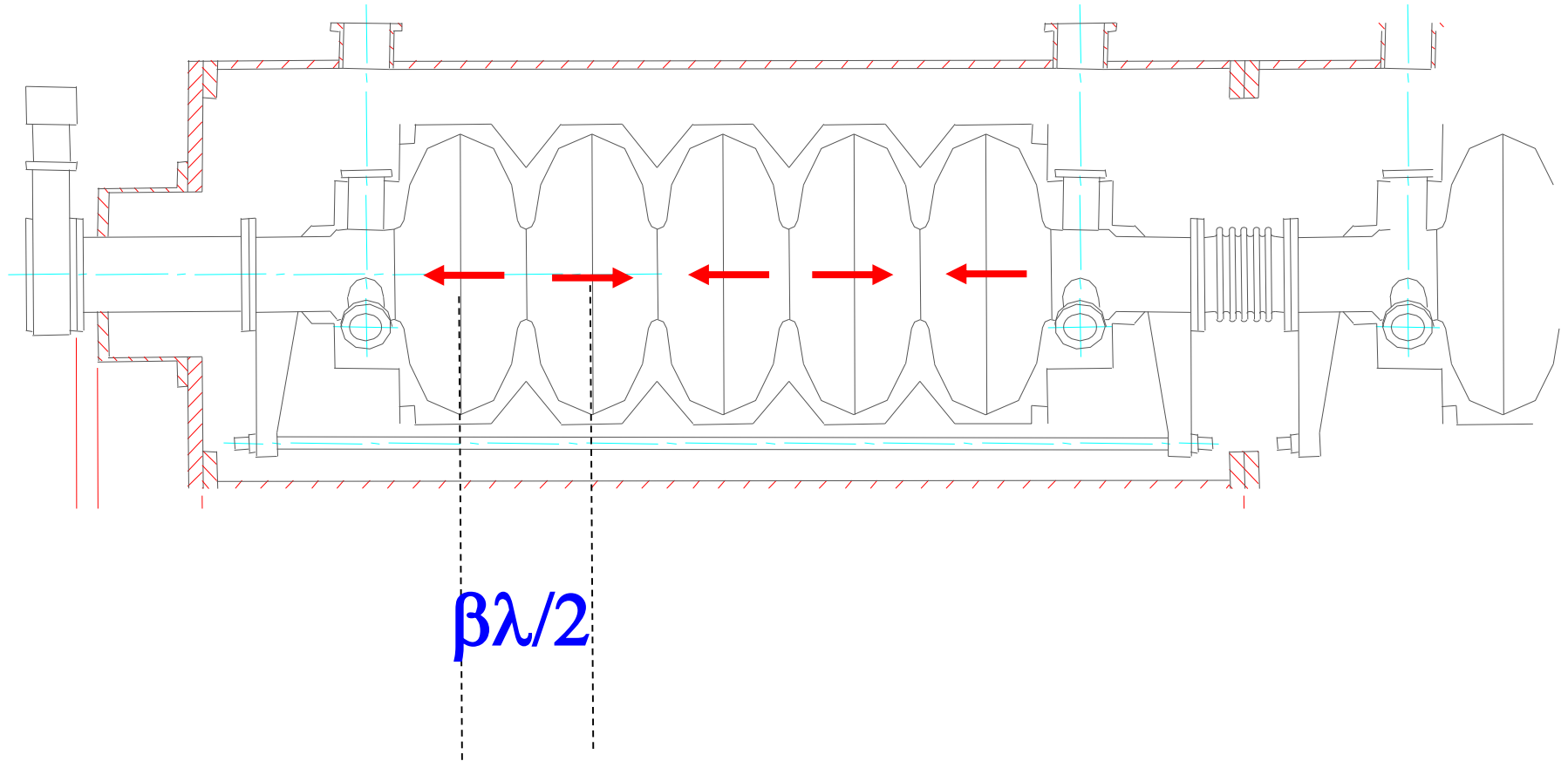


- Low energy section prepares the structure of the beam and guarantees beam quality
- High energy section needs low losses and high efficiency

- Third lesson; RFQs and IFMIF
- Second lesson: linac dynamics and ESS

RF aspects

Gli acceleratori lineari : cavità RF

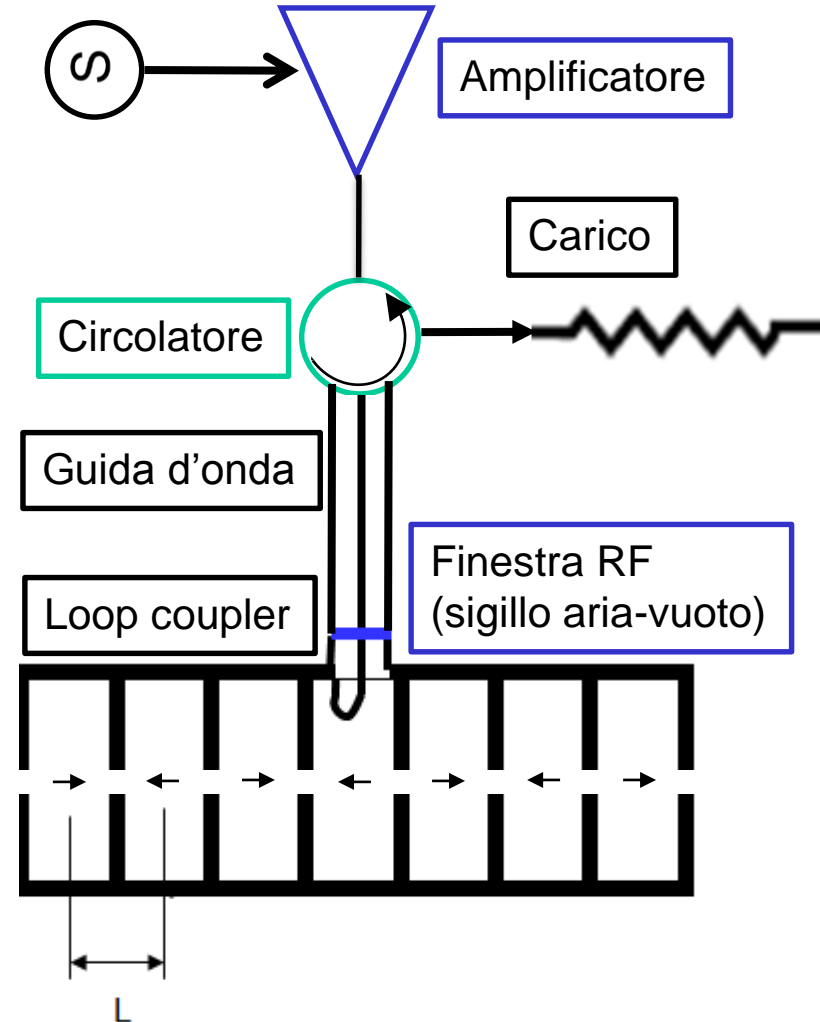


Linac RF ad onda stazionaria

- Linac: acceleratore RF a singolo passaggio
- potenzialmente
 - Alta intensità di fascio accelerato P_b
 - Alta potenza RF dissipata P_{rf}
- Necessaria alta efficienza energetica

$$\eta = \frac{\eta_{RF} P_b}{P_d + P_b} = \frac{\eta_{RF}}{1 + \frac{P_d}{P_b}}$$

η_{RF} efficienza del sistema RF
(conversione potenza elettrica dalla rete)

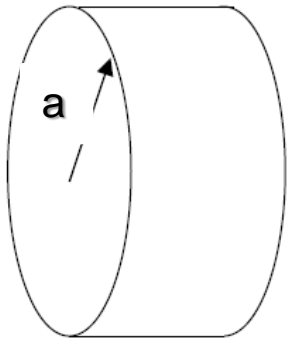


Parametri fisici di una cavità RF

- Nella cavità, per una data frequenza f_0 è risolta l'equazione elettromagnetica delle onde con condizione al contorno di conduttore perfetto.

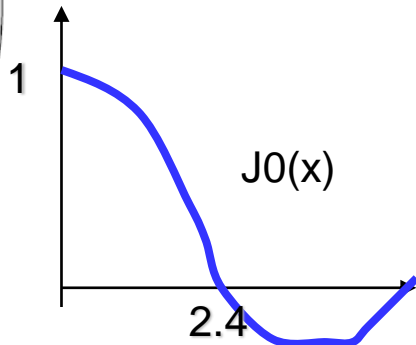
$$\nabla^2 \vec{E} = -\frac{\omega^2}{c^2} \vec{E}$$

- Esempio di cavità di cui è nota la soluzione analitica: modo accelerante TM_{010}
 - CELLA SINGOLA O PILL-BOX



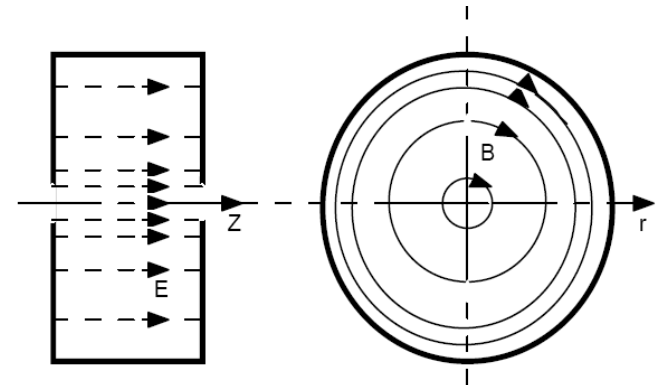
$$E_z(r, t) = E_0 J_0(2\pi r / \lambda) \cos(2\pi f_0 t)$$

$$B_\theta(r, t) = -\frac{E_0}{c} J_1(2\pi r / \lambda) \sin(2\pi f_0 t)$$



$$J_0(2\pi a / \lambda) = J_0(2.405) = 0 \quad f_0 = 2.405c / a$$

$J_0(x)$ e $J_1(x)$ funzioni di Bessel di prima specie



Parametri fisici di una cavità RF

- Nella cavità, per una data frequenza f_0 è risolta l'equazione elettromagnetica delle onde con condizione al contorno di conduttore perfetto.

$$\nabla^2 \vec{E} = -\frac{\omega_0^2}{c^2} \vec{E}$$

- Esempio di cavità multi cella di cui è nota la soluzione analitica: modo accelerante TM_{01n}

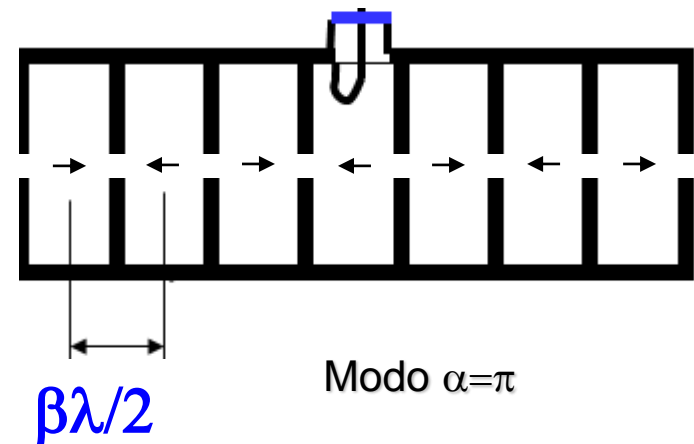
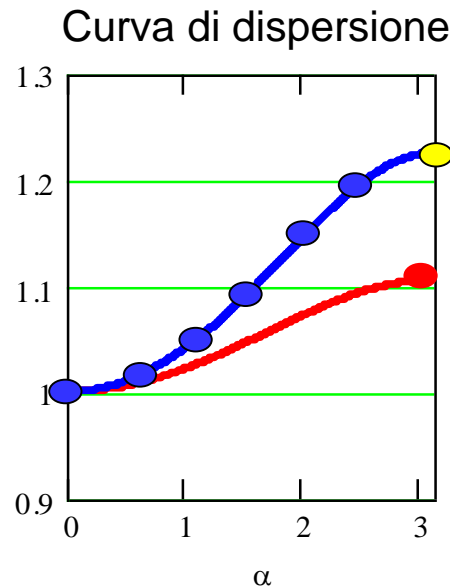
$$E_z(r, t) = E_0 J_0(2\pi r / \lambda) \cos(\alpha n) \cos(2\pi f_n t)$$

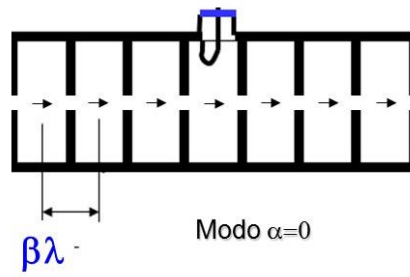
$$f_n = \frac{f_0 \sqrt{1+k}}{\sqrt{1+k \cos \alpha n}}$$

$$\frac{\sqrt{1+1}}{\sqrt{1+1 \cdot \cos(\alpha)}} \quad \text{---}$$

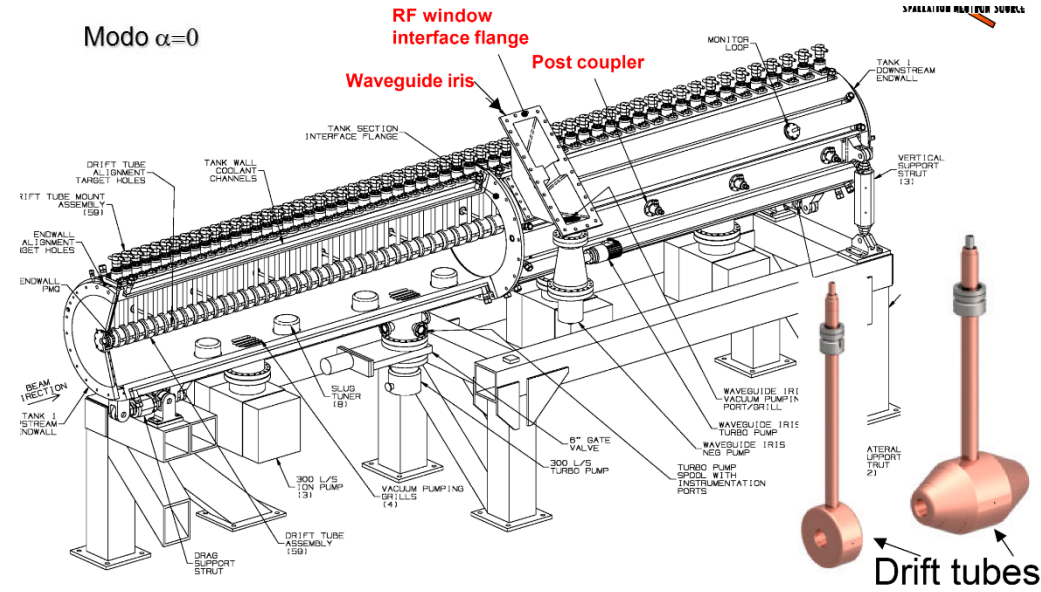
$$\frac{\sqrt{1+2}}{\sqrt{1+2 \cdot \cos(\alpha)}} \quad \text{---}$$

k coefficiente di accoppiamento

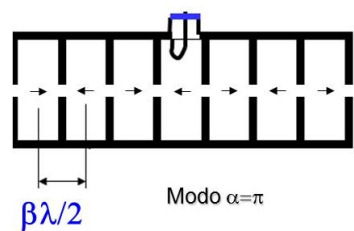
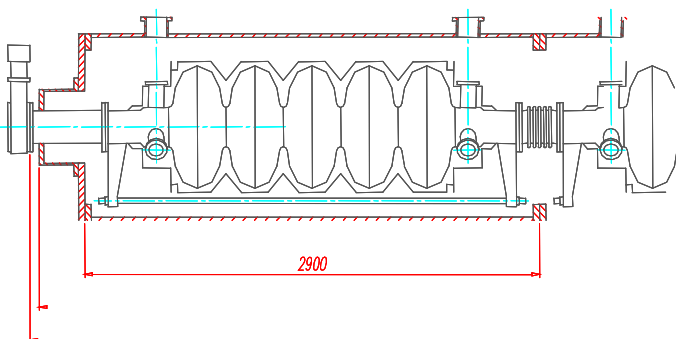




DTL o Alvarez

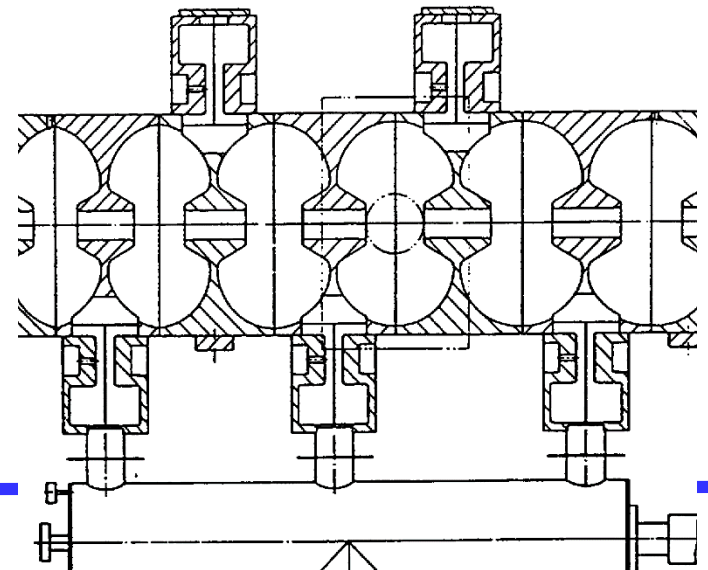
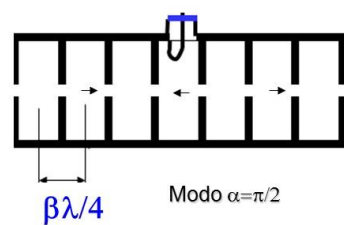


Superconducting elliptical cavity



Side coupled linac

Modo $\alpha=\pi/2$



Parametri fisici di una cavità RF

- Nella cavità, per una data frequenza f_0 è risolta l'equazione elettromagnetica delle onde con condizione al contorno di conduttore perfetto.

$$\nabla^2 \vec{E} = -\frac{\omega_0^2}{c^2} \vec{E}$$

f_0 **frequenza di risonanza** del modo di operazione

$$U = \frac{1}{4} \int_{Vol} (\epsilon_0 |\mathbf{E}|^2 + \mu_0 |\mathbf{H}|^2) dV$$

Energia elettromagnetica media immagazzinata
nel volume della cavità (in risonanza i due addendi sono uguali)

$$P_d = \sqrt{\frac{\pi \mu_0 f_0}{4\sigma}} \int_S |\hat{\mathbf{i}}_n \times \mathbf{H}|^2 dS = R_s \int_S |\hat{\mathbf{i}}_n \times \mathbf{H}|^2 dS$$

Potenza dissipata sulla superficie
metallica S (di resistenza superficiale R_s)

$$Q = \frac{2\pi f_0 U}{P_d}$$

Fattore di merito della cavità: Per cavità in Rame ($\sigma=5.8 \cdot 10^7$ S/m) valori tipici di Q sono nell'intervallo 5000-50000.

$$R_{sh} = \frac{|V|^2}{P_d}$$

Shunt Impedance: è una figura di merito che indica quanto efficacemente la cavità è in grado di accelerare a scapito della potenza dissipata: Divisa per Q non dipende dalla resistività della superficie

$$\frac{R_{sh}}{Q} = \frac{|V|^2}{2\pi f_0 U}$$

Why a superconducting linac?

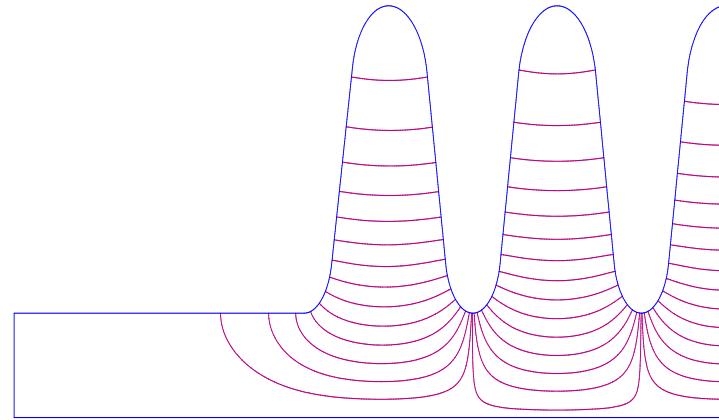
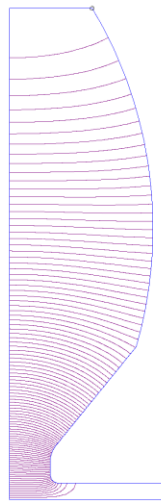
- Normal conducting

$$\eta = \frac{\eta_{RF}}{1 + \frac{P_d}{P_b}} = \frac{\eta_{RF}}{1 + \frac{E}{QI \left[\frac{r}{Q} \right]}}$$

- Superconducting

$$\eta = \frac{P_b}{\frac{P_b + P_d}{\eta_{RF}} + \frac{P_d}{\eta_{cryo}}} \approx \frac{\eta_{RF}}{1 + \frac{\eta_{RF}}{\eta_{cryo}} \frac{E}{QI \left[\frac{r}{Q} \right]}}$$

- $\eta_{RF} \approx .65$ RF efficiency
- $\eta_{cryo} \approx .02$ cryogenic efficiency
- P_b beam power
- P_d dissipated power
- r/Q shunt impedance per unit length (geometrical factor)
- I beam intensity
- E average acceleration



	SCL	Superconducting	
Frequency	425	352.2	MHz
Q	2.80E+04	2.00E+09	
beta	0.44	0.50	
Beam bore diameter	16.00	94.4	mm
r	38.00	2.22E+05	MΩ/m
r/Q	1357.	110.	Ω/m
I	30.	30	mA
E	2.	2	MV/m
η	0.24	0.644	

The static losses in the cryostats (to be added for the superconducting linac) can be dominating.

Beam dynamics

acceleration: relativistic kinematics

- Electrostatic acceleration: a particle with charge e , generated in a source at potential V , once in the transport line at ground potential has a kinetic energy

$$W = eV$$

- An adimensional energy γ and velocity β are defined according to:

$$\gamma = 1 + \frac{W}{mc^2} \quad \vec{v} = c\vec{\beta}$$

- with m mass of the particle (938 MeV/c² protons, $A \cdot 931.5$ MeV/c² for a nucleus of mass number A , 0.511 MeV/c² for electrons), $c = 2.998 \cdot 10^8 \text{ ms}^{-1}$. then

$$\gamma^2 = \frac{1}{1 - \beta^2} \quad \beta^2 = 1 - \frac{1}{\gamma^2}$$

acceleration: relativistic kinematics

- Electrostatic acceleration: a particle with charge e , generated in a source at potential V , once in the transport line at ground potential has a kinetic energy

$$W = eV$$

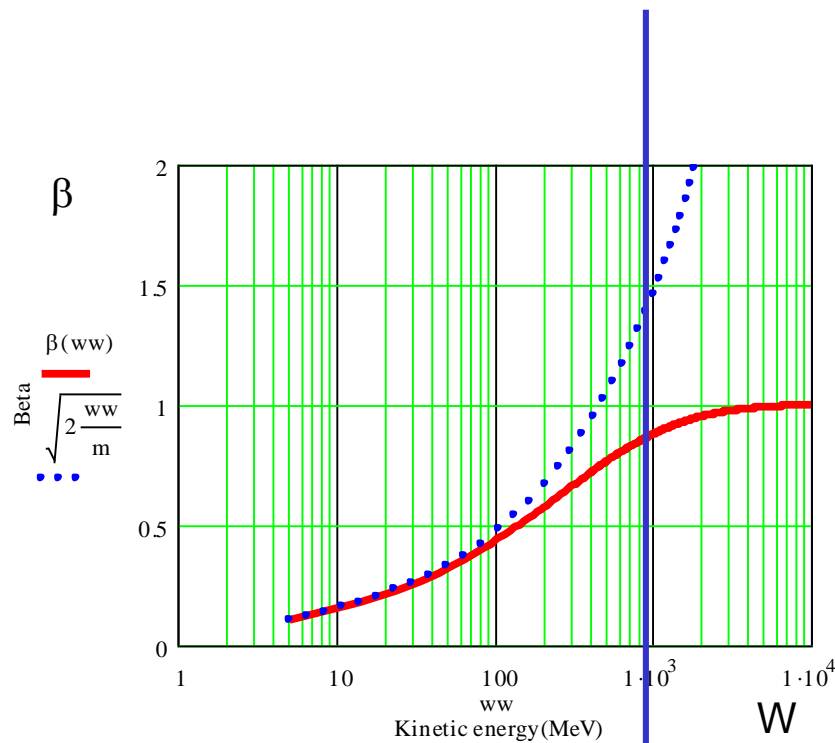
- An adimensional energy γ and velocity β are defined according to:

$$\gamma = 1 + \frac{W}{mc^2} \quad \vec{v} = c\vec{\beta} \quad \boxed{E = Mc^2}$$

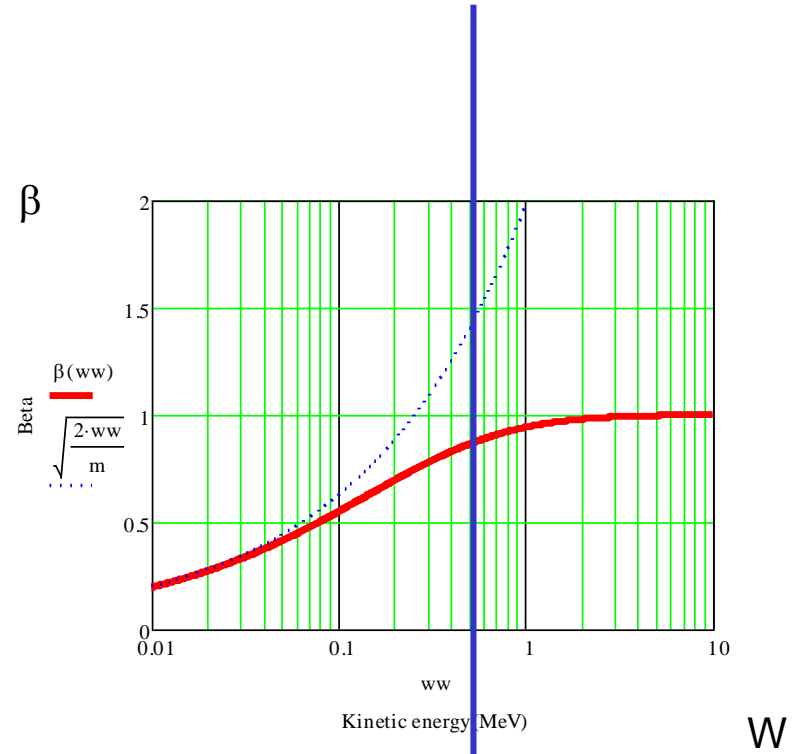
- with m mass of the particle (938 MeV/c² protons, $A \cdot 931.5$ MeV/c² for a nucleus of mass number A , 0.511 MeV/c² for electrons), $c = 2.998 \cdot 10^8 \text{ ms}^{-1}$. then

$$\gamma^2 - \beta^2 \gamma^2 = 1 \quad \beta^2 = 1 - \frac{1}{\gamma^2} \quad \boxed{[mc^2]^2 = E^2 - p^2 c^2}$$

acceleration: relativistic kinematics



Proton velocity ($mc^2=938$ MeV)
And non relativistic approximation



Electron velocity ($mc^2=0.511$ MeV)

Triangolo

Energy γ

$$\frac{\Delta\beta\gamma}{\beta\gamma} = \beta^2 \frac{\Delta\gamma}{\gamma}$$

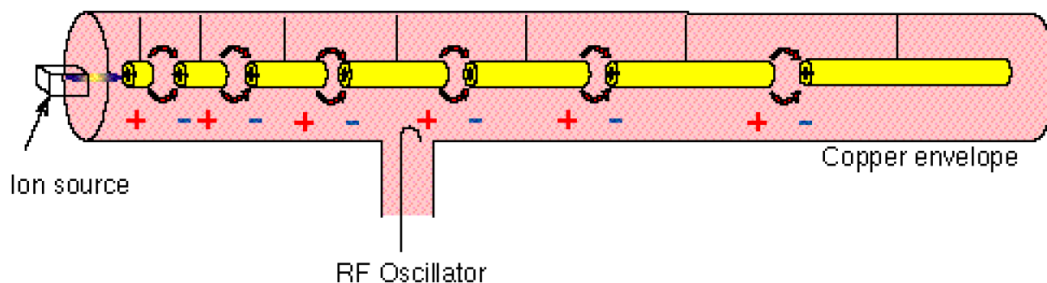
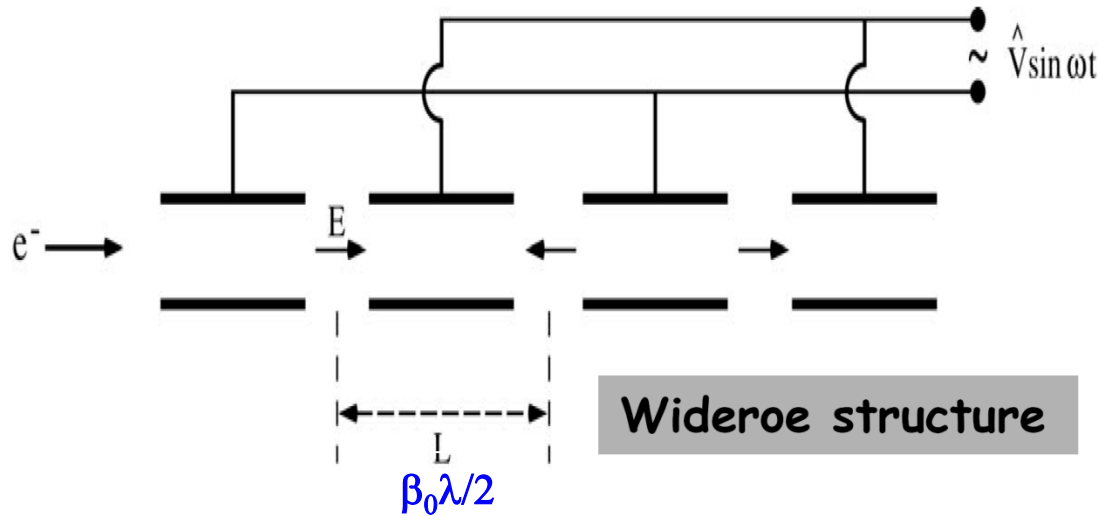
$$\frac{\Delta\gamma}{\gamma} = \beta^2 \gamma^2 \frac{\Delta\beta}{\beta}$$

Momentum $\beta\gamma$

Velocity β

$$\frac{\Delta\beta}{\beta} = \gamma^2 \frac{\Delta\beta\gamma}{\beta\gamma}$$

Linear accelerator (linac)

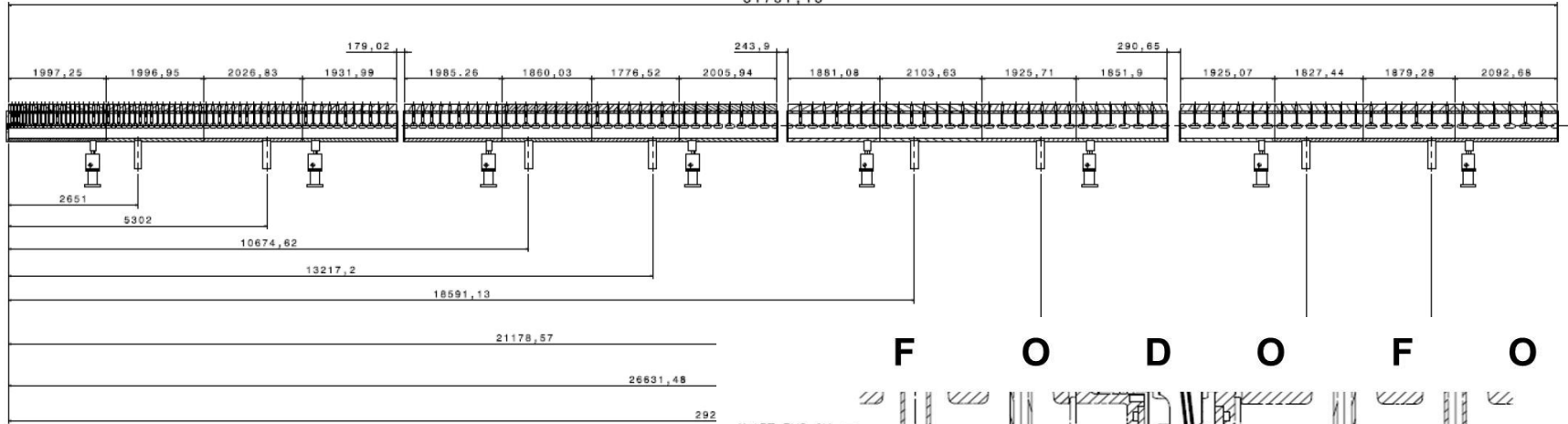


- The distance after each accelerating gap defines the synchronous velocity β_0 , then the nominal energy w_0 and its increase after the accelerating gap

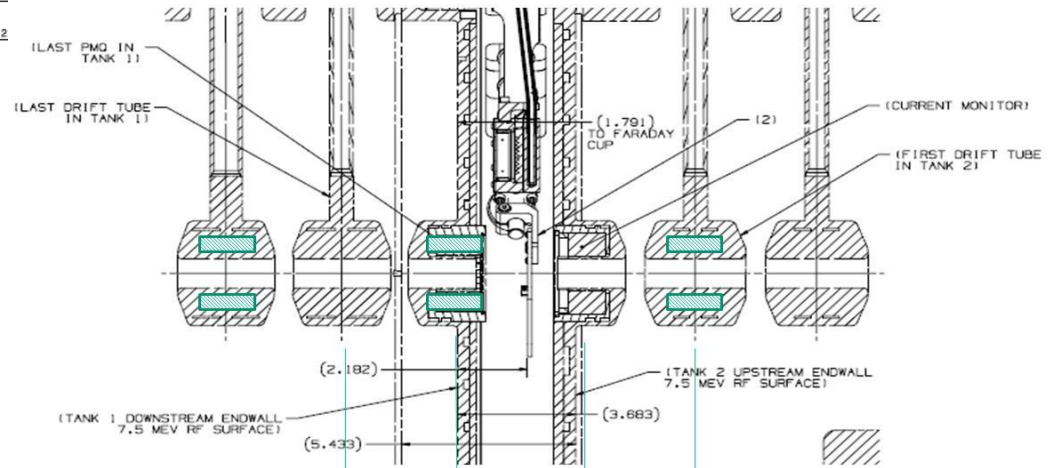
$$\frac{dw_0}{dn} = eV \cos \phi_0$$

- ϕ_0 is the synchronous phase, dn is an adimensional variable increasing of a unit after each period

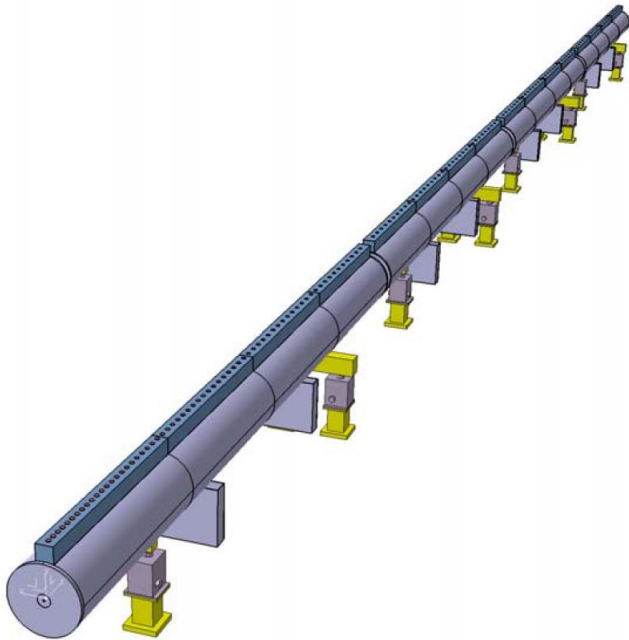
31781, 13



F O D O F O



$\beta\lambda$ $\beta\lambda$ $\beta\lambda$



DTL designed for ESS 3.5-90 MeV 65 mA pulsed

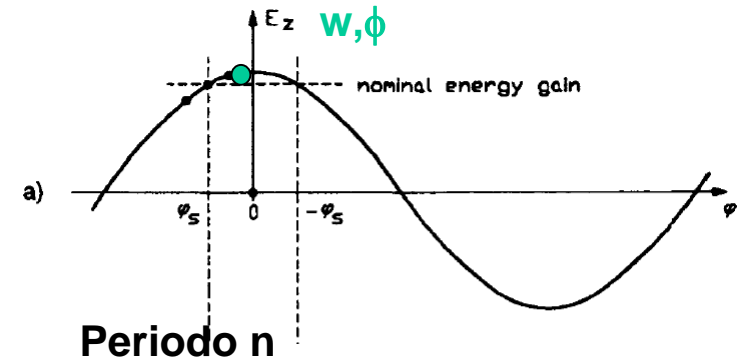
The generic particle: phase stability

The generic particle, with phase ϕ and energy w , will withstand after each gap e variation

$$\frac{d(w - w_0)}{dn} = eV[\cos \phi - \cos \phi_0]$$

While after the length $\beta_0 \lambda / 2$ of the period it will arrive with a delay respect to the nominal particle:

$$\frac{d(\phi - \phi_0)}{dn} \approx -\pi \frac{\beta - \beta_0}{\beta} = -\pi \frac{w - w_0}{\beta^2 \gamma^3 mc^2}$$



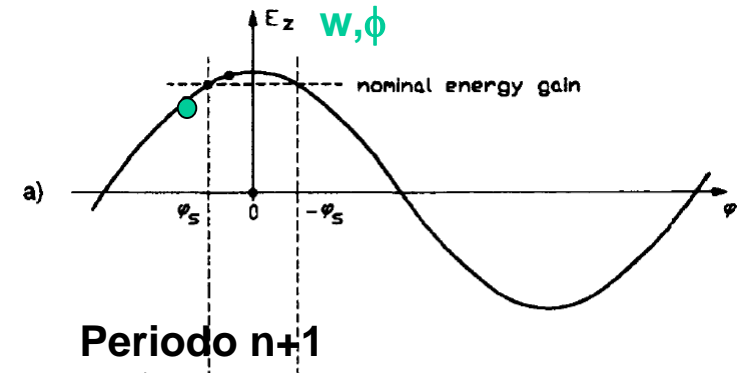
The generic particle: phase stability

The generic particle, with phase ϕ and energy w , will withstand after each gap e variation

$$\frac{d(w - w_0)}{dn} = eV [\cos \phi - \cos \phi_0]$$

While after the length $\beta_0 \lambda / 2$ of the period it will arrive with a delay respect to the nominal particle:

$$\frac{d(\phi - \phi_0)}{dn} \approx -\pi \frac{\beta - \beta_0}{\beta} = -\pi \frac{w - w_0}{\beta^2 \gamma^3 mc^2}$$



The generic particle: phase stability

The generic particle, with phase ϕ and energy w , will withstand after each gap e variation

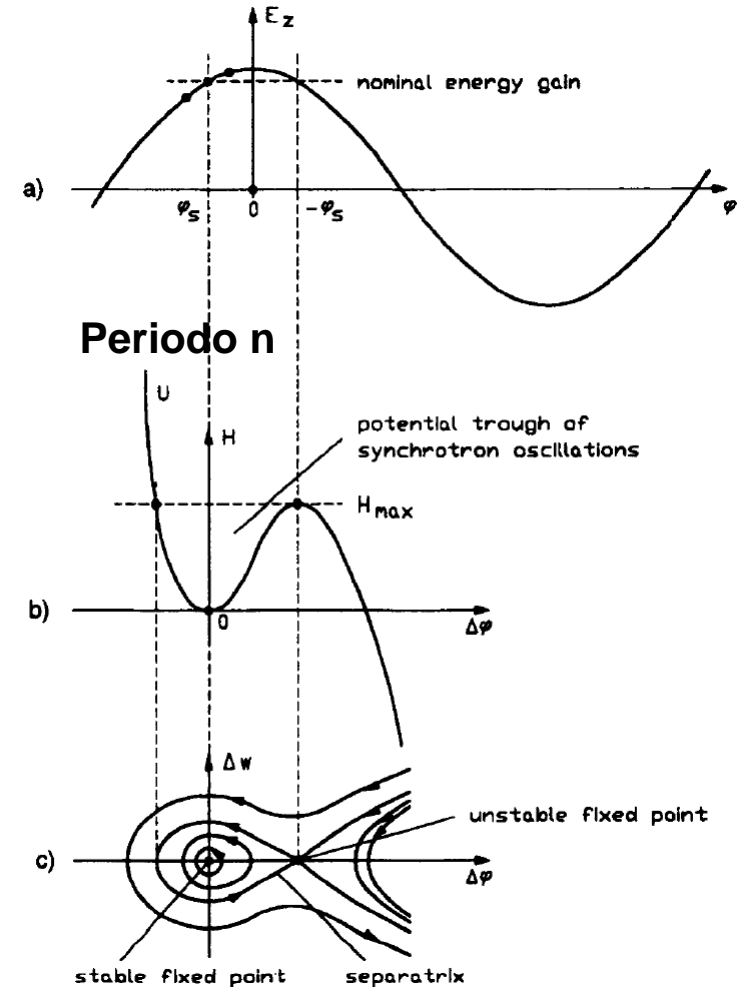
$$\frac{d(w - w_0)}{dn} = eV [\cos \phi - \cos \phi_0] = \frac{\partial H}{\partial \phi}$$

While after the length $\beta_0 \lambda / 2$ of the period it will arrive with a delay respect to the nominal particle:

$$\frac{d(\phi - \phi_0)}{dn} \approx -\pi \frac{\beta - \beta_0}{\beta} = -\pi \frac{w - w_0}{\beta^2 \gamma^3 mc^2} = -\frac{\partial H}{\partial w}$$

The evolution of the system is described by the Hamiltonian

$$H(w, \phi) = \frac{\pi (w - w_0)^2}{2 \beta^2 \gamma^3 mc^2} + \underbrace{eV [\sin \phi - \phi \cos \phi_0]}_{U(\phi)}$$



RF defocusing

- The transverse electric field is also determined by the quasi electrostatic hypothesis+cylindrical symmetry:

$$\text{div}\vec{E} = 0 \quad \Rightarrow \quad \frac{\partial E_r}{\partial r} = -\frac{1}{2} \frac{\partial E_z}{\partial z}$$

$$\begin{aligned} \frac{\partial E_r}{\partial r} &= -\frac{e}{2L} \int dz \frac{\partial E_z}{\partial z} \cos\left(\frac{2\pi z}{\beta\lambda} + \phi\right) = \frac{e}{2L} \int dz E_z \frac{\partial}{\partial z} \cos\left(\frac{2\pi z}{\beta\lambda} + \phi\right) = -\frac{\pi e}{\beta\lambda L} \int dz E_z \sin\left(\frac{2\pi z}{\beta\lambda} + \phi\right) = \\ &= -\frac{\pi e}{\beta\lambda L} \sin\phi \int dz E_z \cos\left(\frac{2\pi z}{\beta\lambda}\right) = -\frac{\pi e V}{\beta\lambda L} \sin\phi = -\frac{\pi e E_a}{\beta\lambda} \sin\phi \end{aligned}$$

That can be substituted in the transverse equation of motion

$$\begin{aligned} x'' + [K + K_{RF}]x &= 0 \\ K_{RF} &= \pi \frac{eE_a \sin\phi_0}{\beta^3 \gamma^3 mc^2 \lambda} \end{aligned}$$

NOTE: this derivation is non relativistic and gives an inaccurate $1/\gamma$. The $1/\gamma^3$ can be calculated either Calculating the electric field in particle rest frame and applying Lorenz transformation or considering the in Laboratory frame the magnetic field here neglected.

Solution in term of Floquet functions

- The solution of Hill equation

$$x'' + K(s)x = 0 \quad K(s+L) = K(s)$$

Can be written in the form $x = a(s)e^{i\psi(s)}$ where, separating real and imaginary components, one gets

$$a'' + Ka - a\psi'^2 = 0$$

$$2\psi' a' + a\psi'' = 0$$

The second equation is solved by:

$$\psi' = \frac{\varepsilon}{a^2}$$
$$a'' + Ka - \frac{\varepsilon^2}{a^3} = 0$$

$$a(s+L) = a(s)$$

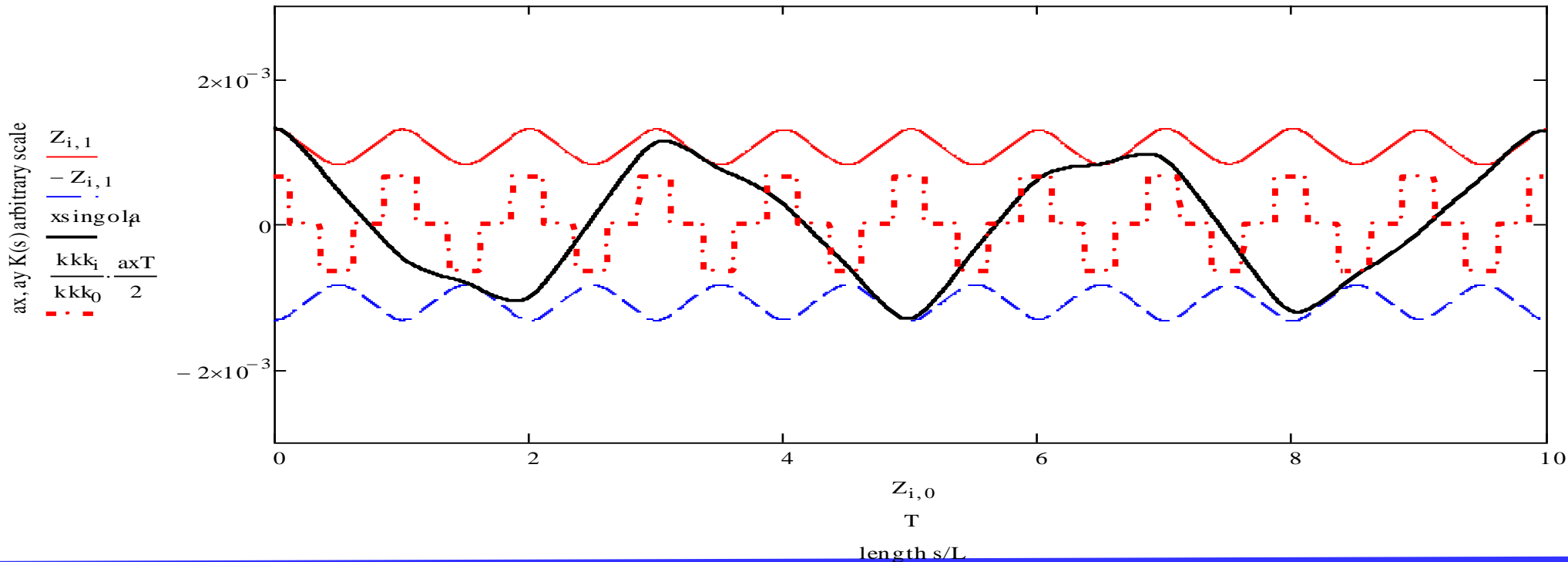
$$\mu = \int_{s_0}^s \psi' ds = \int_{s_0}^s \frac{\varepsilon ds}{a^2}$$

Where ε emittance is a constant, a beam envelope. It is defined then a function $\beta(s)$ **betatron function** with the following relation

$$a(s) = \sqrt{\varepsilon\beta(s)} \quad \Rightarrow \quad x(s) = \sqrt{\varepsilon\beta(s)} \cos\left(\int_{s_0}^s \frac{ds}{\beta(s)} + \delta\right)$$

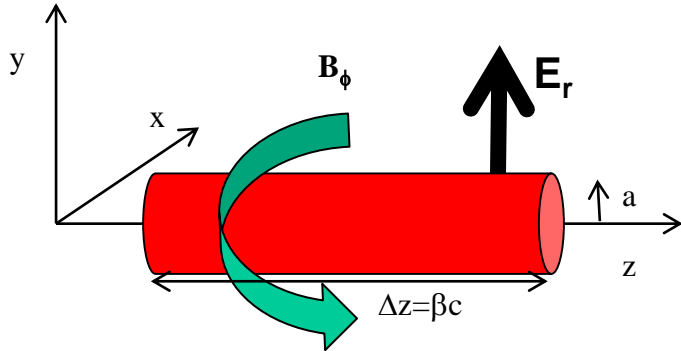
Solution in term of Floquet functions

$$a(s) = \sqrt{\varepsilon\beta(s)} \Rightarrow x(s) = \sqrt{\varepsilon\beta(s)} \cos\left(\int_{s_0}^s \frac{ds}{\beta(s)} + \delta\right)$$



Campi elettromagnetici generati dal fascio

(distribuzione omogenea)



$$2\pi r E_r \Delta z = \frac{1}{\epsilon_0} \left(\frac{r}{a}\right)^2 \Delta z \frac{I}{\beta c} \Rightarrow E_r = \frac{1}{2\pi\epsilon_0} \frac{I}{\beta c} \begin{cases} \frac{r}{a^2} & \text{if } r \leq a \\ \frac{1}{a} & \text{if } r > a \end{cases}$$

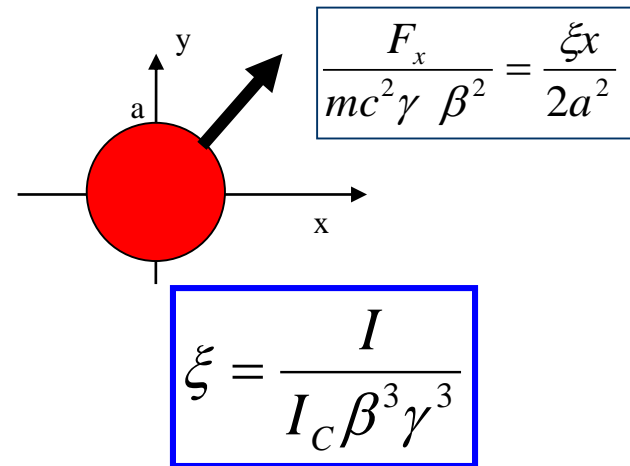
$$2\pi r B_\phi = \mu_0 \left(\frac{r}{a}\right)^2 I \Rightarrow B_\phi = \frac{\mu_0}{2\pi} I \begin{cases} \frac{r}{a^2} & \text{if } r \leq a \\ \frac{1}{a} & \text{if } r > a \end{cases}$$

$$F_r = e[E_r - B_\phi \beta c] = \frac{1}{2\pi\epsilon_0} \frac{I}{\beta c} (1 - \beta^2 c^2 \mu_0 \epsilon_0) \dots = \frac{1}{2\pi\epsilon_0} \frac{I}{\beta \gamma^2 c} \begin{cases} \frac{r}{a^2} & \text{if } r \leq a \\ \frac{1}{a} & \text{if } r > a \end{cases}$$

Carica Spaziale

Bassa energia

Campi per una densità di carica omogenea



$I_C = \frac{\pi\epsilon_0}{e} mc^3 = 7.8 \text{ MA}$ corrente caratteristica per protoni

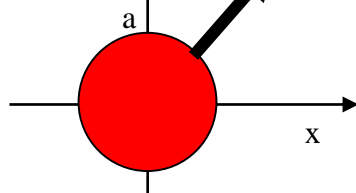
Electro magnetic fields generated by the beam

Space charge

Fields generated by a homogeneous current

$$\frac{F_x}{mc^2 \gamma \beta^2} = \frac{\xi x}{2a^2}$$

$$F_x = e[E_r - \beta c B_\phi] = \frac{eI}{\beta c \pi \epsilon_0 a^2} [1 - \beta^2]$$



$$\xi = \frac{I}{I_C \beta^3 \gamma^3}$$

$I_C = \frac{\pi \epsilon_0}{e} mc^3 = 7.8 \text{ MA}$ characteristic current for protons

The effect of space charge is to mitigate the external focusing

$$x'' + \left[K(s) + K_{RF} - \frac{\xi}{a^2} \right] x = 0$$

If the charge distribution is not homogeneous (as it often happens) the force becomes non linear (aberrations that can spoil beam quality)

Solution in term of Floquet functions

- The solution of Hill equation

$$x'' + \left[K(s) + K_{RF} - \frac{\xi}{a^2} \right] x = 0 \quad K(s+L) = K(s)$$

Can be written in the form $x = a(s)e^{i\psi(s)}$ where, separating real and imaginary components, one gets

$$\begin{aligned} a'' + (K + K_{RF})a - \frac{\xi}{a} - a\psi'^2 &= 0 \\ 2\psi'a' + a\psi'' &= 0 \end{aligned}$$

The second equation is solved by:

$$\begin{aligned} \psi' &= \frac{\varepsilon}{a^2} \\ a'' + (K + K_{RF})a - \frac{\xi}{a} - \frac{\varepsilon^2}{a^3} &= 0 \end{aligned}$$

Where ε emittance is a constant, a beam envelope.

$$x(s) = a(s) \cos \left(\int_{s_0}^s \frac{\varepsilon ds}{(a(s))^2} + \delta \right)$$

Solution in term of Floquet functions

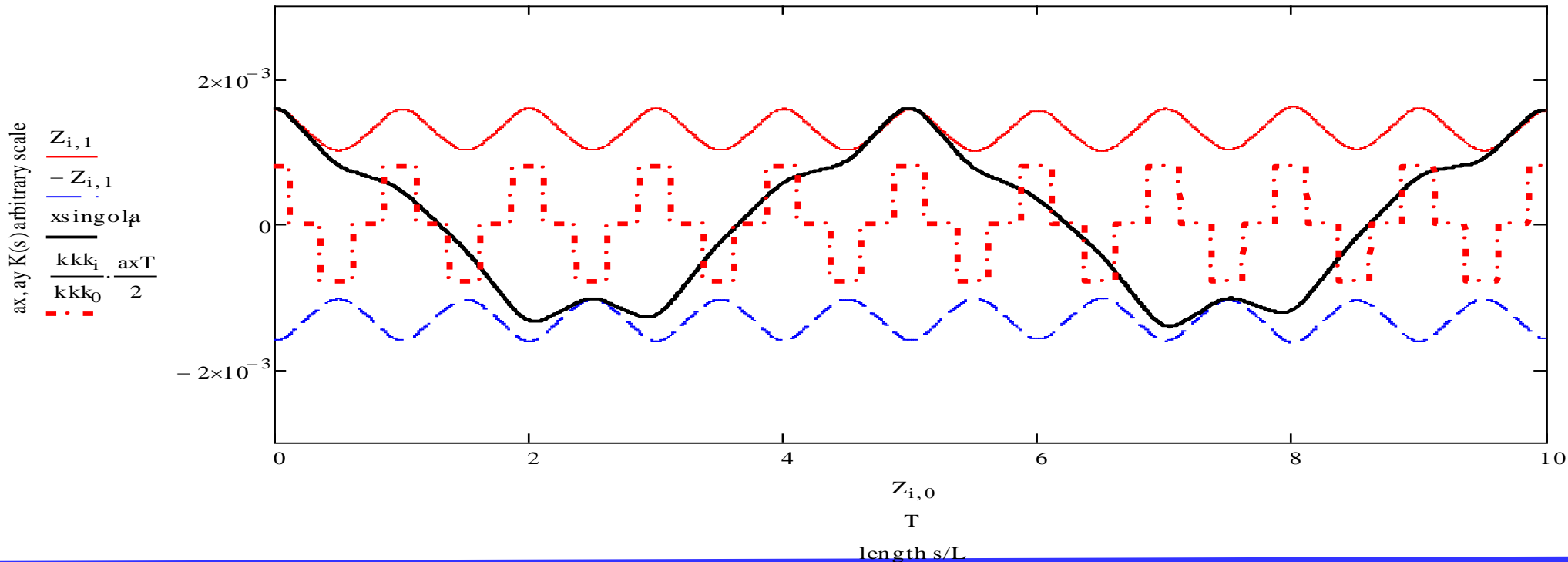
$$x(s) = a(s) \cos \left(\int_{s_0}^s \frac{\varepsilon ds}{(a(s))^2} + \delta \right)$$

$$\sigma_0 \cdot \frac{180}{\pi} = 54.61705$$

$$\mu \cdot \frac{180}{\pi} = 36.31235$$

$$\sqrt{2 \cdot (\sigma_0^2 + \mu^2)} \cdot \frac{180}{\pi} = 92.75354$$

$$\sqrt{\sigma_0^2 + 3 \cdot \mu^2} \cdot \frac{180}{\pi} = 83.29936$$



Laminar and low current limit

- The envelope equation can be written according to

$$a'' + Ka - \frac{\varepsilon^2}{a^3} \left[1 + \frac{\xi a^2}{\varepsilon^2} \right] = 0$$
$$a'' + Ka - \frac{\xi}{a} \left[1 + \frac{\varepsilon^2}{\xi a^2} \right] = 0$$

- With the two limit cases

$$\frac{\xi a^2}{\varepsilon^2} \ll 1$$
$$\frac{\xi a^2}{\varepsilon^2} \gg 1$$

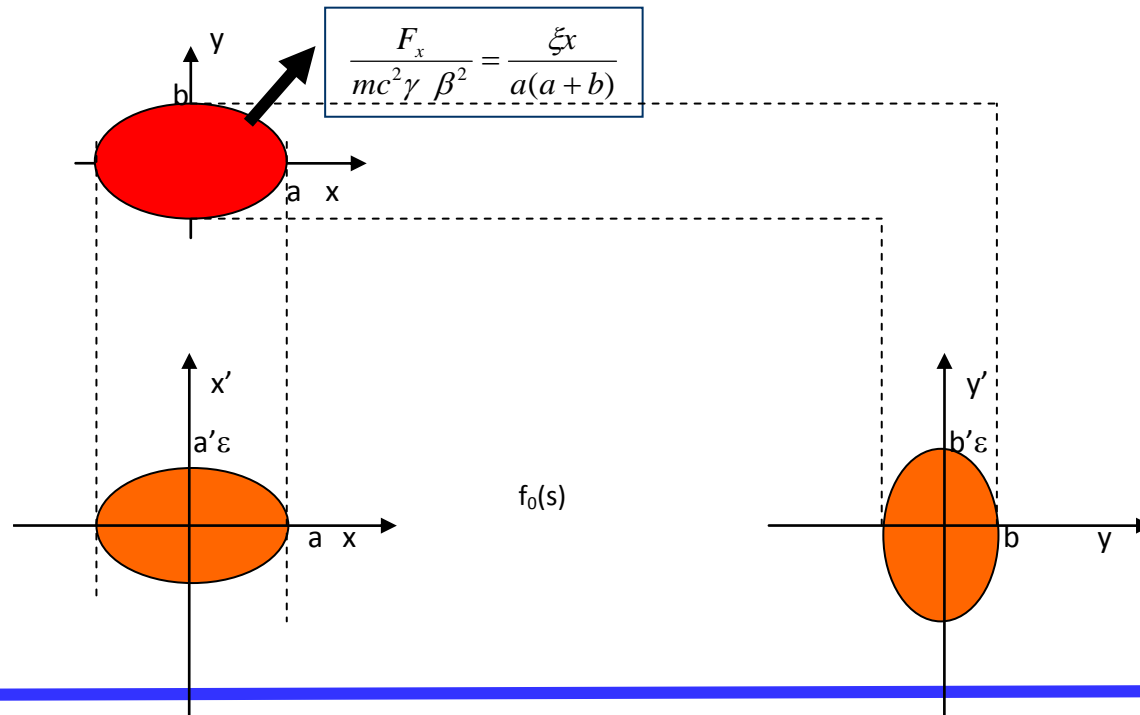
Negligible space charge

Negligible emittance (laminar flow)

- Large beam dimension corresponds to important space charge (not completely obvious).

K-V distribution

- It exists a distribution, the Kapchinskij Vladimirskij (KV), that gives a homogeneous charge density (in $x y$ space) and at the same time is defined on emittance ellipsoids (invariants in phase space).
- The behavior of more realistic distributions can be evaluated starting from KV (r.m.s characteristics).



Instabilities

- Given the periodic particle distribution in our accelerator

$$f_0(\vec{x}, \vec{p}, t + T) = f_0(\vec{x}, \vec{p}, t)$$

- $f(\vec{x}, \vec{p}, t) d^3x d^3p$ number of particles in the elementary volume
- Due to **external forces**+**e.m. fields generated by the beam**, for a small initial deviation from f_0 the distribution will evolve (linearly) according to:

$$f(\vec{x}, \vec{p}, t) = f_0(\vec{x}, \vec{p}) + f_1 e^{-i\Omega t}$$

- If Ω has a positive imaginary the beam is unstable,

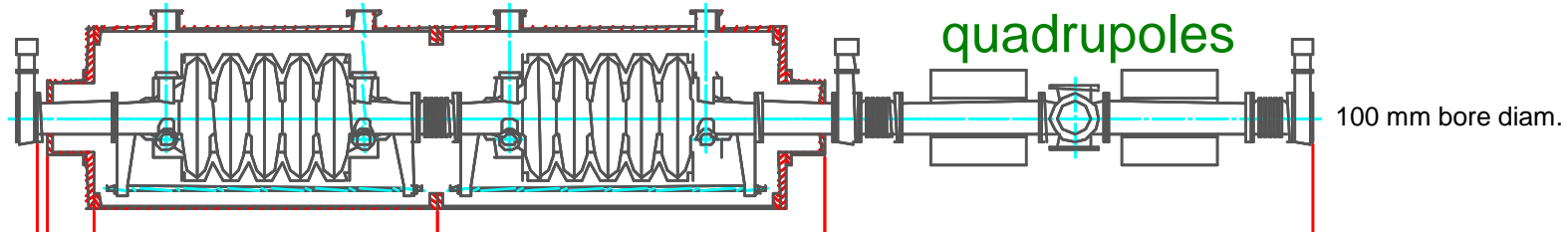
$$\tau = \frac{1}{\text{Im}\Omega} \geq 0$$

and τ is the instability **rise time**.

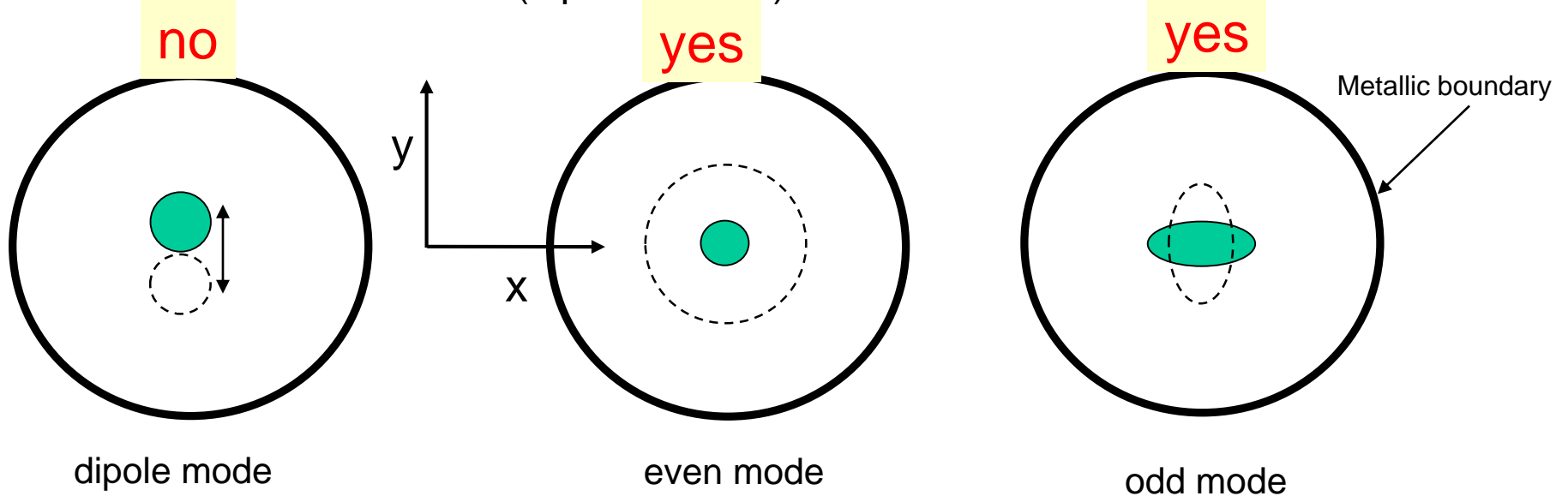
- **Threshold** is the minimum beam current that gives Ω complex.

Instabilities in p-linacs

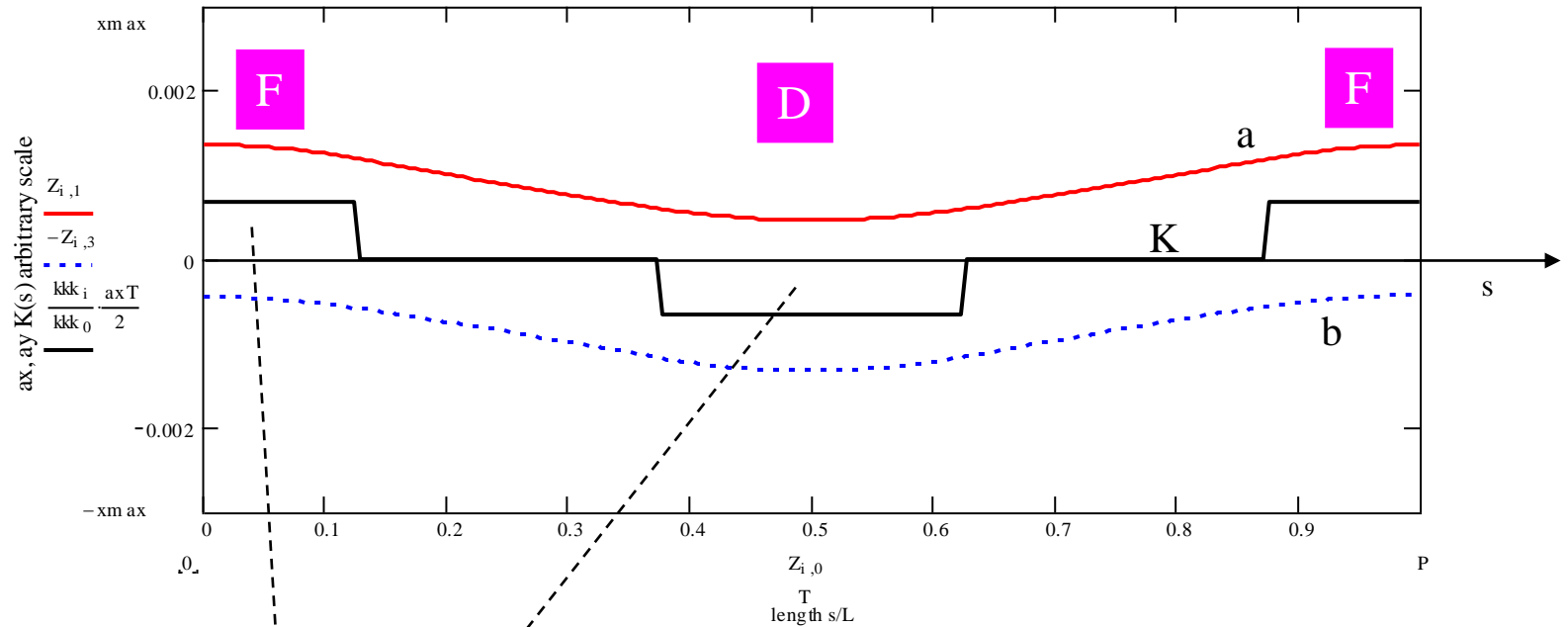
- Large beam hole, low frequency (.3-.8 GHz), low γ .



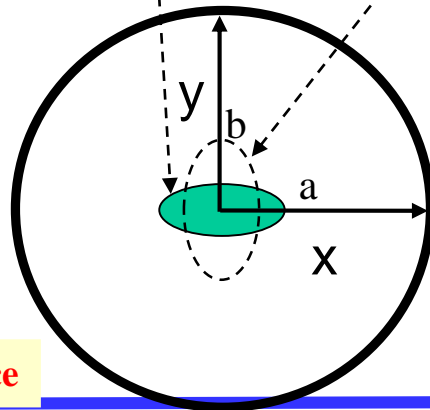
- Beam generated fields do not know the center of the structure and can not excite the motion of the beam cm (dipole modes).



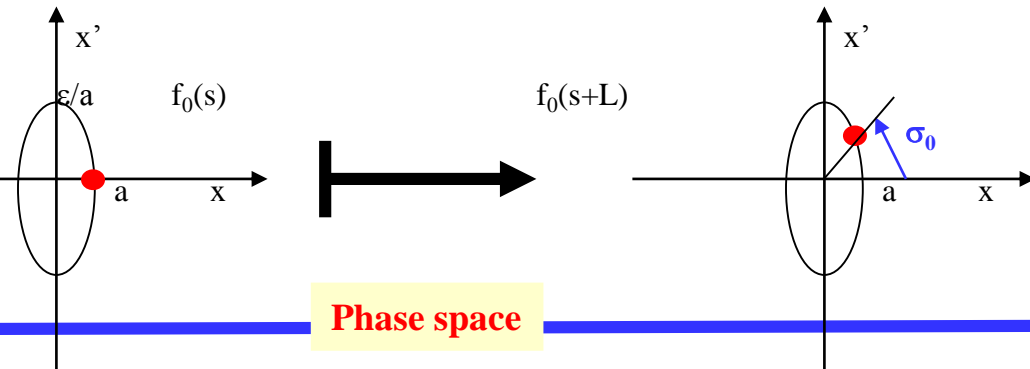
FODO cell



a and b periodic (matched) envelopes



Real space



Phase space

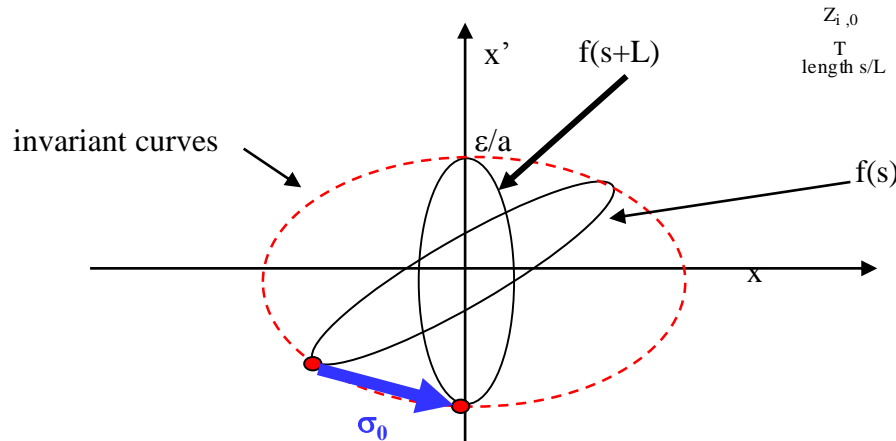
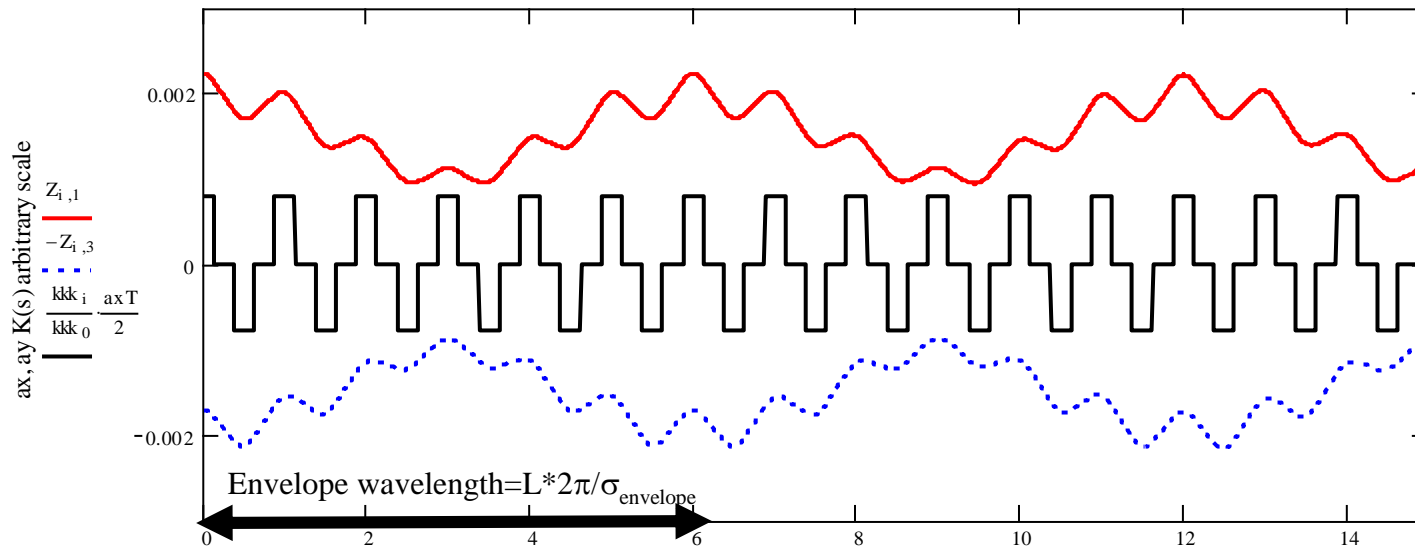
Envelope oscillations: low current

$$\sigma_0 \cdot \frac{180}{\pi} = 29.85764$$

$$\mu \cdot \frac{180}{\pi} = 29.85764$$

$$\sqrt{2 \cdot (\sigma_0^2 + \mu^2)} \cdot \frac{180}{\pi} = 59.71528$$

$$\sqrt{\sigma_0^2 + 3 \cdot \mu^2} \cdot \frac{180}{\pi} = 59.71528$$



- Vertical and horizontal motion are decoupled.

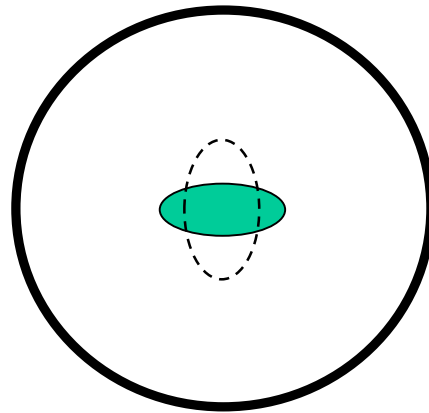
- The envelope phase advance is $2\sigma_0$, since after half turn of the red point the particle distribution is identical.

$$\sigma_0 \cdot \frac{180}{\pi} = 29.85764 \quad \mu \cdot \frac{180}{\pi} = 14.72113 \quad \sqrt{2(\sigma_0^2 + \mu^2)} \cdot \frac{180}{\pi} = 47.07845 \quad \sqrt{\sigma_0^2 + 3\mu^2} \cdot \frac{180}{\pi} = 39.26339$$

Envelope modes with space charge

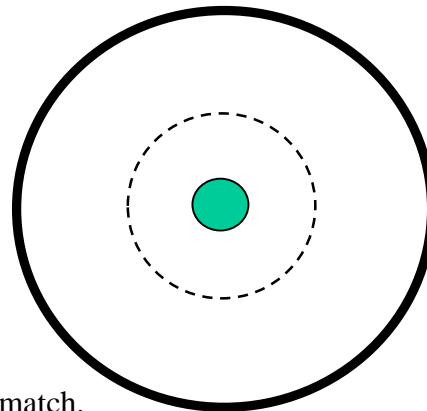
$$\sigma_{odd} = \sqrt{3\sigma^2 + \sigma_0^2}$$

odd mode

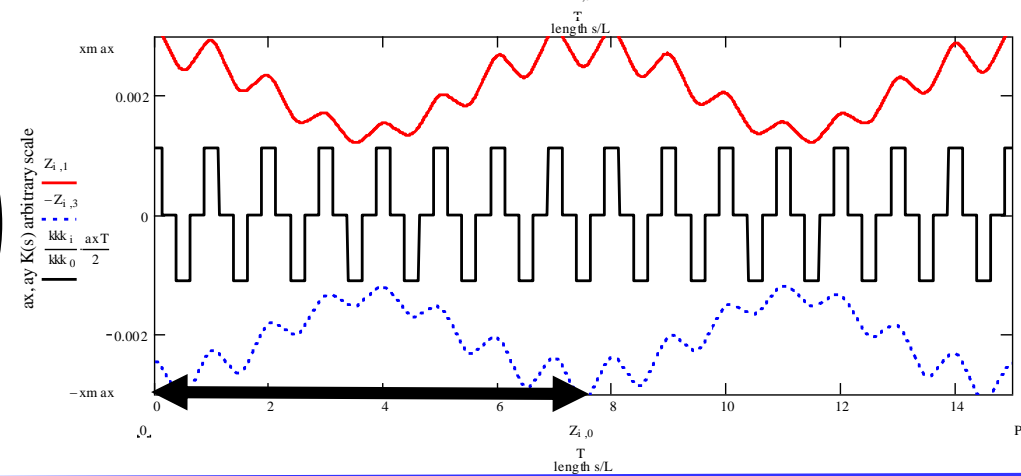
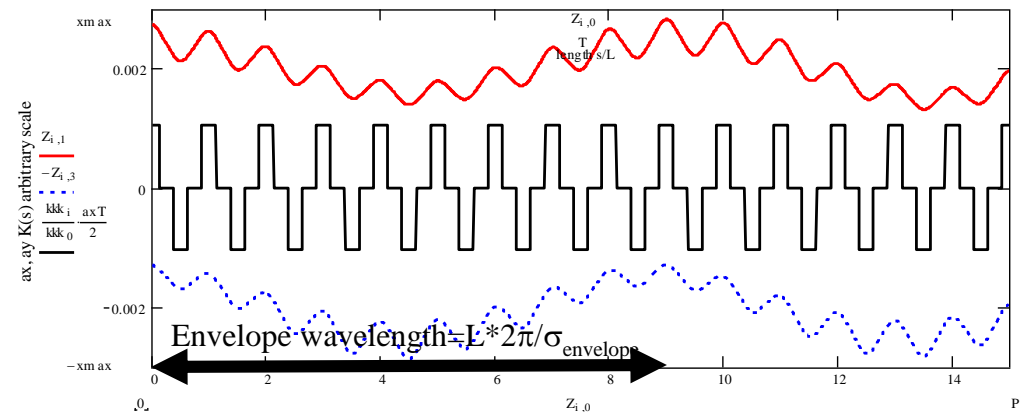
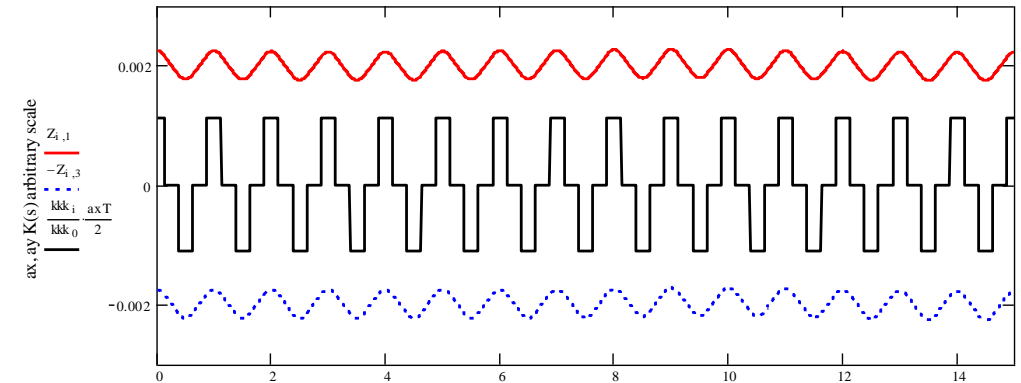


$$\sigma_{even} = \sqrt{2(\sigma^2 + \sigma_0^2)}$$

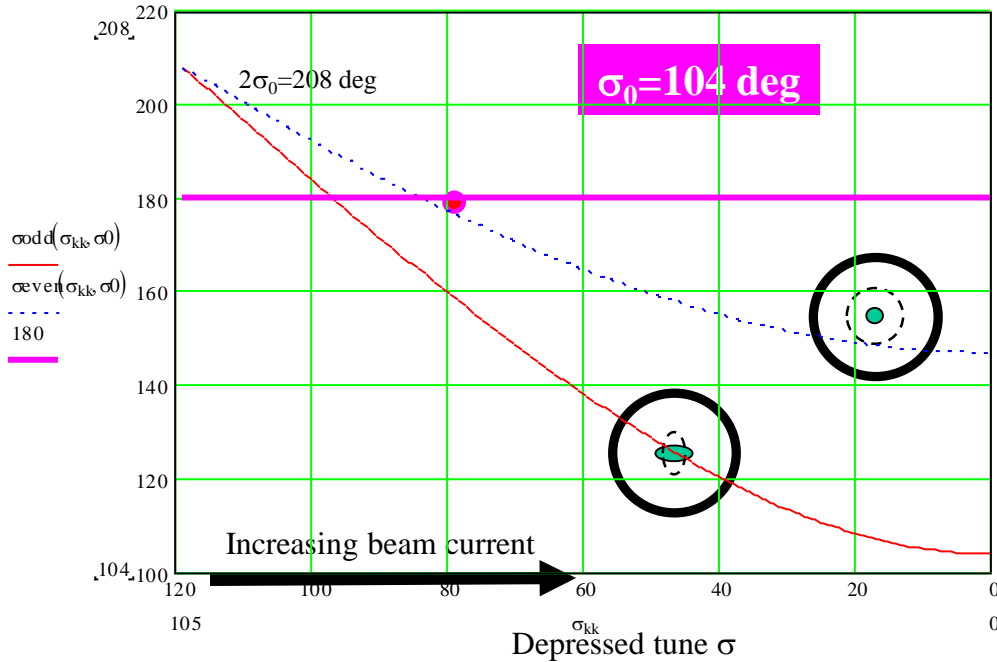
even mode



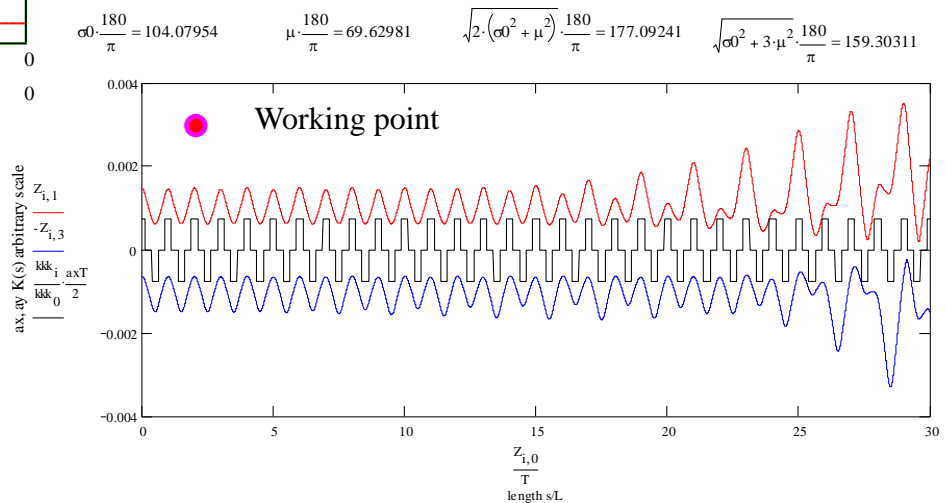
In both cases we start with 40% mismatch.



Envelope instability



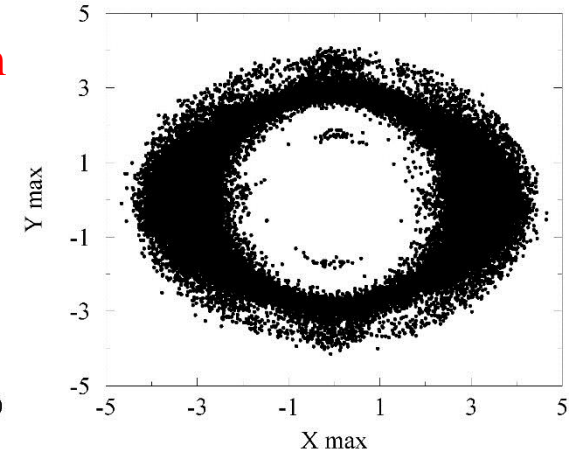
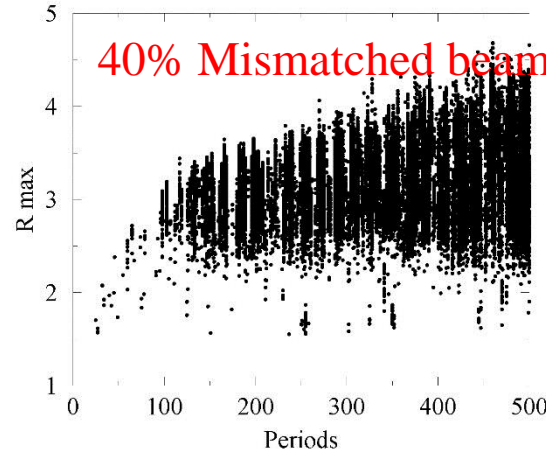
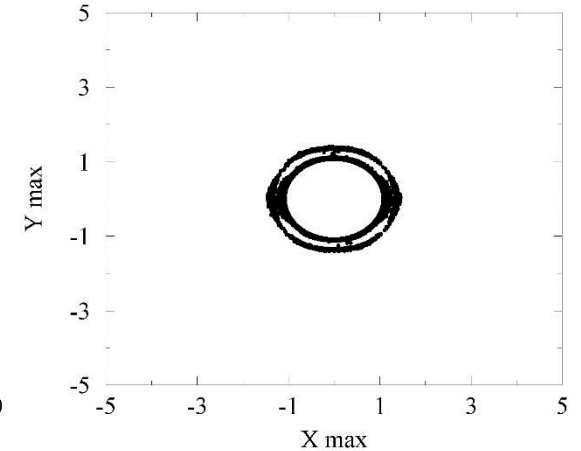
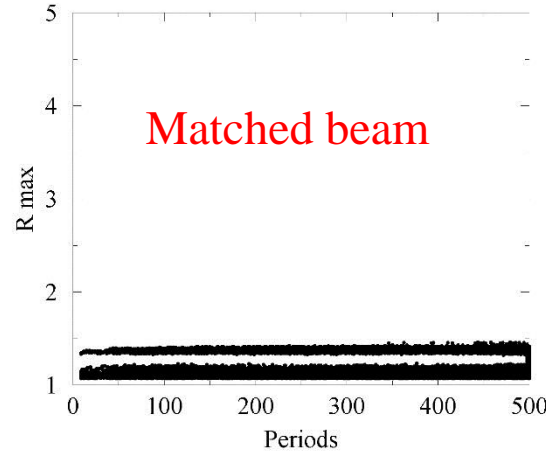
- When $\sigma_{\text{envelope}} = 180^\circ$ a half integer resonance is crossed and the solution becomes exponential (Instability!)



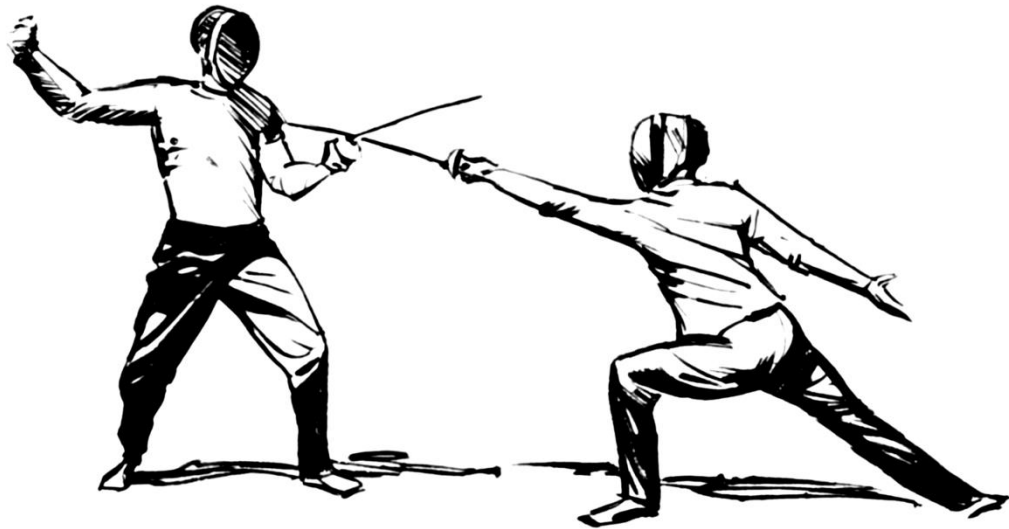
The residual mismatch due to numerical errors is enough to make the instability evident.

Single particle effects: beam halo

- New high intensity proton linacs require an extremely good control of beam losses.
- Typically the required 1 W/m of beam losses means $10^{-7}/\text{m}$ for 1 GeV 10 mA
- In computer simulations one can see a cloud of few particles around the beam core (**beam halo**) when the beam is mismatched

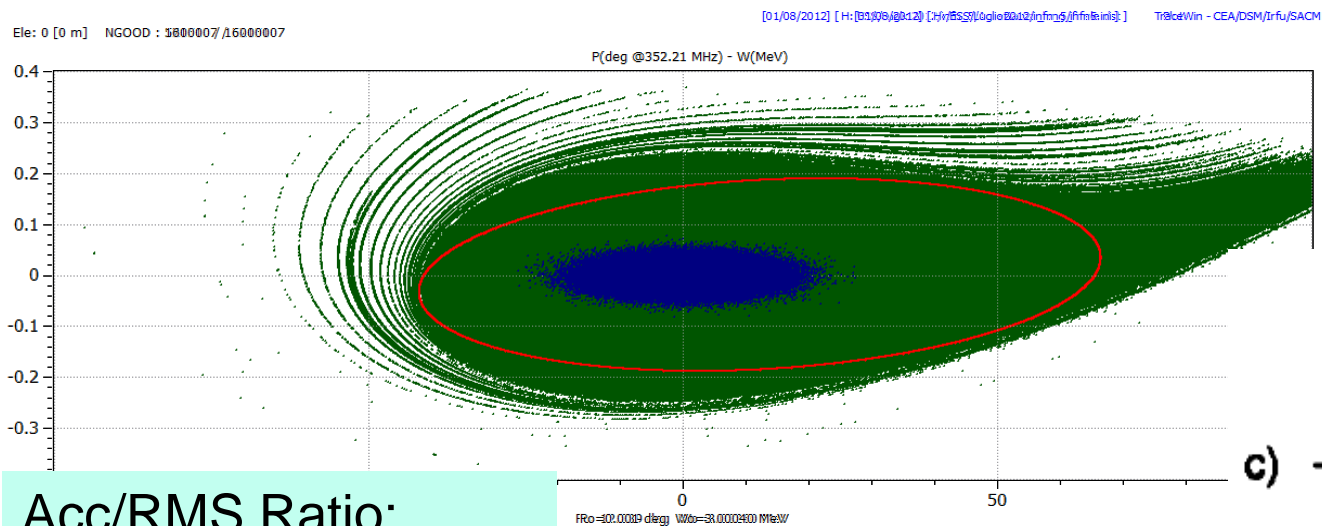


From academy to competition

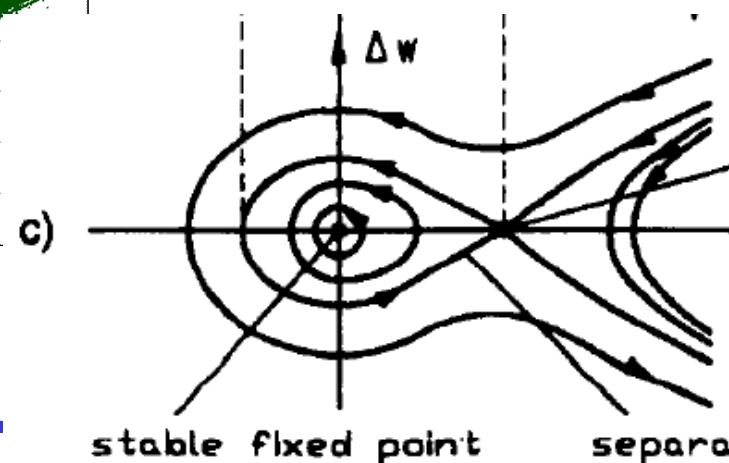


- The acceptance in a linac (ESS Drift tube linac, 3-78 MeV 50 mA) has not the shape of the hamiltonian separatrix but is the so called golf club.
- This is due to the fact that the adiabatic invariant are indeed varying relatively fast respect to the typical time of the system, the longitudinal oscillation period.
- In practice theory gives guide lines, but design is benchmarked on computer simulations

Max Longitudinal acceptance=10 degMeV



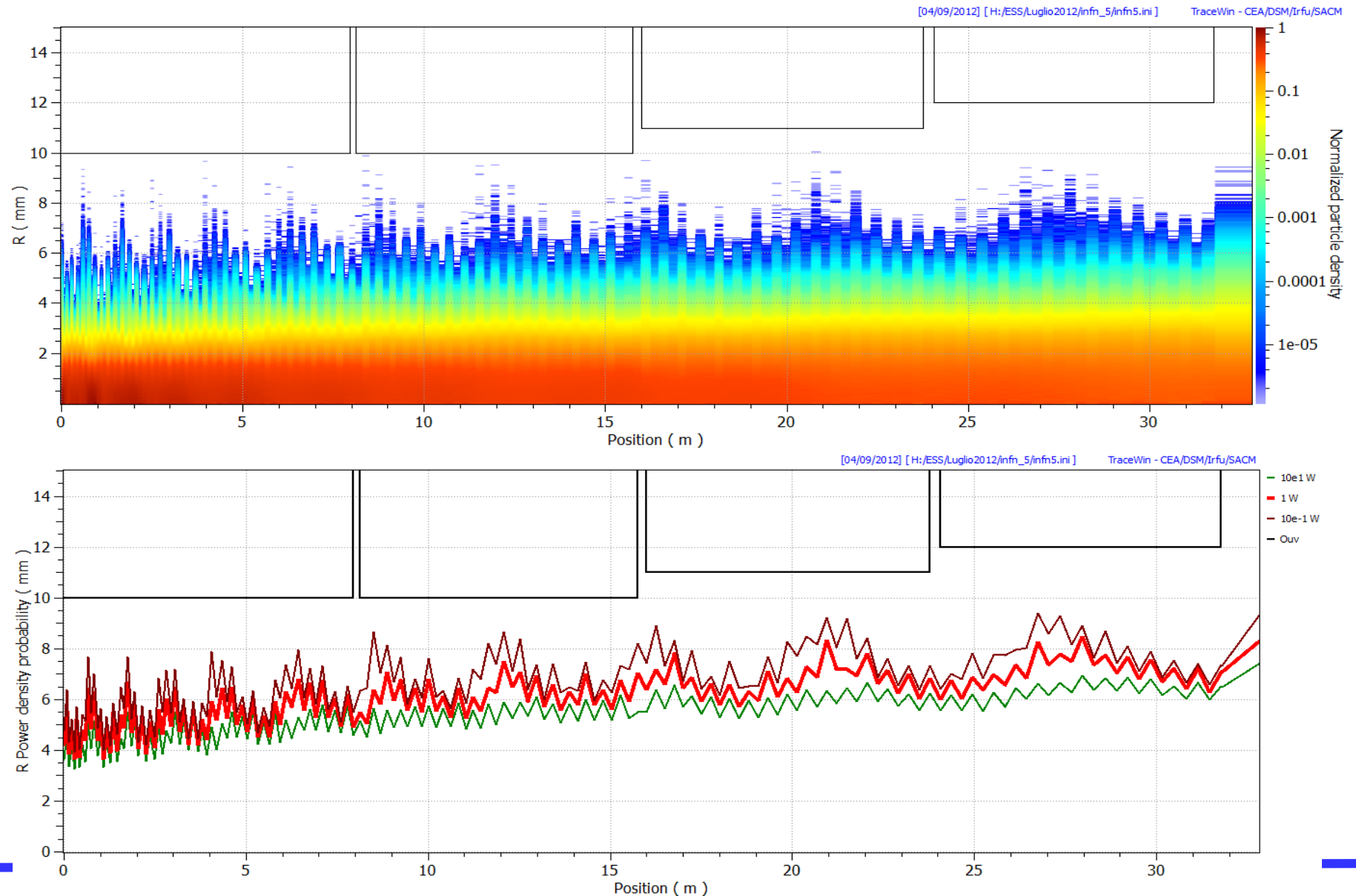
Acc/RMS Ratio:
Longitudinal=91



Computer codes

- Modern computer codes can give a good description of the accelerator, with use of field mapping in RF cavities and magnetic lenses, space charge, image fields.
- The 10^6 macro particle level can be reached (i.e. W losses for a MW beam) and is significative for radiation protection estimation (prompt radiation and activation).
- Algorithms are available for systematic simulation of construction errors.
- Design codes are available to optimize structures and apply design principles.

Beam Density with Input distribution Gaussian 6σ



Mode coupling

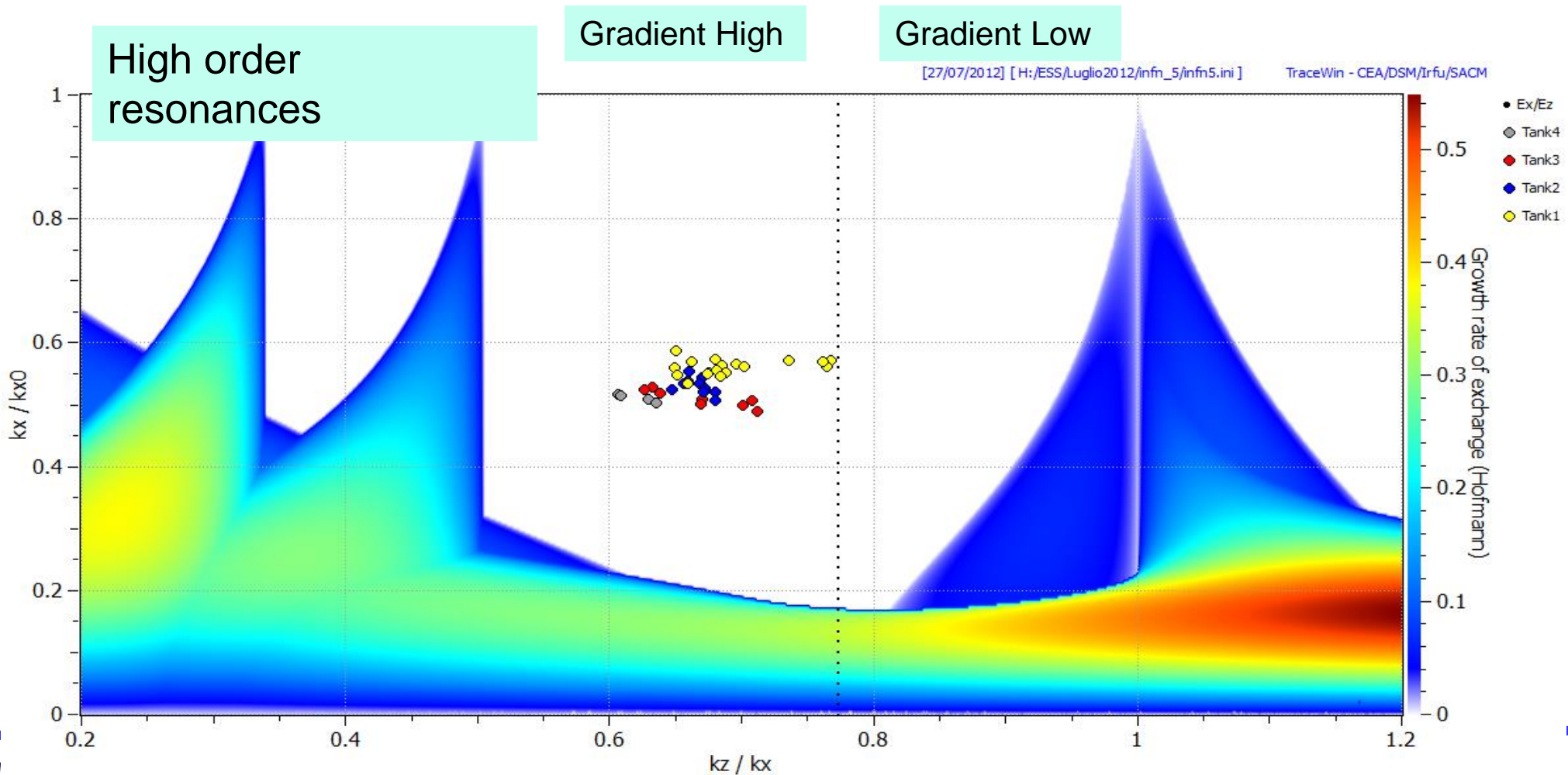
- Small losses and emittance degradations are related to very basic issues that we try to tackle in the design.
- Particles can reach large amplitude due to resonances and mode coupling.
 - Respect to a synchrotron the lattice is smoother (σ_{ot} low), so structural resonances with envelope modulation are unimportant
 - betatron (x,y) and synchrotron (z) oscillation are similar, so coupling is possible
 - In case of space charge, the envelope oscillation due to mismatch couples to the single particle oscillation

$$x'' + \left[K(s) + K_{RF} - \frac{\xi}{a^2} \right] x = 0$$

$$K_{RF} = \pi \frac{eE_a \sin \phi}{\beta^3 \gamma^3 mc^2 \lambda} \approx \pi \frac{eE_a}{\beta^3 \gamma^3 mc^2 \lambda} \sin \left[\phi_0 + A \cos \left(\frac{\sigma_z s}{L} \right) \right]$$

$$a = a_0 + A \cos \left(\frac{\sigma_{envelope} s}{L} \right)$$

Equipartitioning all along the DTL



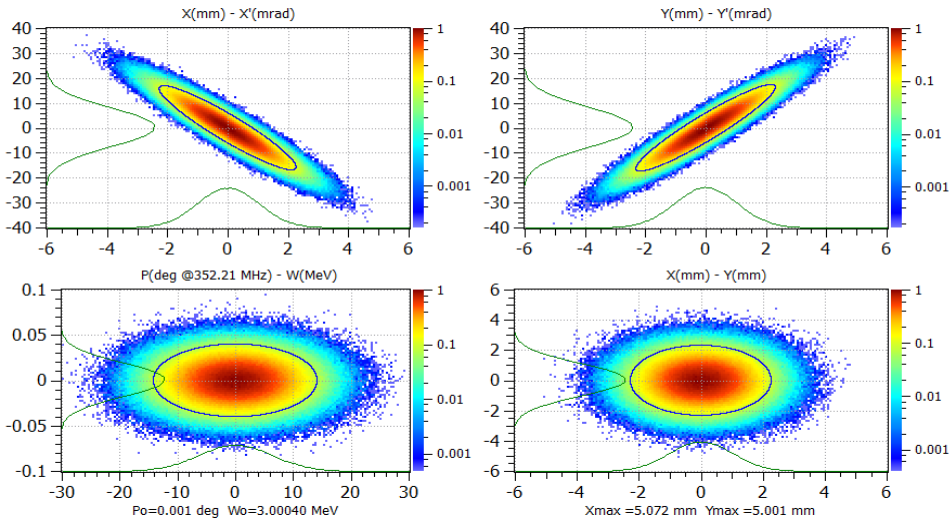
Example of error study on the DTL

- All errors apply together with a Uniform input beam distribution with added a “halo” distribution with 3times the emittance and 3σ as gaussian size distribution, 0.625% of the beam as halo, i.e. 1kW.
- 100 random DTL generated.
- $1.6 \cdot 10^5$ particles i.e. 1 W for particle at 50 mA, 80 MeV.

Gaussian 6 σ

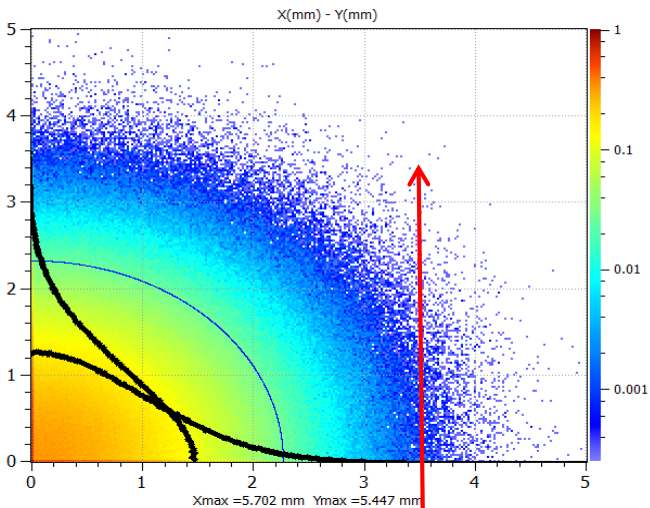
Ele: 0 [0 m] NGOOD : 1600000 / 1600000

[04/09/2012] [H:/ESS/Luglio2012/inf5_5/inf5.ini] TraceWin - CEA/DSM/Irfu/SACM



[04/09/2012] [H:/ESS/Luglio2012/inf5_5/inf5.ini] TraceWin - CEA/DSM/Irfu/SACM

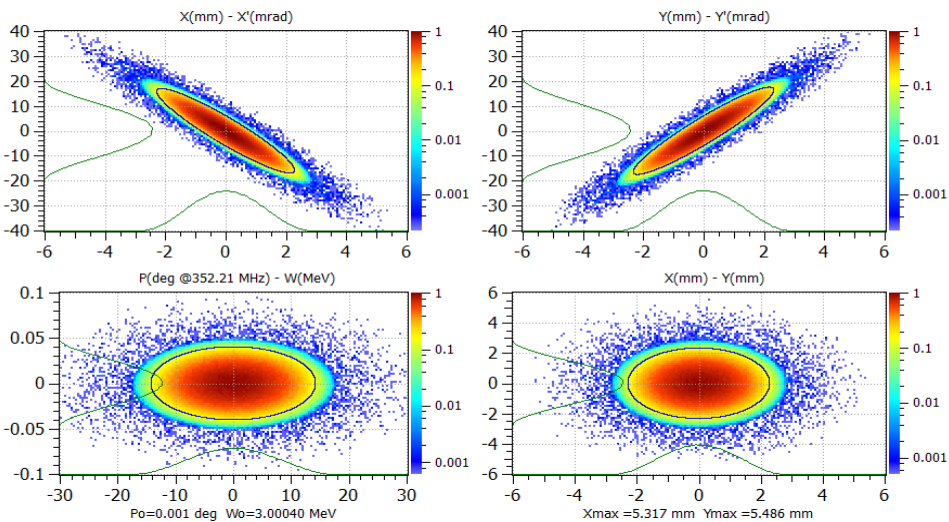
Ele: 0 [0 m] NGOOD : 16000000 / 16000000



Uniform+Halo

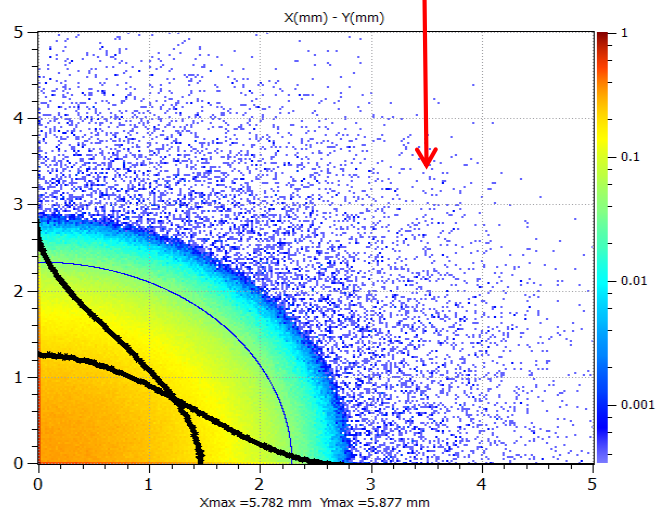
Ele: 0 [0 m] NGOOD : 1600000 / 1600000

[04/09/2012] [H:/ESS/Luglio2012/inf5_5/inf5.ini] TraceWin - CEA/DSM/Irfu/SACM

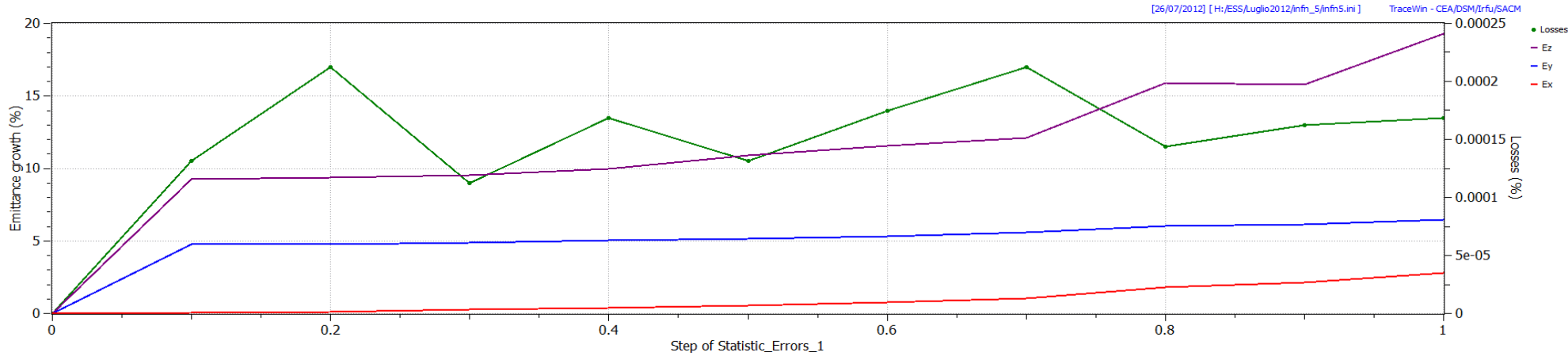


[04/09/2012] [H:/ESS/Luglio2012/inf5_5/inf5.ini] TraceWin - CEA/DSM/Irfu/SACM

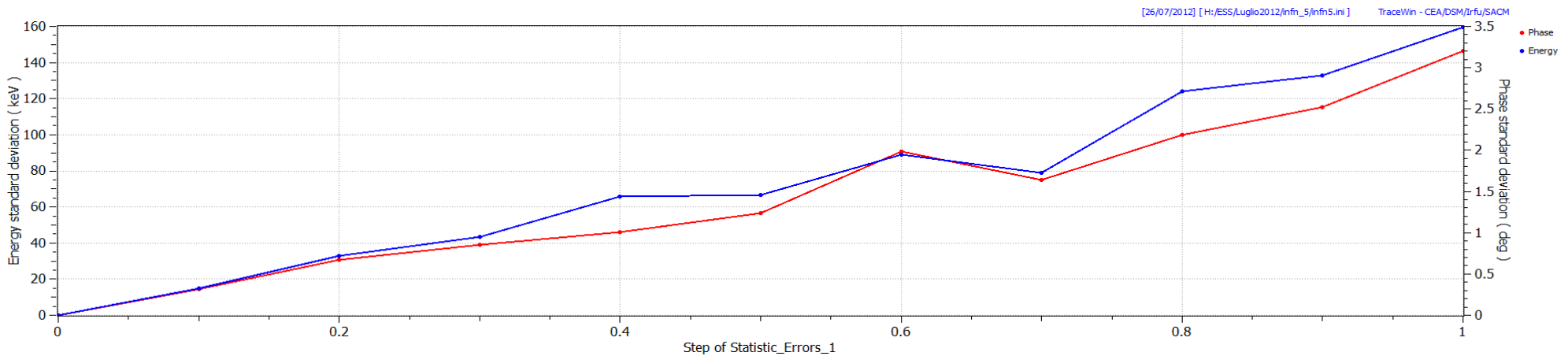
Ele: 0 [0 m] NGOOD : 16000000 / 16000000



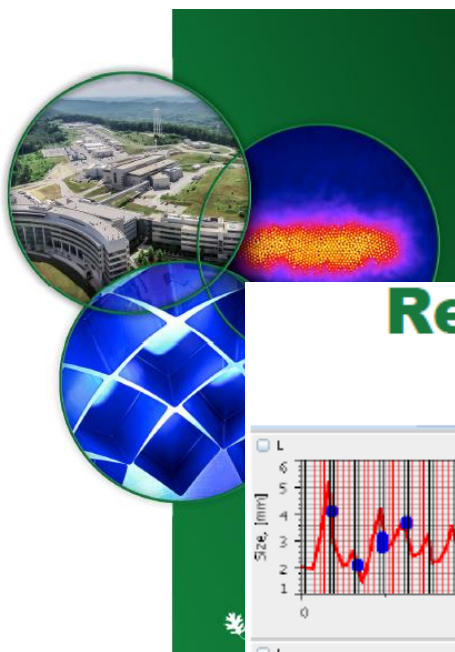
Errors results on ϕ s without correction Steerers



Step 1 \equiv Maximum ϕ s shake cell by cell of $\pm 5^\circ$



Fifteen Year Perspective on the Design and Performance of the SNS Accelerator

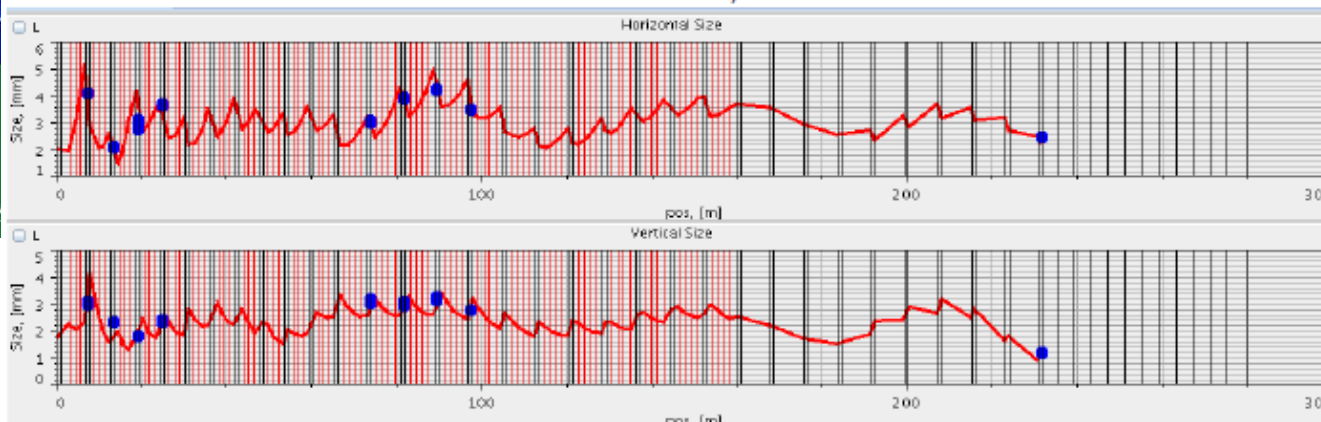


S. Cousineau
 (On behalf of the SNS project)
 HB2016, Sweden
 July 04, 2016

SNS is managed by UT-Battelle
 for the US Department of Energy

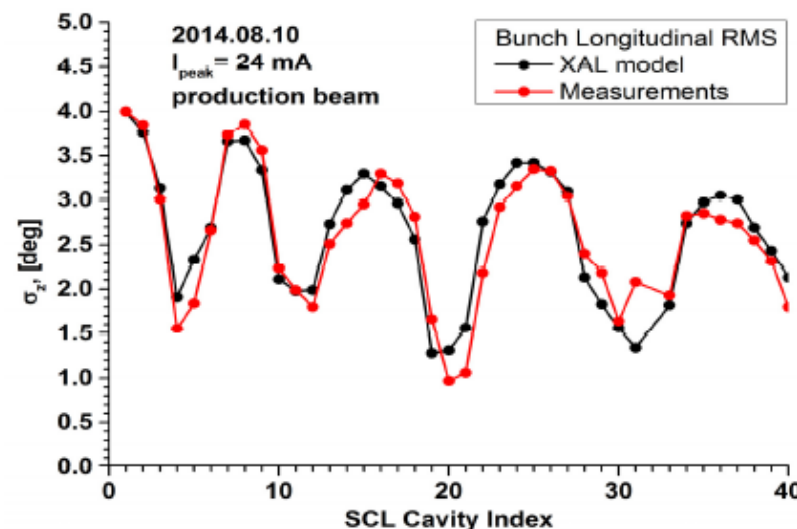
Reality: No Matching in the Linac

Transverse Beam Size SCL, fit to measured RMS

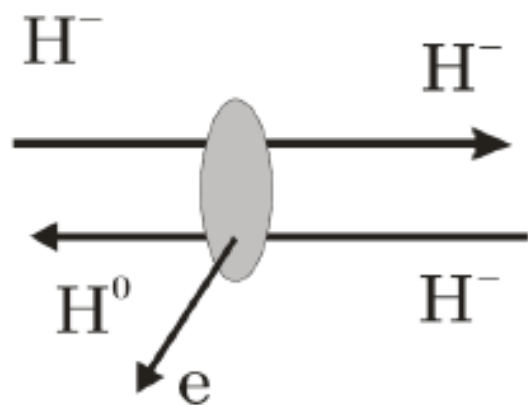


- Beam is mismatched, transverse and long., throughout entire linac.
- After multi-year effort, model now agrees with measurement for RMS

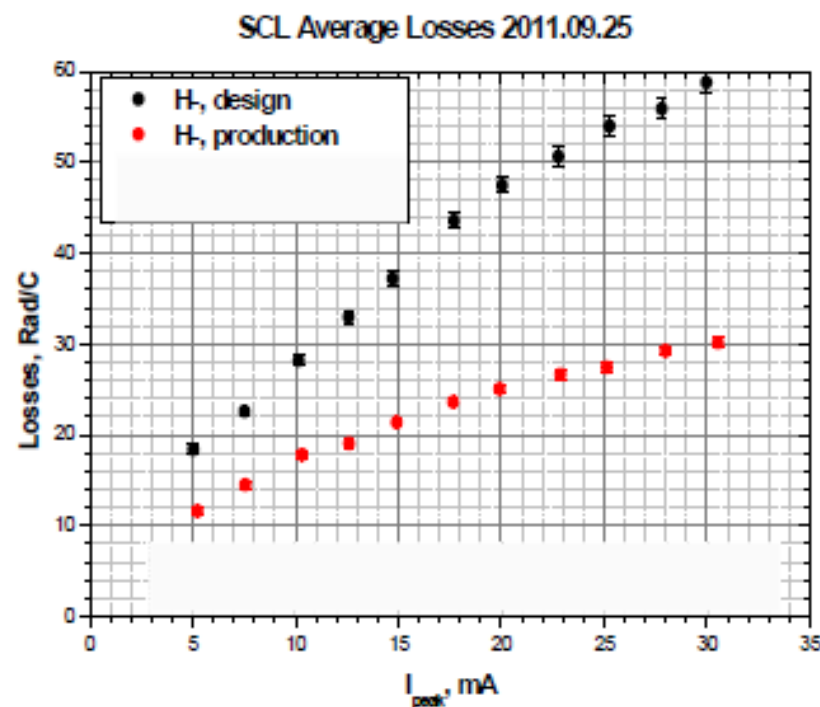
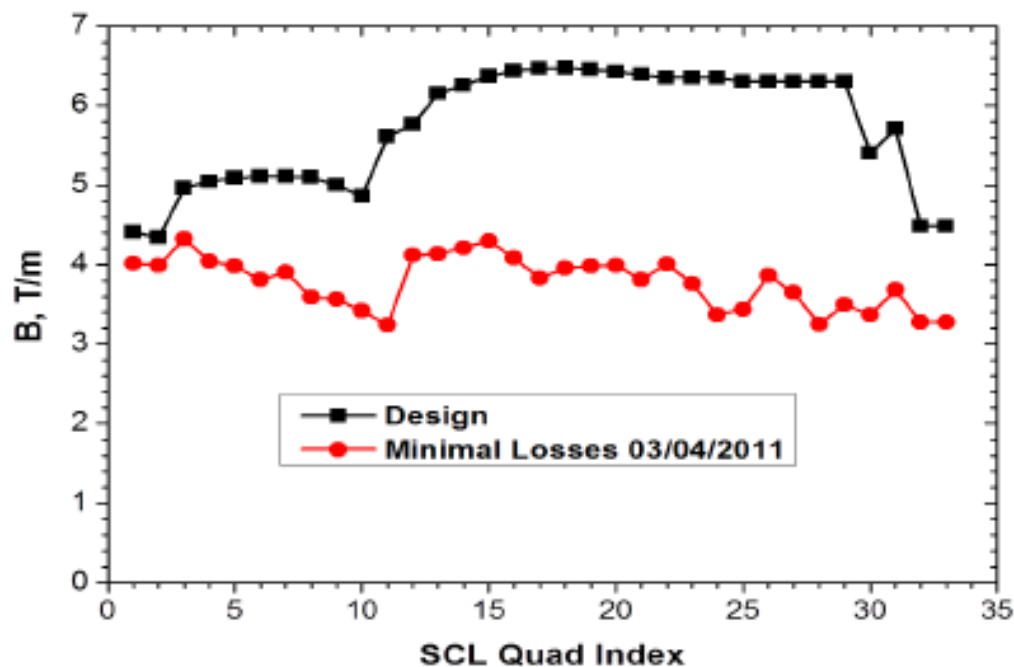
See Shishlo WEPM2Y1



Reality: Impact of H⁻ Intrabeam Stripping



- Saw much more beam loss than expected.
- Factor ~2 decrease in quad strength reduced losses significantly.
- Later realized (and confirmed) H⁻ intrabeam stripping.

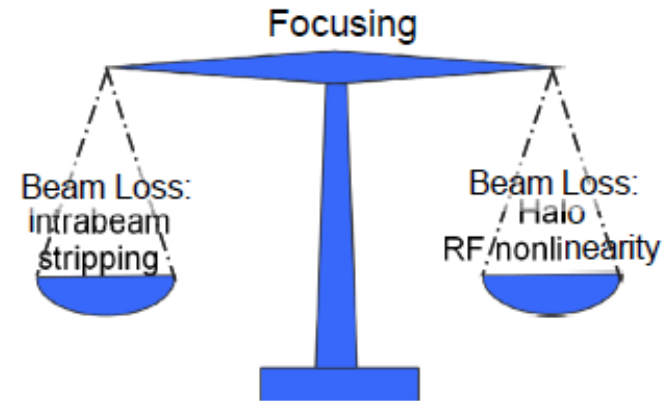


Understanding Our Linac Beam Loss

More quad defocusing increases beam loss – we have reach the limit.

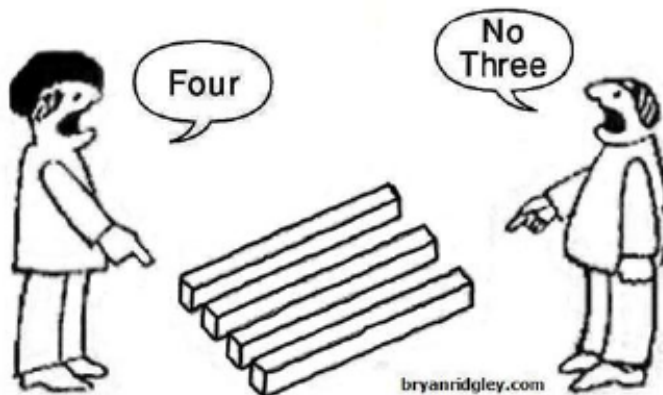
Presently, $\frac{\text{RMS Beam Size}}{\text{SCL Bore}} \approx 10$

We don't understand the remaining beam loss.
Probably 'halo', but from what? How much?



Many ideas of what defines “halo”:

Reality can be so complex that equally valid observations from differing perspectives can appear to be contradictory.



- At SNS we are going to define halo as **$10^{-4} - 10^{-6}$ of peak density** (per 2014 Workshop on Beam Halo Monitoring).
- Some SNS diagnostics can measure this level. (See Aleksandrov -THAM5Y01)
- Models are now ready to attack this problem (see Shishlo WEP2Y1)

Conclusions

- The basic principles of linear accelerators have been synthetically reviewed. They are
 - RF acceleration, necessary to overcome the basic limitation of the possible electrostatic tension.
 - Alternating gradient, necessary because of the proprieties of our basic lens, the magnetic quadrupole.
 - Phase stability, necessary because of the RF acceleration, can be described with a nice integrable system
- But real world is more complicated, x, y, z are coupled by RF field, errors and space charge, and to transport a beam is almost always an adventure.
- Sometimes unforeseen phenomena like intrabeam stripping occurs
- The design and optimization of an effective RF accelerator (with resonable capital cost, RF consumption, reliable and resistent against construction errors...) is a very interesting and intellectually rewarding activity

A European research center for the world



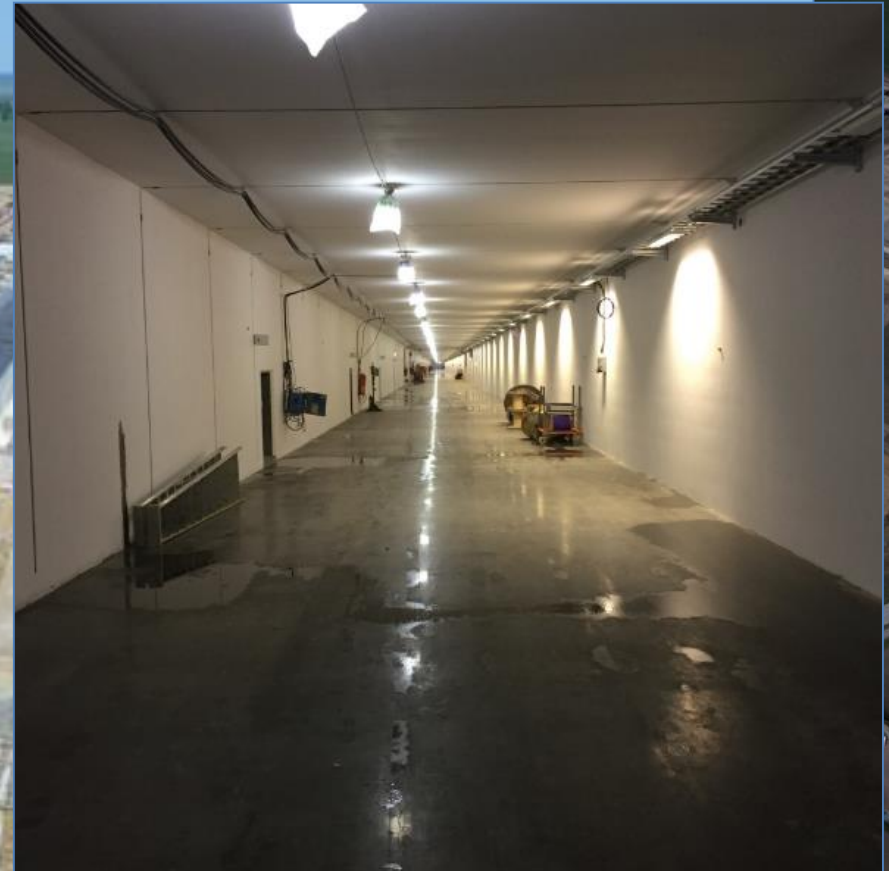
**SCIENCE
VILLAGE**
SCANDINAVIA

MAX IV

MEDICIN
VILLAGE

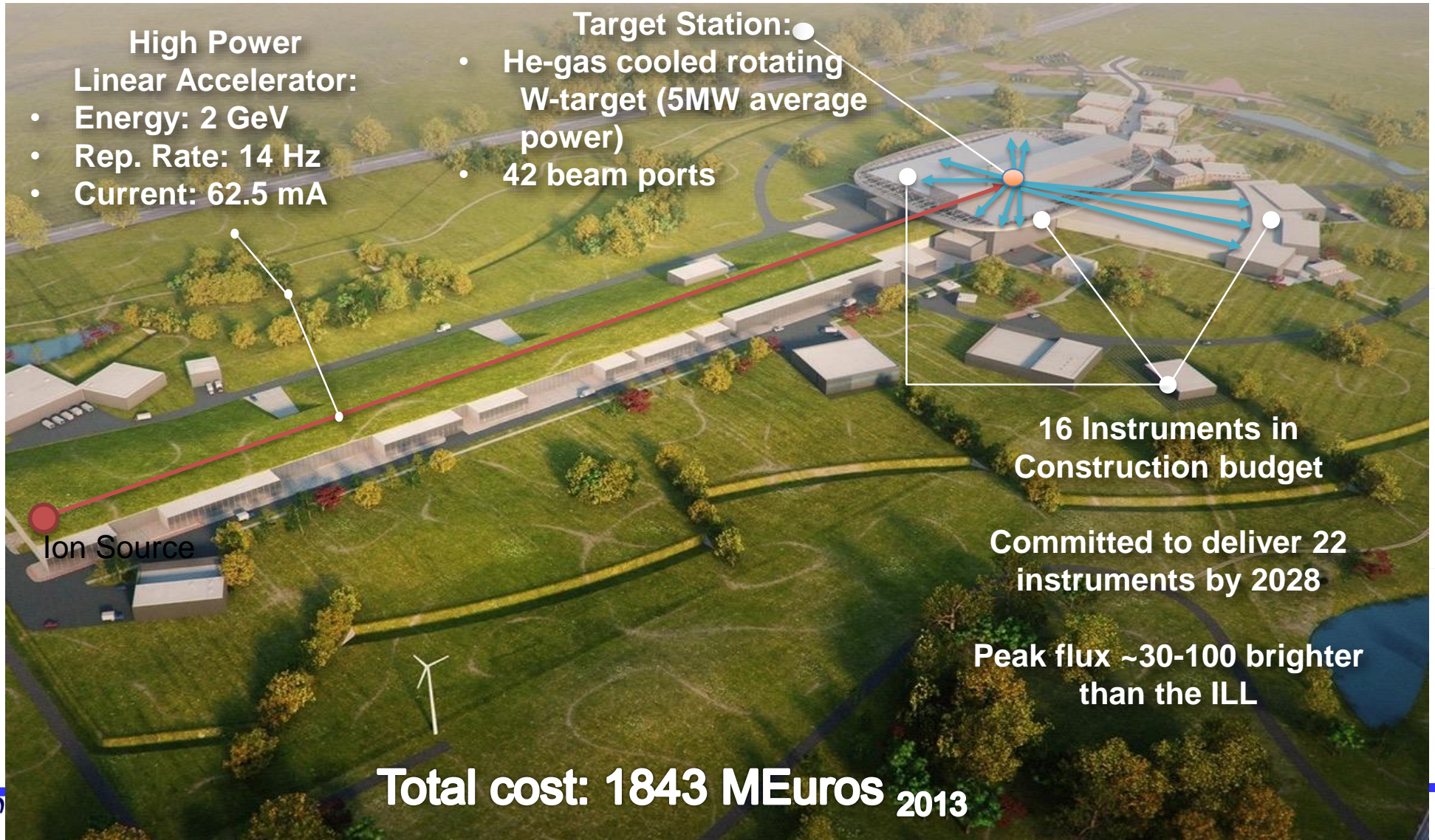
ess
EUROPEAN
SPALLATION
SOURCE

Progress on civil construction

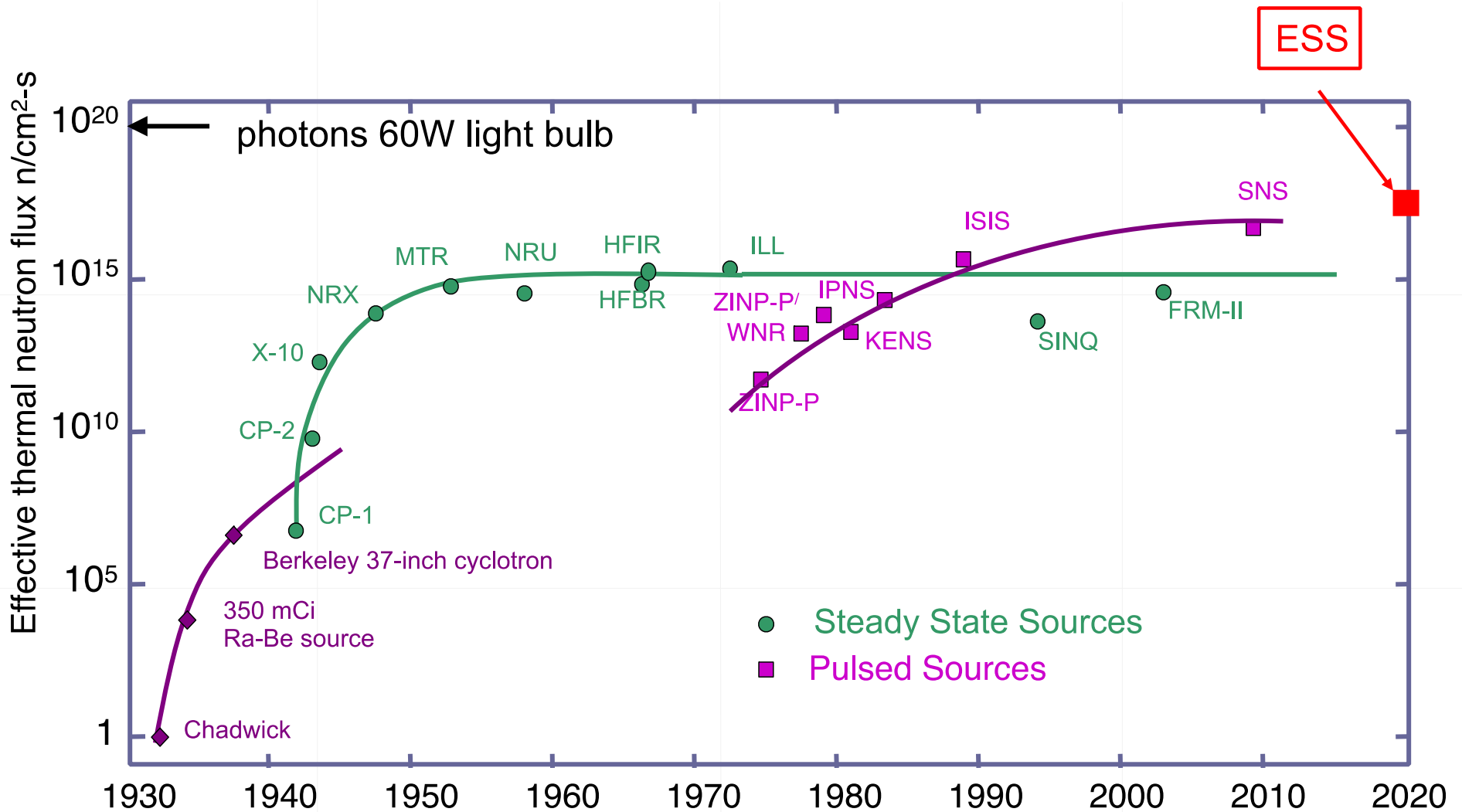


27 April 2016

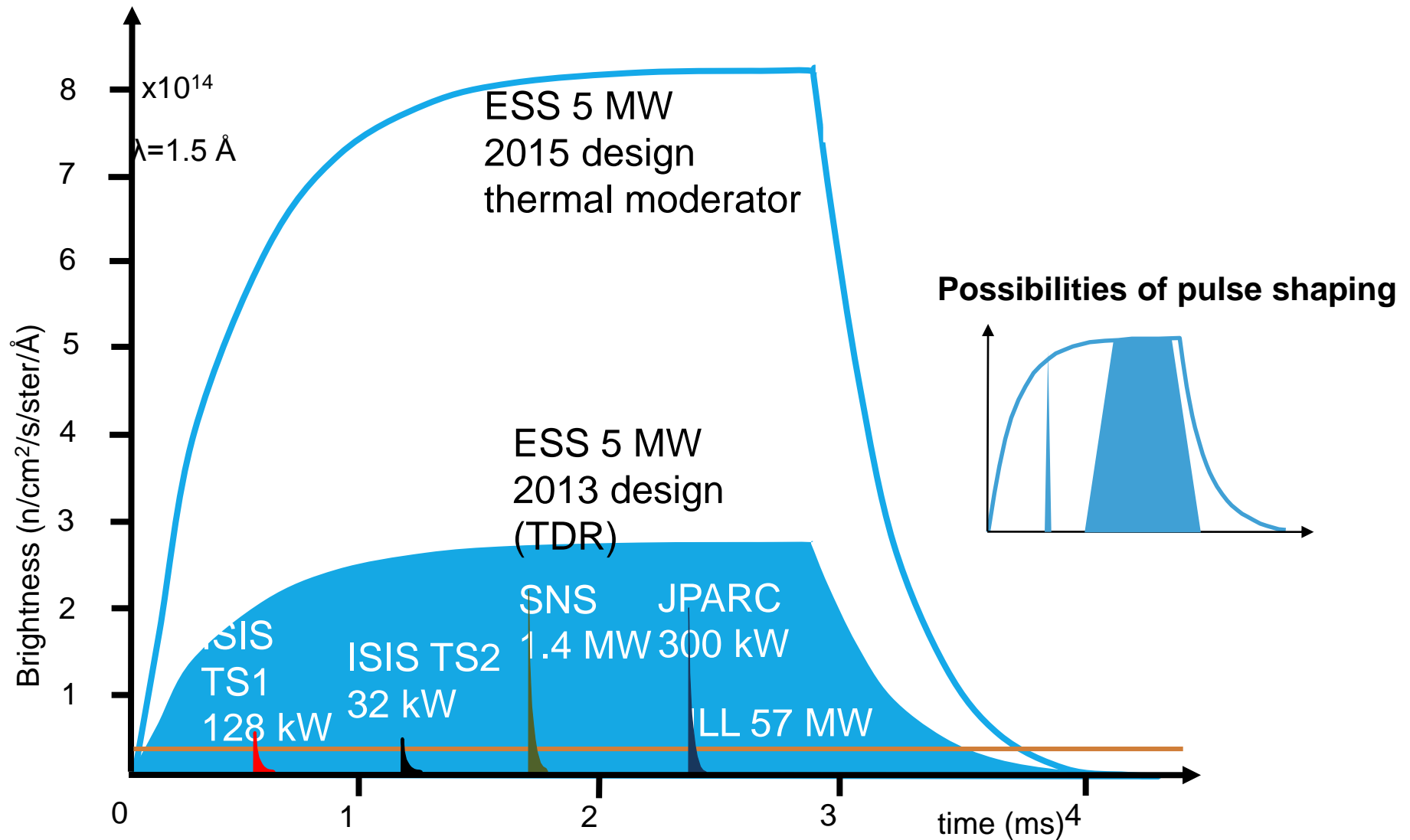
ESS design



Evolution of neutron sources



ESS long pulse potential (not in scale)



Accelerator Technical performances

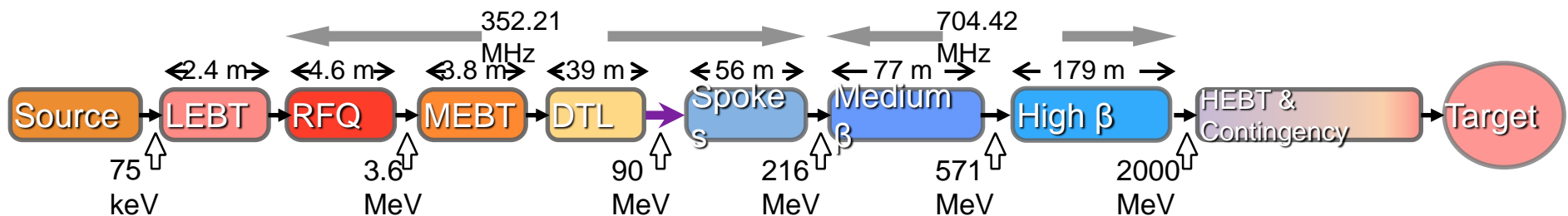
Design Drivers:

High Average Beam Power
5 MW
High Peak Beam Power
125 MW
High Availability
> 95%

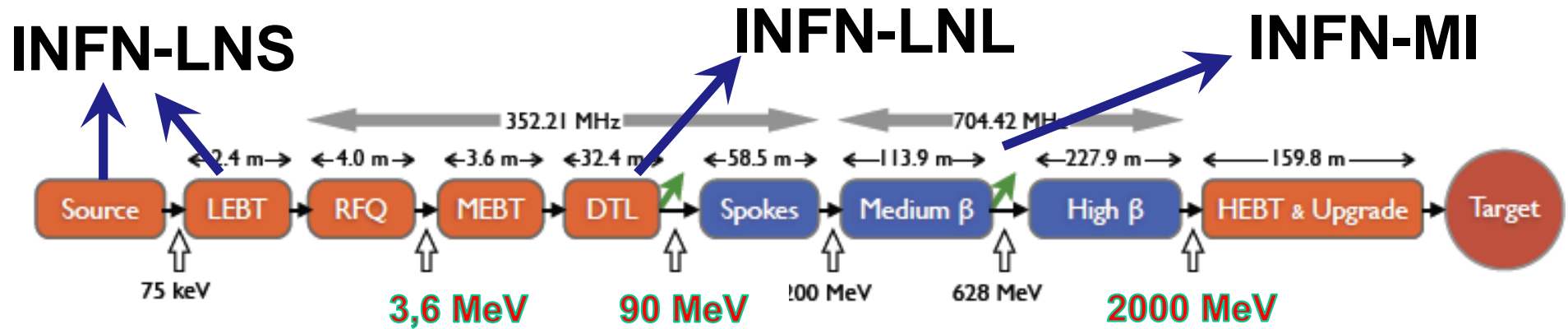


Key parameters:

- 2.86 ms pulses
- 2 GeV
- 62.5 mA peak
- 14 Hz
- Protons (H⁺)
- Low losses
- Minimize energy use
- Flexible design for mitigation and future upgrades



INFN contribution to the European Spallation Source



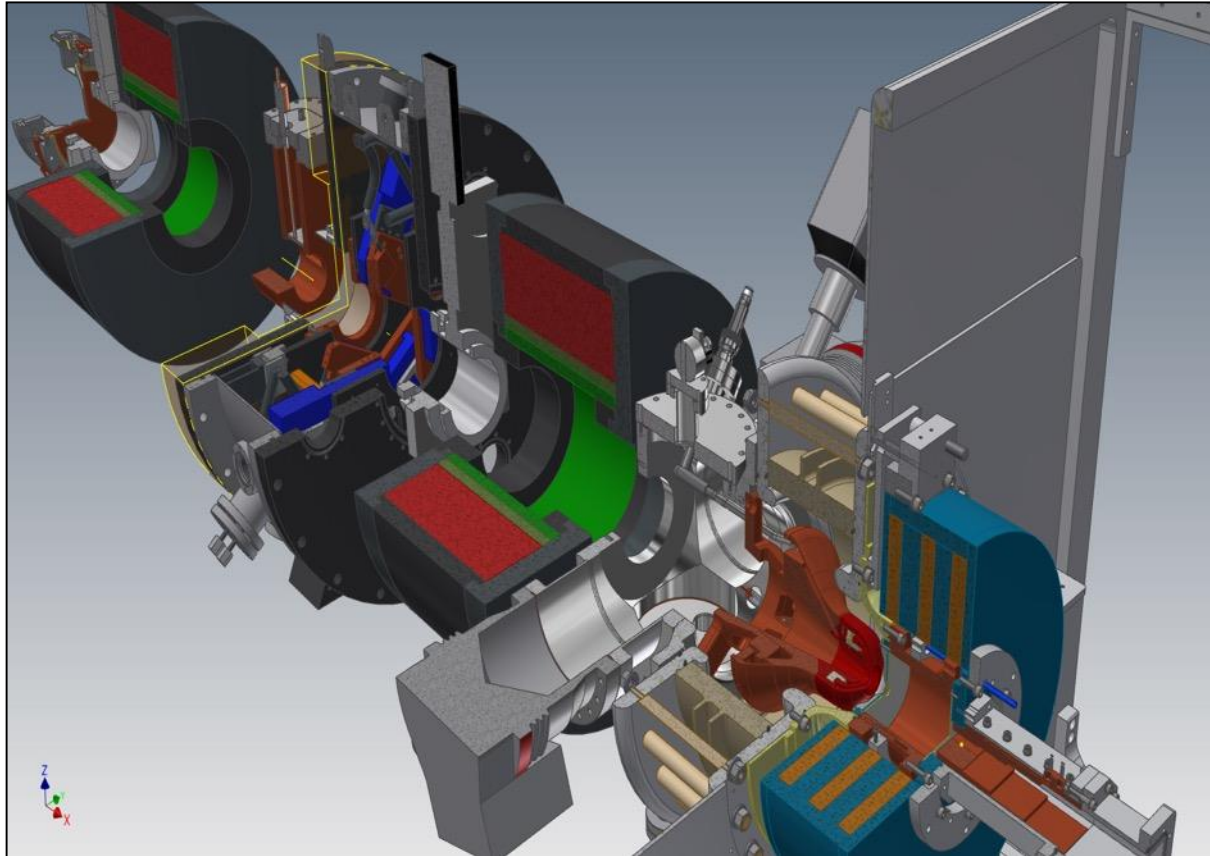
INFN is in charge of the management of the WP3-Normal Conducting Linac

1. **Ion Source & LEBT** (INFN-Laboratori Nazionali del Sud, Italy),
2. **RFQ** (CEA-IRFU, France),
3. **MEBT** (ESS Bilbao, Spain)
4. **Drift Tube Linac with some diagnostics** (INFN-Laboratori Nazionali di Legnaro, Italy)

Other INFN groups are involved in the in-kind contribution to ESS:

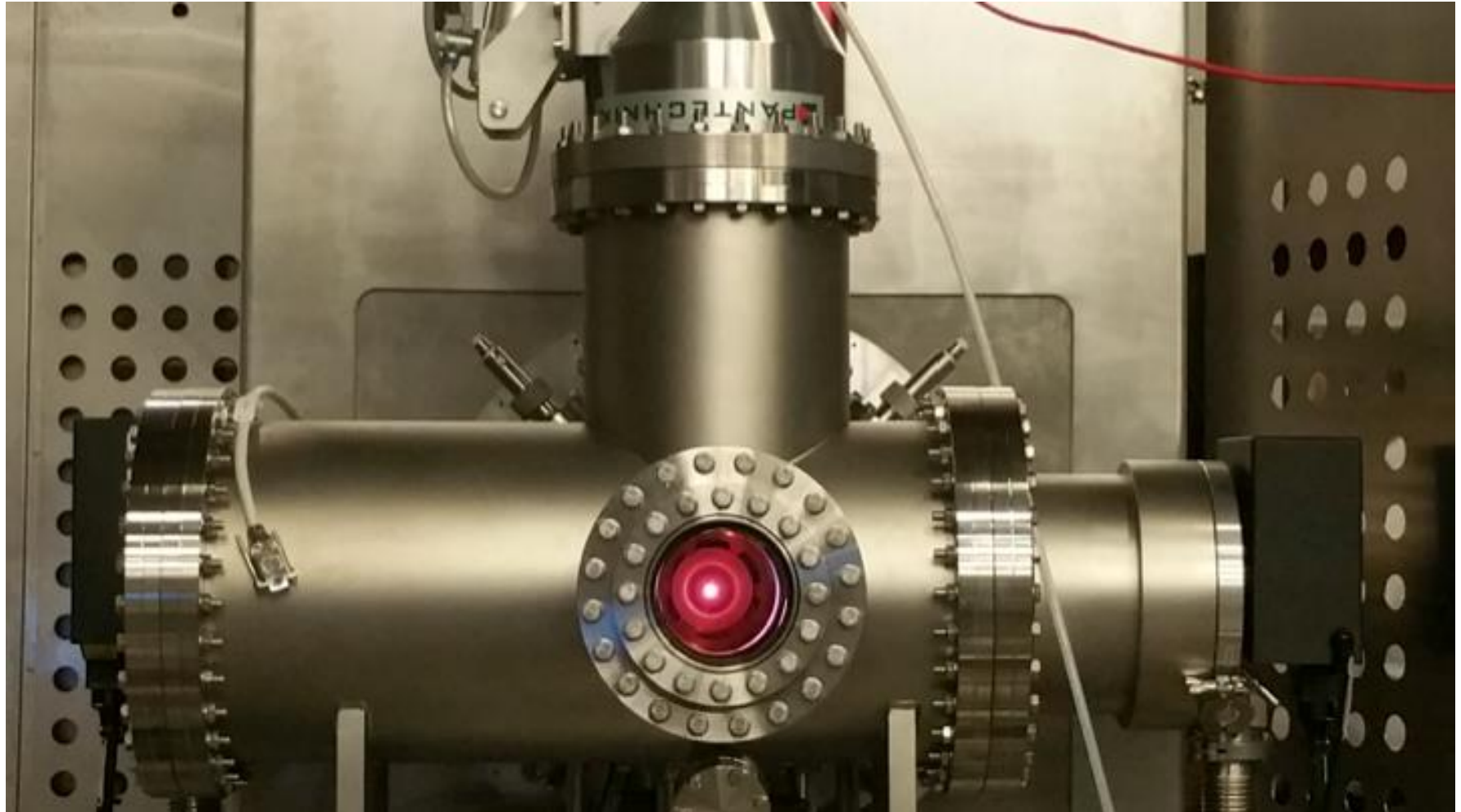
5. **Milan (superconducting elliptical cavities for WP5)**: INFN is involved in the design and construction of SC elliptical cavities of medium beta section (Milan-Lasa)
→ **know-how for ESS construction, industrial background for series construction**
→ **LNL for ICS + LNS, LNL&Milan for support to commissioning (t.b.d. in details)**

Ion Source & LEBT



- Maximum proton beam current at the target: 62.5 mA (>90 mA of source's output current)
- Pulse during neutron production: 2.86 ms
- Beam Stability: $\pm 2.5\%$
- Beam emittance 0.25π mm mrad
- The peak beam current must be variable from 6.3 mA to 62.5 mA (step size of 6.3 mA, precision of 1.6 mA)

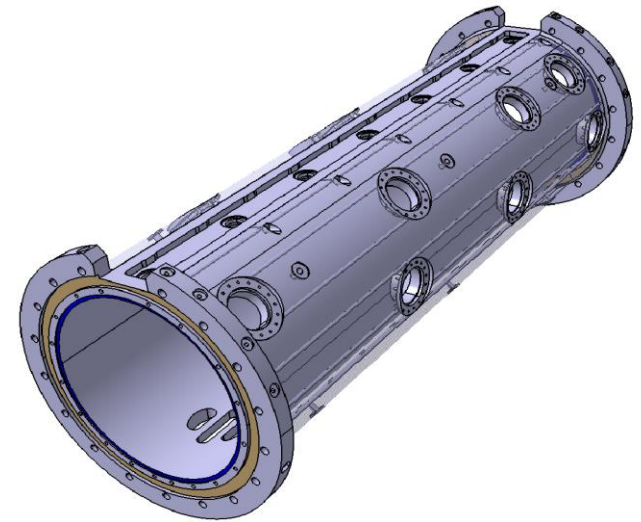
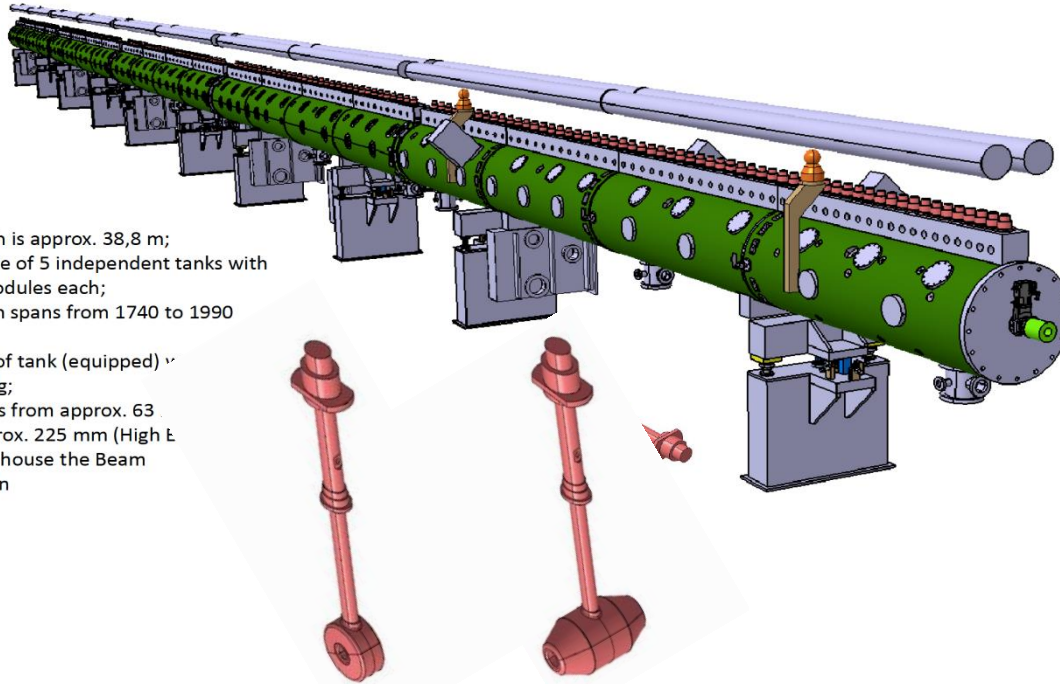
First plasma in the ion source in Catania



INFN-LNL and Torino contribution - DTL

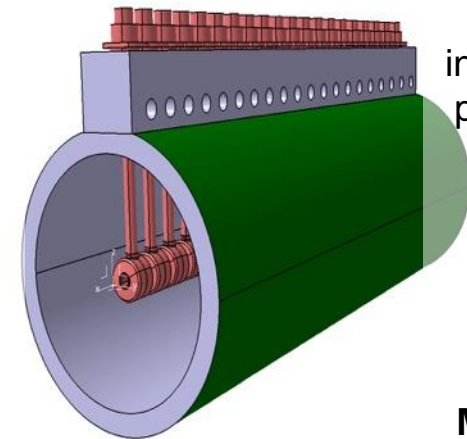
General characteristics and design criteria of the DTL

- DTL total length is approx. 38,8 m;
- The DTL is made of 5 independent tanks with 4 segments/modules each;
- Segment length spans from 1740 to 1990 mm;
- Each segment of tank (equipped) v approx. 1700 kg;
- DT length spans from approx. 63 Energy) to approx. 225 mm (High E
- 4 Intertanks to house the Beam instrumentation



Requirement	Target value	Comment
Particle type	H+	H- are possible
Input energy	3.62 MeV	+ 50 keV
Output energy	90 MeV	
Input current	62.5 mA	Peak, (2.86 ms long with a repetition rate of 14 Hz)
Input emittance	0.28 mm mrad	Transverse RMS normalized
	0.15 deg MeV	Longitudinal RMS
Emittance increase in the DTL	<10%	Design
Beam losses	<1 W/m	Above 30 MeV
RF frequency	352.21 MHz	
Duty cycle	<6%	
Peak surface field	<29 MV/m	1.6 Ekp
RF power per tank	<2.2 MW	Peak, dissipated+beam load, including
Module length	<2 m	Design constraint
Focusing structure	FODO	Empty tubes for Electro Magnetic Dipoles (EMDs) and Beam Position Monitors (BPMs) to implement beam corrective schemes
PMQ field	<62 T/m	

GIRDER (EN AW5083 Al alloy)
Precise positioning of the DT stem axis in steel bushing
SLAVE

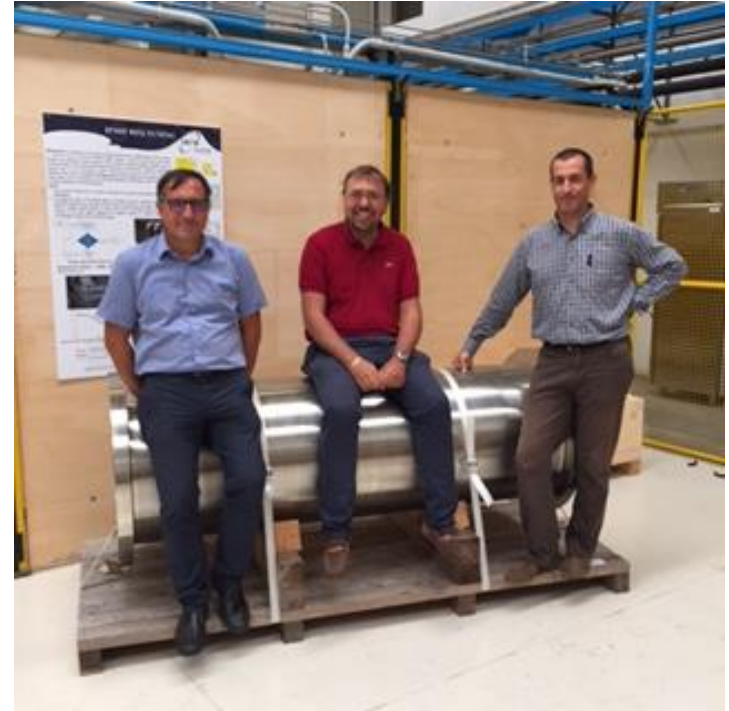


TANK (304L stainless steel)
internal Cu plating on finished surface (Ra 0,8)
high stiffness support
MASTER

Progress on DTL in Legnaro



DTL drift tube prototypes



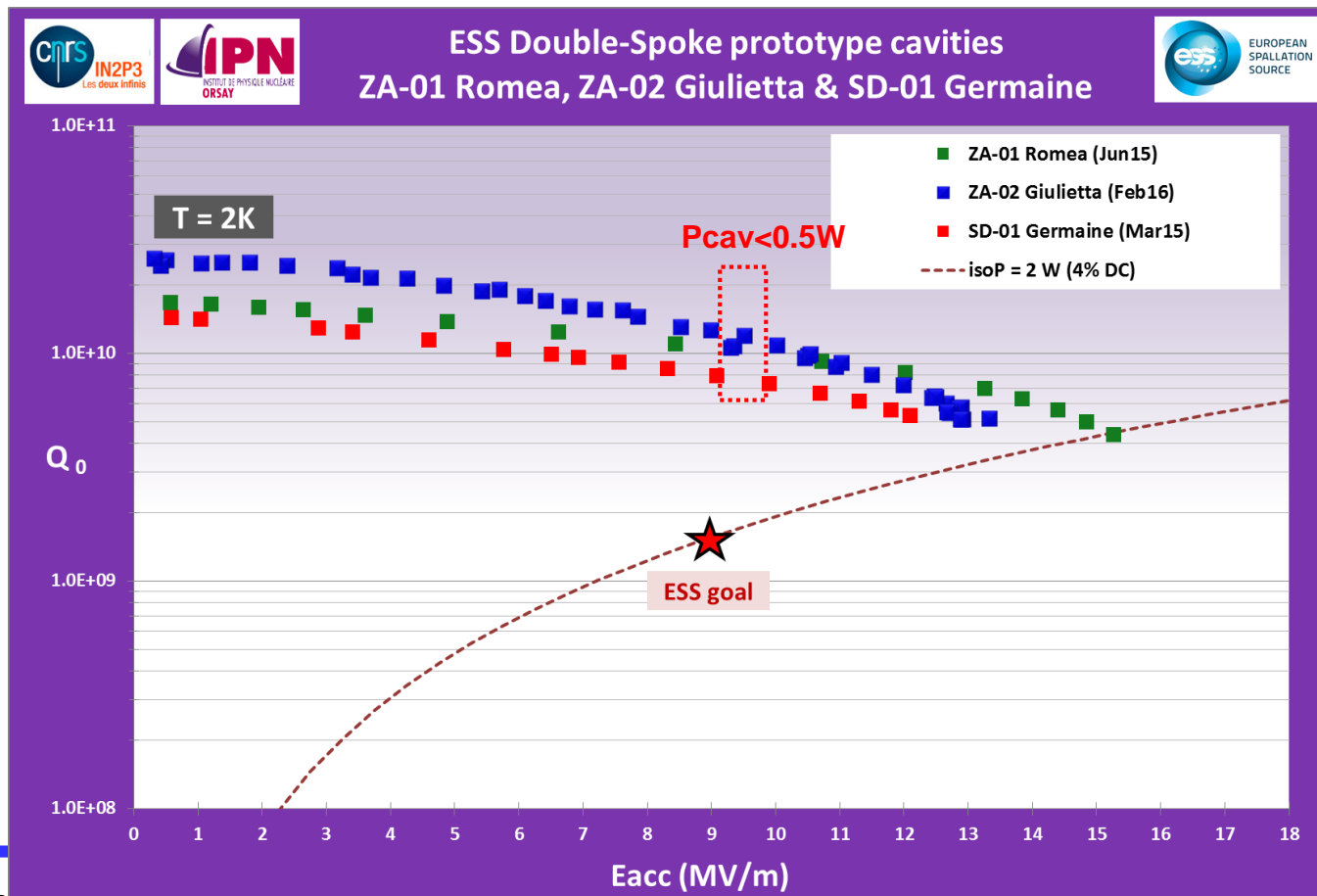
Santo Gammino, Andrea Pisent and Paolo Mereu on the first ESS DTL tank

Spoke Cavities design & prototype performances



Spoke cavity prototype test results (Jan15 – Feb16):

- Excellent performances, well within specifications (both on Eacc & Q_0)



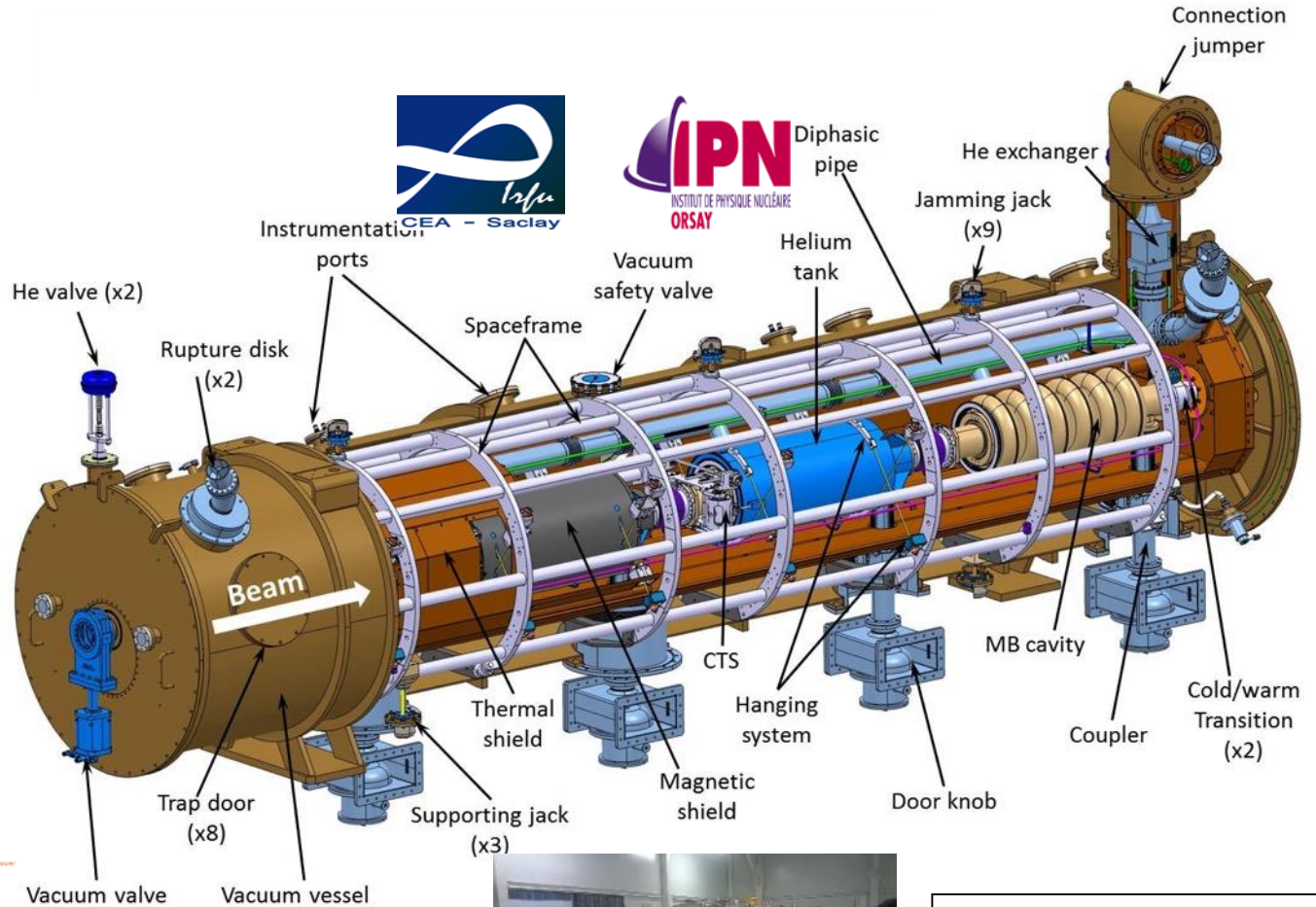
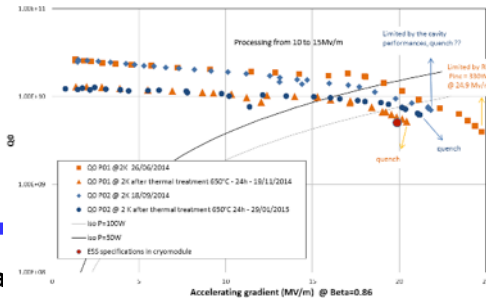
cryomodule



Medium beta cavity prototype

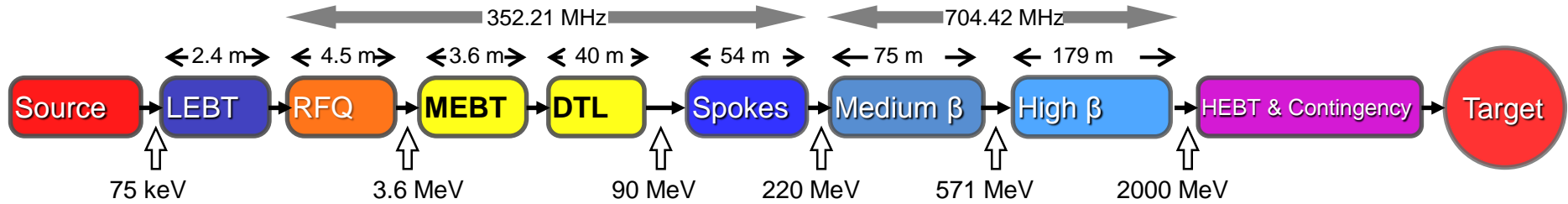


High beta cavity prototype with its helium tank



Blank assembly of the spaceframe inside the vacuum tank

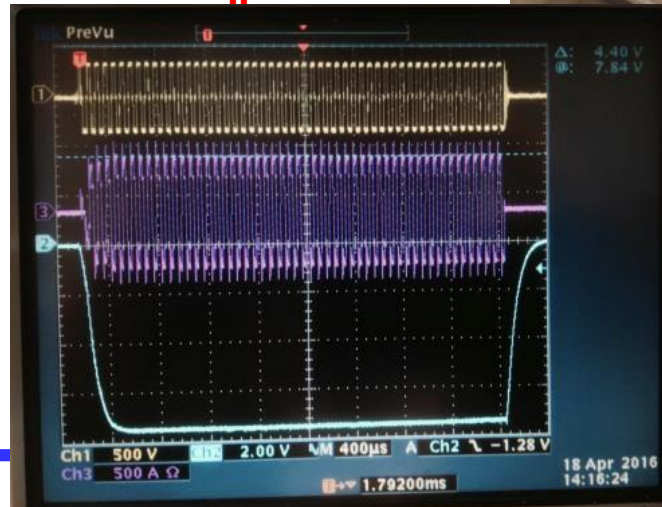
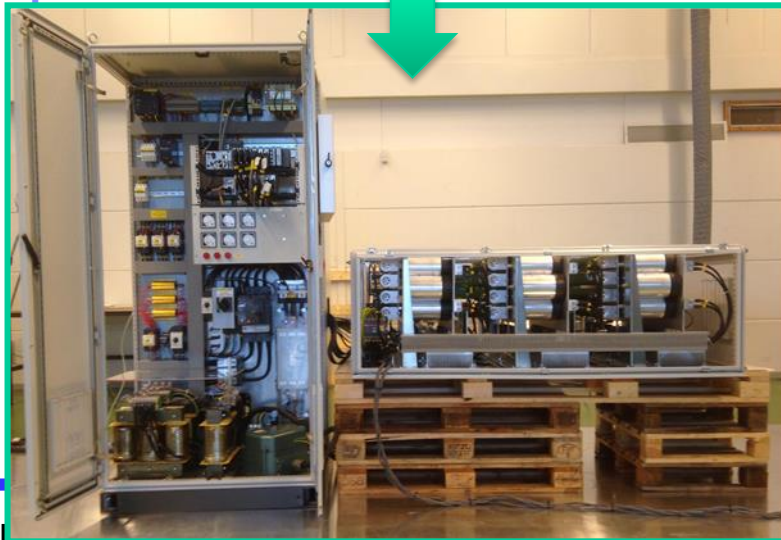
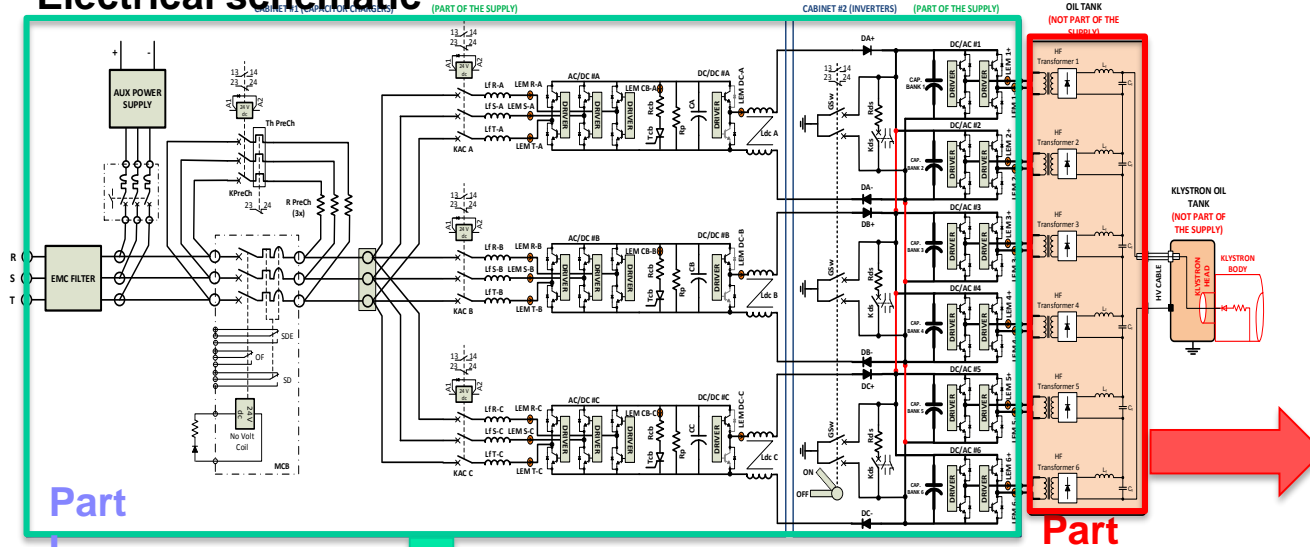
RF Technical performances



	Energy (MeV)	Frequency /MHz	No. of Cavities	βg	Temp / K	RF power /kW
Source	0.075	-	0	-	~300	-
LEBT	0.075	-	0	-	~300	-
RFQ	3.6	352.21	1	-	~300	1600
MEBT	3.6	352.21	3	-	~300	20
DTL	90	352.21	5	-	~300	2200
Spoke	220	352.21	26 (2/CM)	$0.5 \beta_{opt}$	~2	330
Medium β	571	704.42	36 (4/CM)	0.67	~2	870
High β	2000	704.42	84 (4/CM)	0.86	~2	1100
HEBT	2000	-	0	-	~300	-

Modulator SML proto status March 2016

Electrical schematic

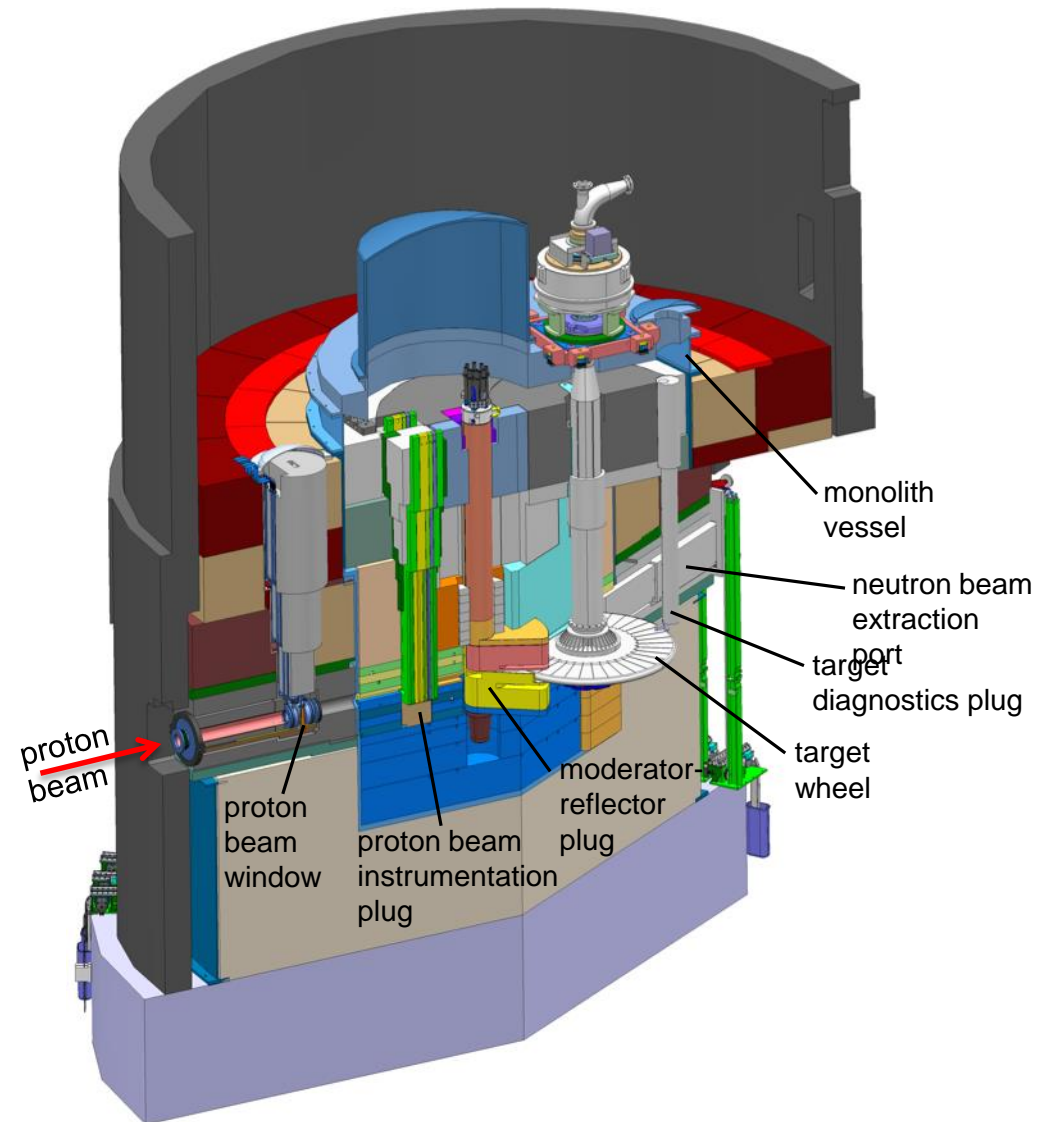


90 kV operation
Closed loop

Target, monolith, moderators etc.

Main components:

- Monolith:
 - Vessel (6 m diameter x 8 m height) (ESS-Bilbao, SP)
 - Steel shielding (6000 tons)
 - Instrumentation plugs (ESS-Bilbao, SP)
 - Proton beam window (ESS-Bilbao, SP)
 - Neutron shutters (ESS-Bilbao, SP)
 - Neutron beam extraction system
- Rotating Tungsten target (ESS-Bilbao, SP)
 - **2.5 m diameter** x 10 cm height
 - 7500 Tungsten bricks (3.5 tons)
 - 0.39 rev./s
- Target He gas-cooling (UJF, CZ)
 - 3 MW capacity
 - 3 kg/s flow rate
 - $\Delta t = 200$ degrees C
- High brightness moderators (FZJ, DE)
 - 2 liquid H₂ moderators
 - Water premoderators and moderators
 - He cryoplant (35 kW – 16 K)



Journey to deliver the world's leading facility for research using neutrons



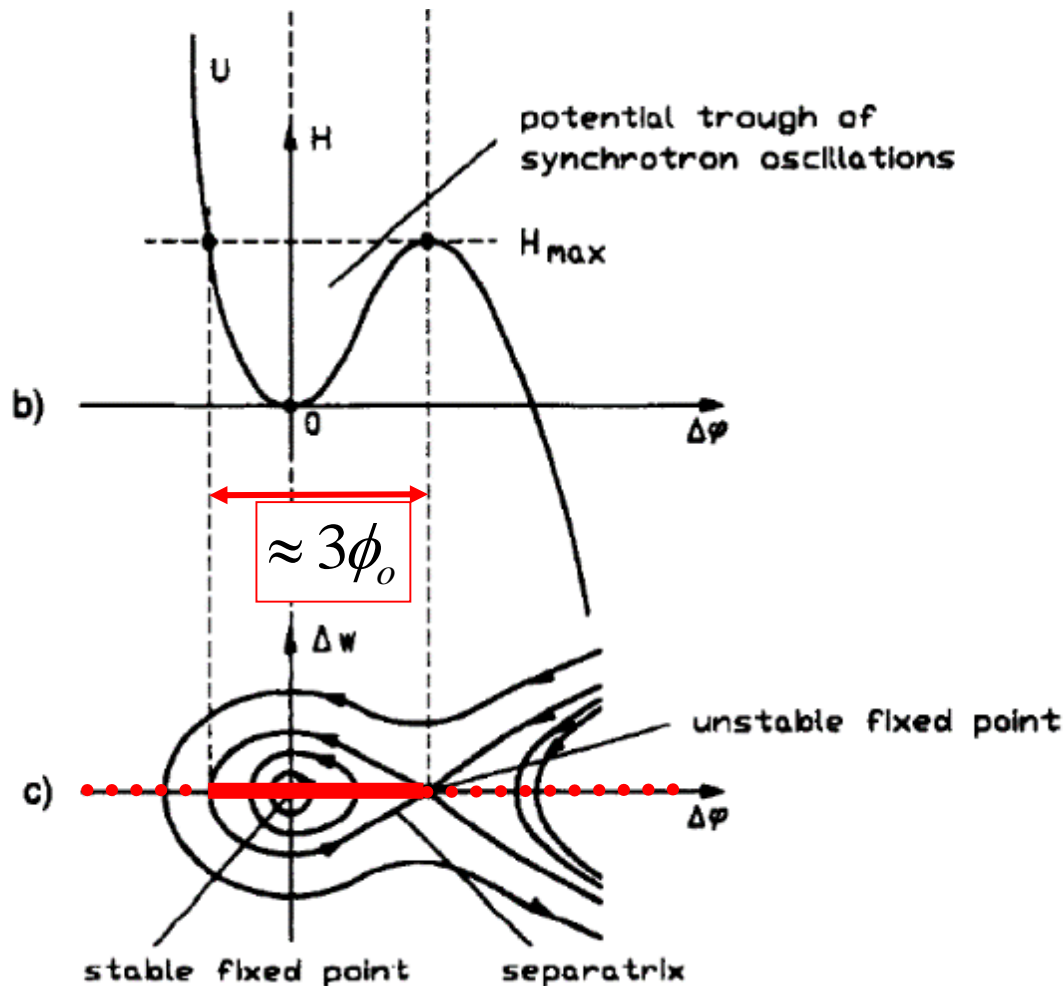
Beam dynamics in RFQ linear accelerators

Andrea Pisent

INFN Laboratori Nazionali di Legnaro

Prologue : bunching in a linac

The problem of capture efficiency in a linac



- Starting with a continuous mono energetic beam from source, only particles in the separatrix will be captured.
- Typically if $\phi_0 = -20^\circ$ only $60/360 = 17\%$ of particles will be captured
- Something must be invented, especially for high intensity or for rare ion beams.

outline

- Wikipedia RFQ “*invented by [Soviet](#) physicists I. M. Kapchinsky and [Vladimir Teplyakov](#) in 1970, the RFQ is presently used as an injector by major laboratories and industries throughout the world for radiofrequency linear accelerators.^[2]”*



- Main features
 - RF acceleration at low energy / replace the high voltage injectors
 - Adiabatic bunching / high capture efficiency

RFQs replace with RF linac electrostatic injectors

example CERN RFQ2

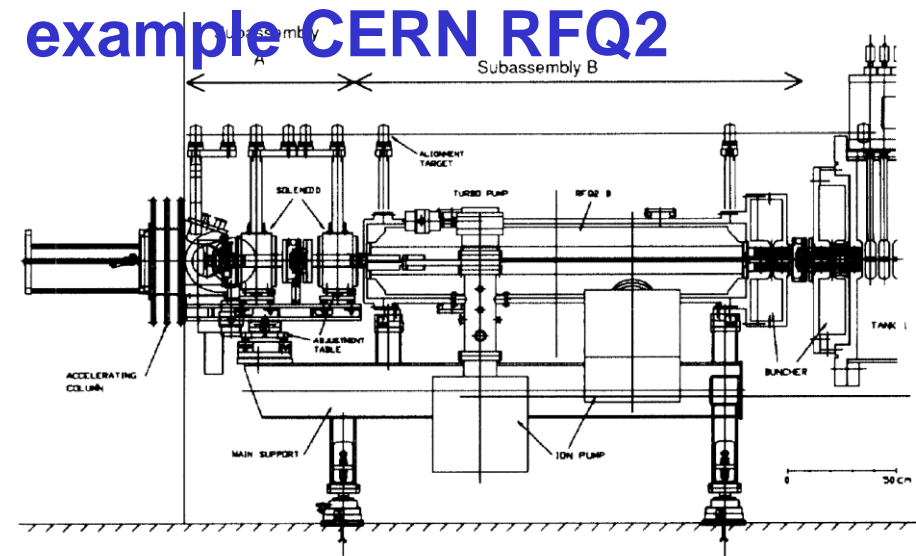
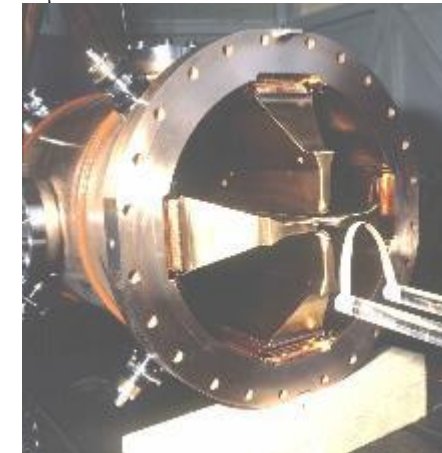


Figure 2. The RFQ2 complex

Main RFQ2 design parameters

RF frequency	202.56 MHz
Input energy	90 KeV
Output energy	750 KeV
Output current	200 mA
Trapping efficiency	~90 %
Vane voltage	178 KV
Final synchronous phase	-35 °
Modulation factor(max)	1.62
Mean aperture radius	7.87 cm
Cavity length	178.5 cm
Vane length	175.2 cm
Cavity diameter	35.4 cm



In operation since 1992

Fusion Material Irradiation Test Project - FMIT

a US Department of Energy project,
accepted as a necessary and vital element for the development of fusion
power.

- Construction project approved 1975
- Accelerator construction undertaken by new Accelerator Technology Division at Los Alamos January 1978, after discussions in 1977.
- No IF's - firm budget and schedule, BUT - huge R&D question - injection of 100 mA cw into DTL required several 100 kV DC injector.
- Discovery of Teplyakov RFQ work in Russia.
- Proposal to DOE for RFQ development, approved!

Arlo Thomas, Jim Potter

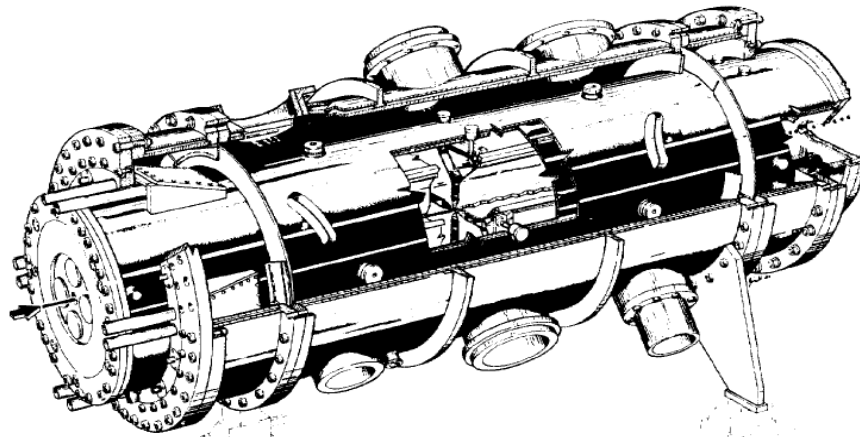
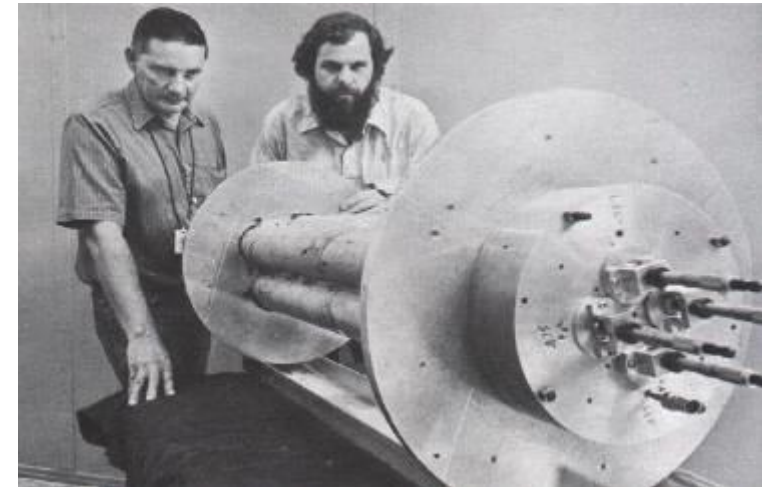


Fig. 1. Initial design of the FMIT RFQ accelerator. The RFQ comprises two coupled, coaxial resonators. The rf power is loop coupled into the outer section, or manifold, which more uniformly distributes the power into the four quadrants of the inner resonator, or core. A 75keV beam is injected (arrow, left in the figure) and accelerated to **2 MeV**.



Courtesy of R. Jameson

RFQs general parameters

	Name	Lab	ion	energy	vane voltage	beam current	power	RF Cu power	Freq.	length		Emax	Power density	
				MeV/u	kV	mA	kW	kW	MHz	m	lambda	kilpat	ave	max
													W/cm ²	W/cm ²
	IFMIF EVEDA	LNL	d	2.5	79-132	130	650	585	175	9.8	5.7	1.8	3.5	60
pulsed	CERN linac 2	CERN	p	0.75	178	200	150	440	202	1.8	1.2	2.5		
	SNS	LBNL	H-	2.5	83	70	175	664	402.5	3.7	5.0	1.85	1.1	10
	CERN linac 3	LNL	A/q=8.3	0.25	70	0.08	0.04	300	101	2.5	0.8	1.9		
CW	LEDA	LANL	p	6.7	67-117	100	670	1450	350	8	9.3	1.8	11.4	65
high p	FMIT	LANL	d	2	185	100	193	407	80	4	1.0	1	0.4	
	IPHI	CEA	p	3	87-123	100	300	750	352	6	7.0	1.7	15	120
	TRASCO	LNL	p	5	68	30	150	847	352	7.3	8.6	1.8	6.6	90
CW	SARAF	NTG	d	1.5	65	4	12	250	176	3.8	2.2	1.6		
mid p	SPIRAL2	CEA	A/q=3	0.75	100-113	5	7.5	170	88	5	1.5	1.65	0.6	19
CW	ISAC	TRIUMF	A/q=30	0.15	74	0	0	150	35	8	0.9	1.15	-	-
lp	PIAVE	LNL	A/q=6	0.58	280	0	0	8e-3 (SC)	80	2.1	0.5	-	-	-

The RFQ is
INFN Italy responsibility

LNL
Padova
Torino
..Bologna



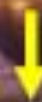
IFMIF-EVEDA RFQ

- 18 modules 9.8 m
- Powered by eight 220 kW rf chains and 8 couplers
- High availability 30 years operation.
- Hands on maintenance
- First complete installation in Japan (Rokkasho site)

$$\frac{d\vec{p}}{dt} = e(\vec{E} + \vec{v} \times \vec{B})$$

+

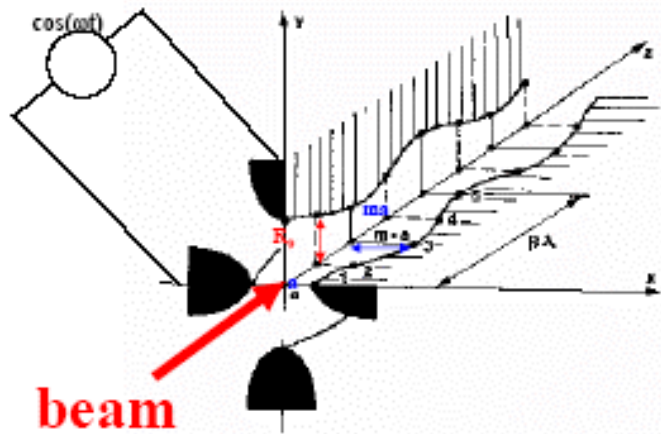
F=eE



-

-

+



Equations of motion

From the two terms potential

$$\Phi(x, y, z) = \frac{V}{2} \left[\frac{x^2 - y^2}{R_0^2} + A I_0(kr) \cos kz \right]$$

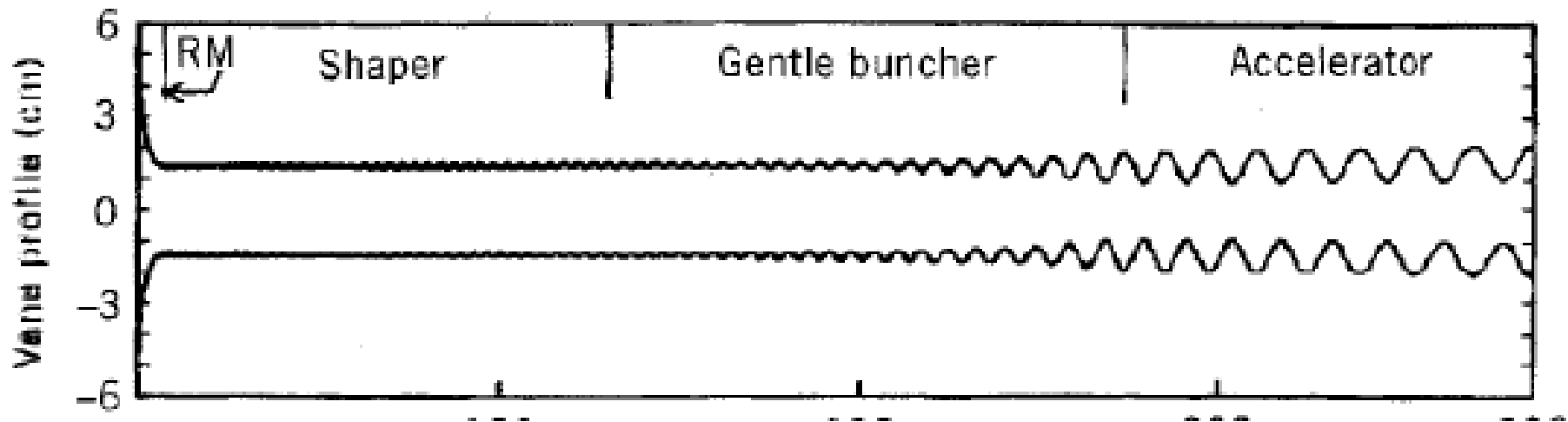
The transverse and longitudinal equations (respect to the parameter $d\tau = \frac{dz}{\beta\lambda}$) read

$$\frac{dw_0}{d\tau} = \left[e \int_0^{2\pi} dz E_z(z) \cos\left(\frac{2\pi z}{\beta\lambda}\right) \right] \cos(\phi) = eAV \frac{\pi}{2} \cos \phi_0$$

$$\frac{d^2 x}{d\tau^2} + [B \cos 2\pi\tau + K_{RF}] x = 0$$

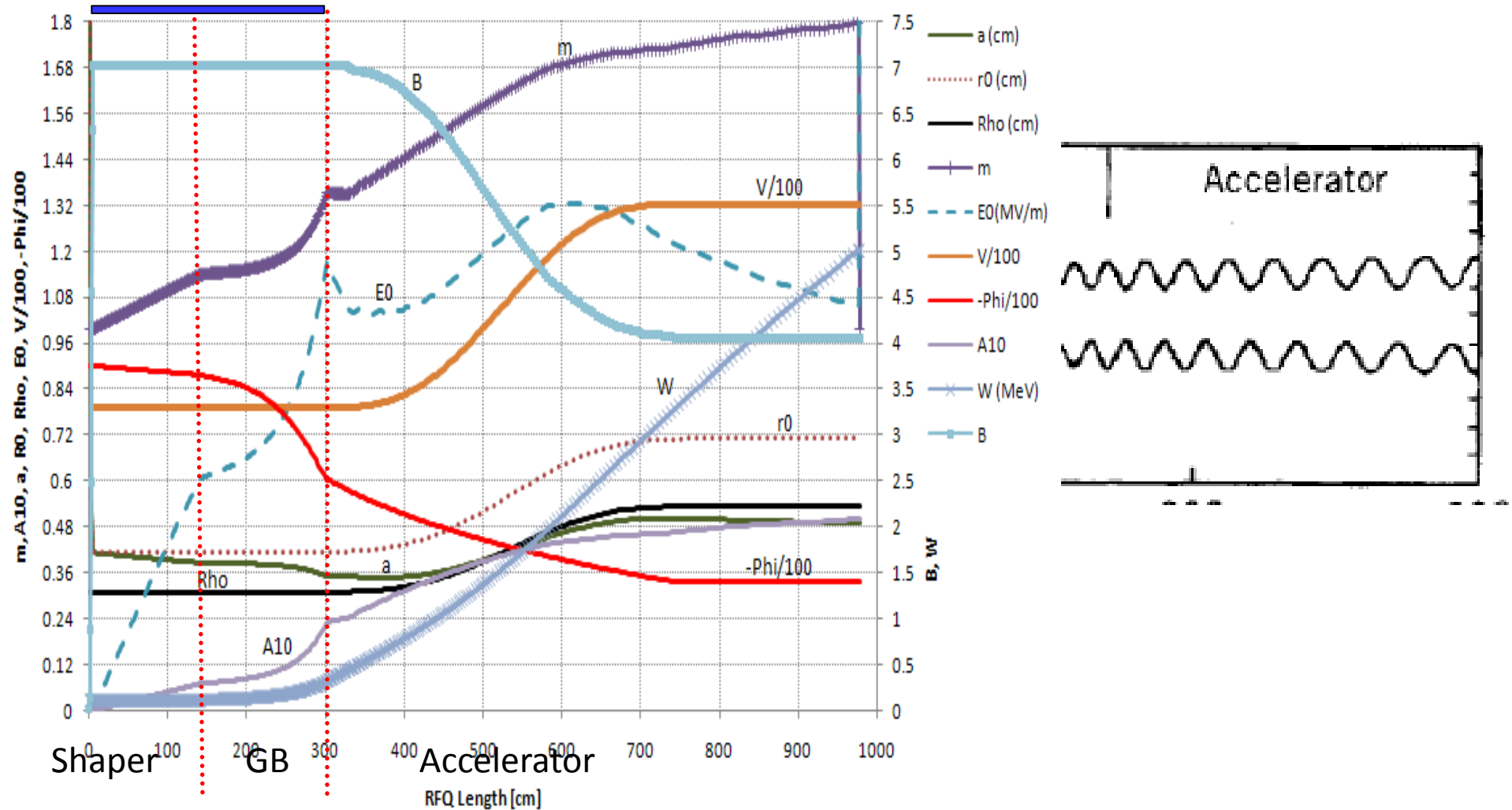
$$K_{RF} = \pi \frac{eE_a \sin \phi_0}{\beta^3 mc^2 \lambda} (\beta\lambda)^2 = \frac{\pi^2}{4} \frac{eAV \sin \phi_0}{\beta^2 mc^2} \quad B = \frac{eV}{mc^2} \frac{\lambda^2}{R_0^2}$$

Beam parameters chosen period by period

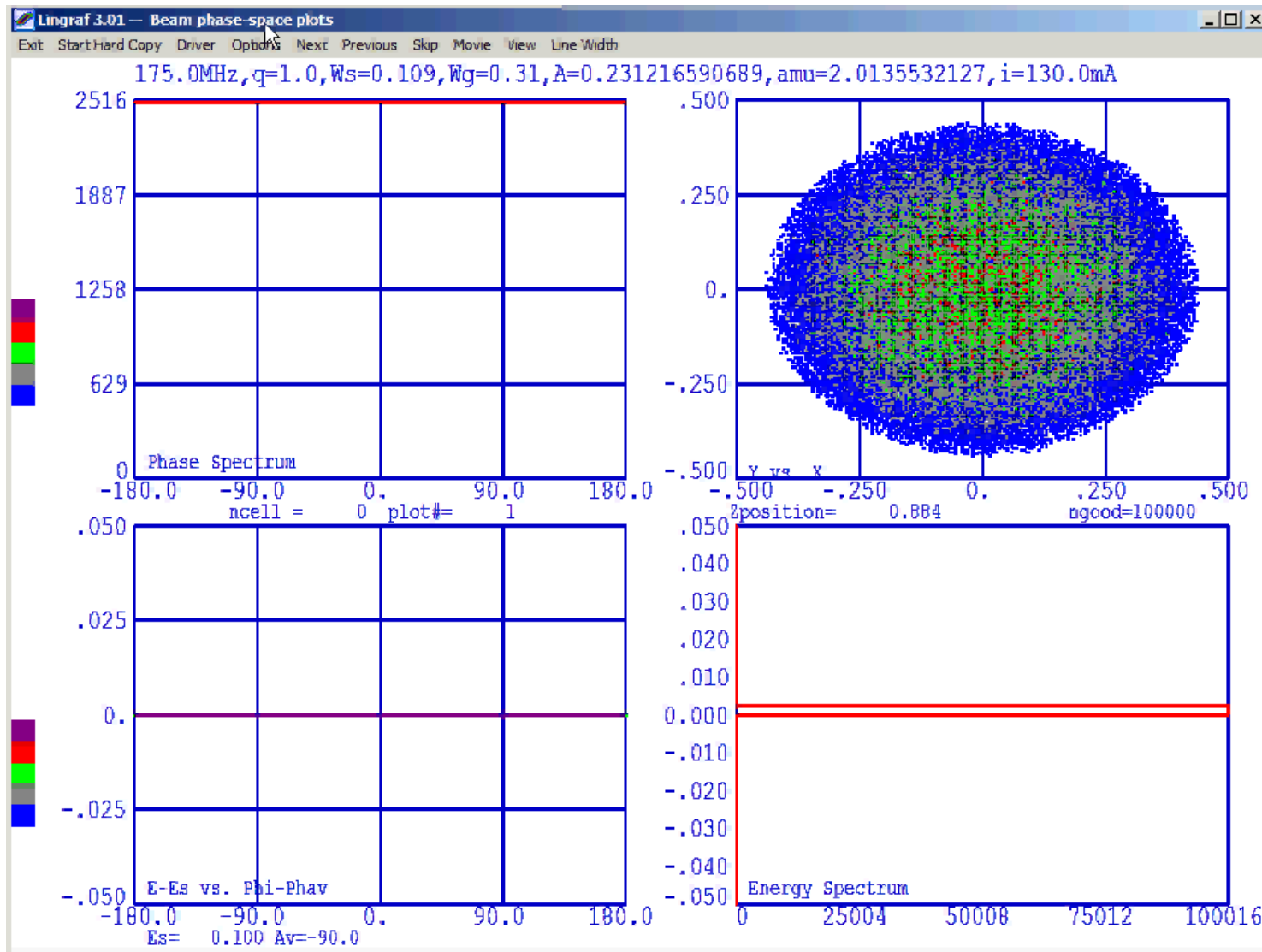


Beam parameters chosen period by period

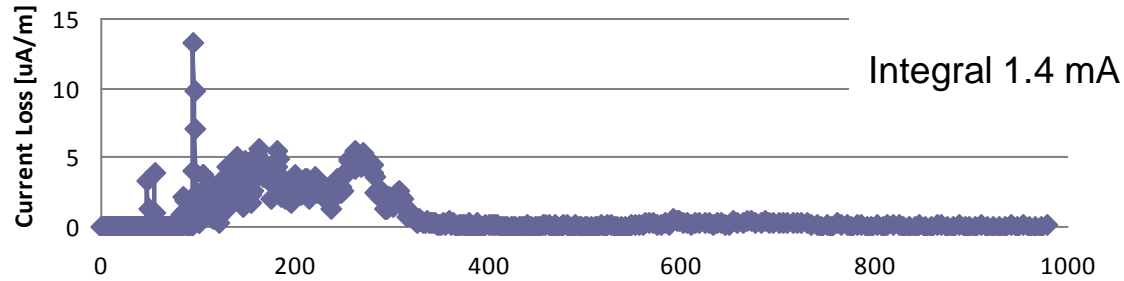
Modulation "m", average aperture "r0" [cm], small aperture "a" [cm], Voltage/100 [kV] E0 [MV/m], Acceleration factor "A10", Energy "W", Focusing "B", -Sync. Phase/100 [deg], Pole tip "rho", along the RFQ



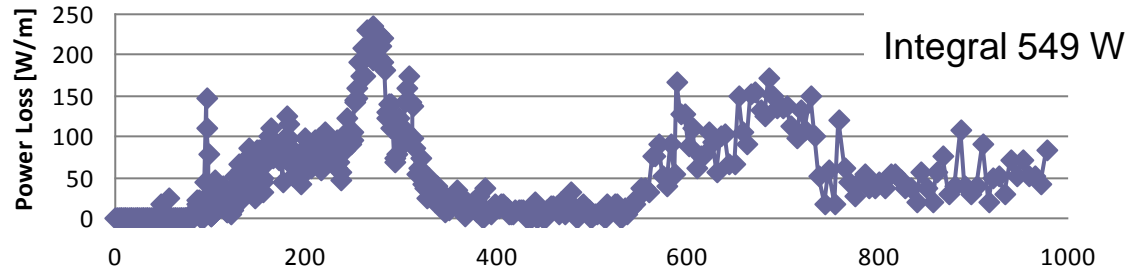
Continuous bunching with RFQ



Beam Loss [uA/m]

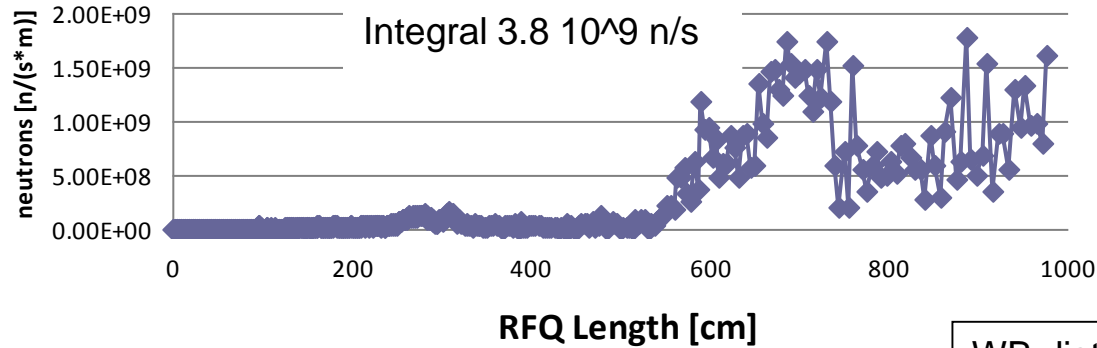


Beam Loss [W/m]



RFQ Length
[cm]

Neutron production estimate [n/(s*m)]



$$n = 5.15 \cdot 10^{-7} N_w^{2.1}$$

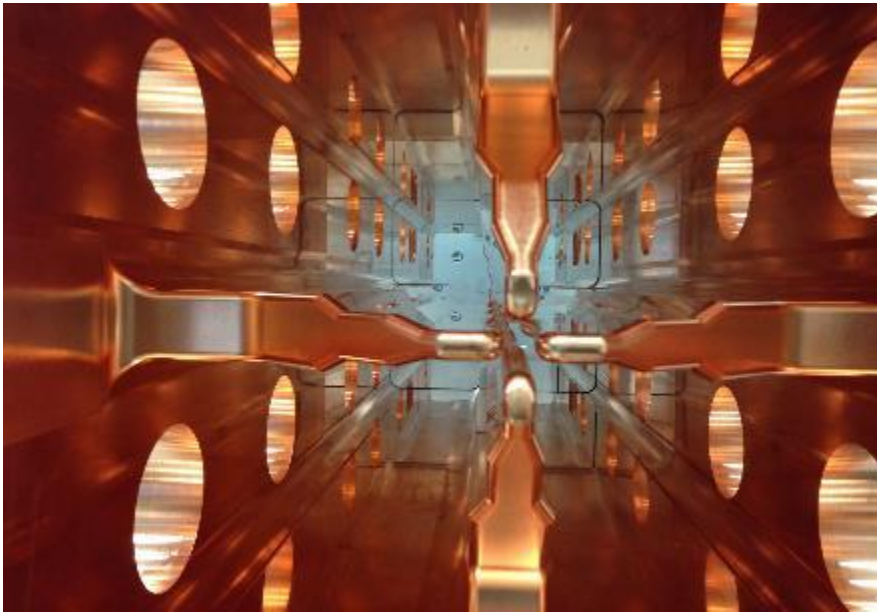
WB distribution 0.25 mm mrad rms norm

RFQ features

- The beam dynamics of an RFQ is written once for ever in the metal.
 - The designer has the choice of modulation parameters in some hundreds of modulation periods.
 - This flexibility allows different approaches and very optimized accelerators for many specific high performance applications.
- BUT
 - Once built the RFQ is not flexible at all, since very few parameters can be changed in operation.
 - The construction has to follow strict tolerances (important technological challenges related to construction and RF tuning).
 - One has to rely on computer simulations and design approaches, since experimental verification of the correctness of the design arrives after many years.

IFMIF

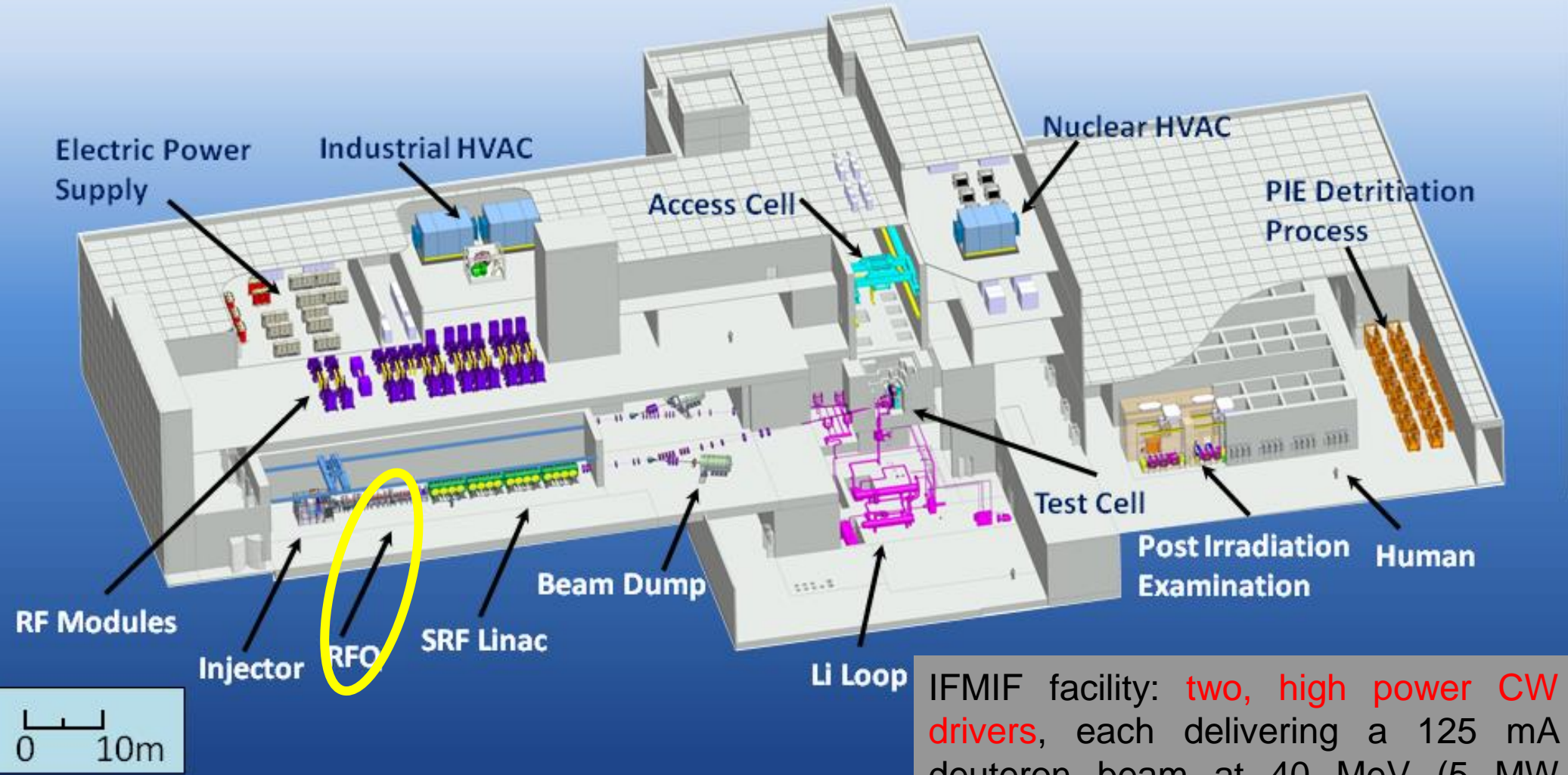
IFMIF-EVEDA RFQ



Input/output Energy	0.1-5	MeV
Duty cycle	cw	
Deuteron beam current	125	mA
Operating Frequency	175	MHz
Length (5.7λ)	9.78	m
Vg (min – max)	79 – 132	kV
R0 (min - max) $\rho/R0=.75$	0.4135 - 0.7102	cm
Total Stored Energy	6.63	J
Cavity RF power dissipation	550	kW
Power density	90	kW/m
Power density (average-max)	3.5-60	kW/cm ²
Quality factor ($Q0/Qsf=0.82$)	13200	
Shunt impedance ($\langle V^2 \rangle L/Pd$)	201	k Ω –m
Frequency tuning	Water temp.	

IFMIF "Artist View"

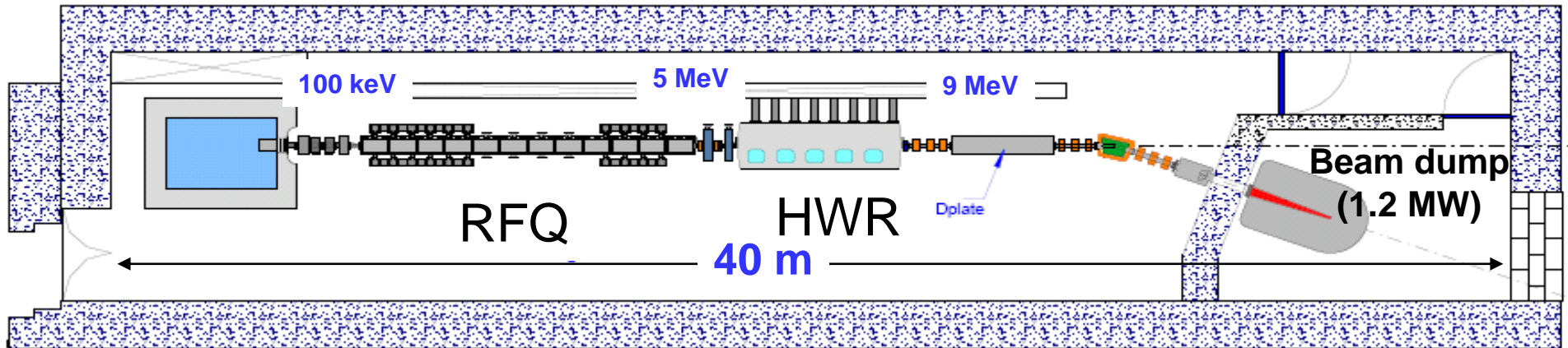
International Fusion Material Irradiation Facility



IFMIF facility: **two, high power CW drivers**, each delivering a 125 mA deuteron beam at 40 MeV (5 MW power) hitting a liquid lithium target in order to yield neutrons (10^{17}s^{-1}) via nuclear stripping reactions.

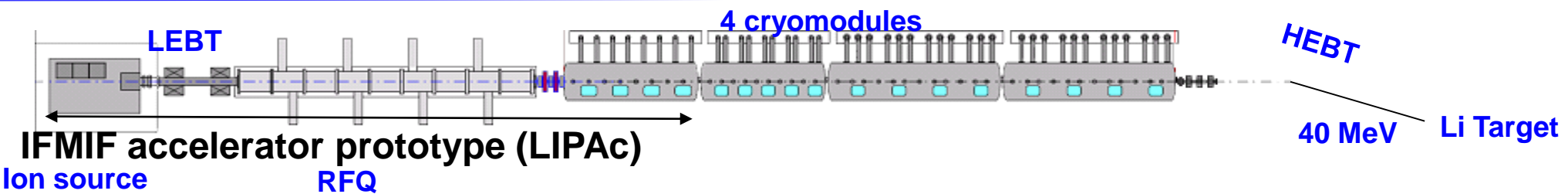
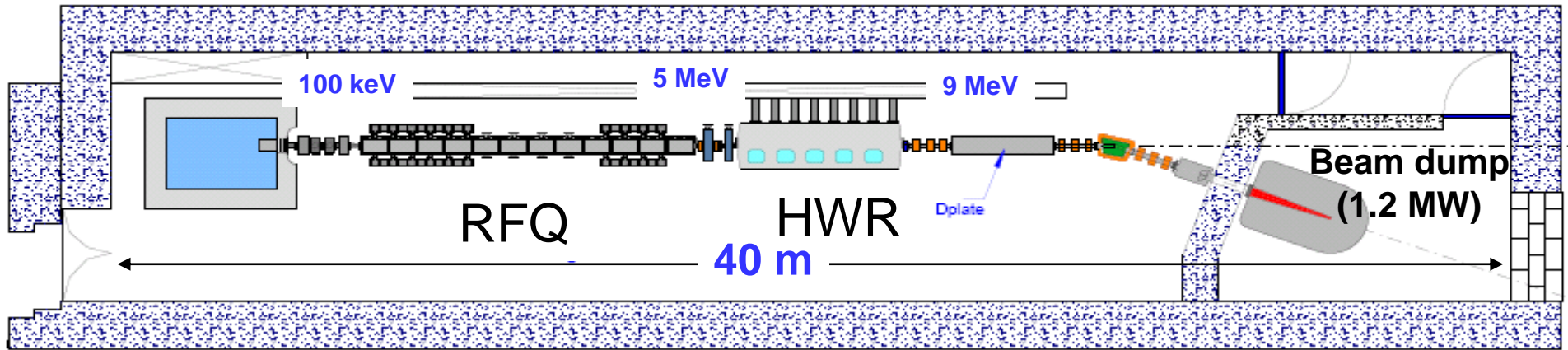
IFMIF EVEDA

- Funded within the Broader Approach to Fusion: construction of a **9 MeV 125 mA cw deuteron accelerator** (LIPAc, Linear IFMIF Prototype Accelerator) to be built in Rokkasho, (Japan), based on a high power RFQ followed by a Half Wave Resonator superconducting



IFMIF EVEDA

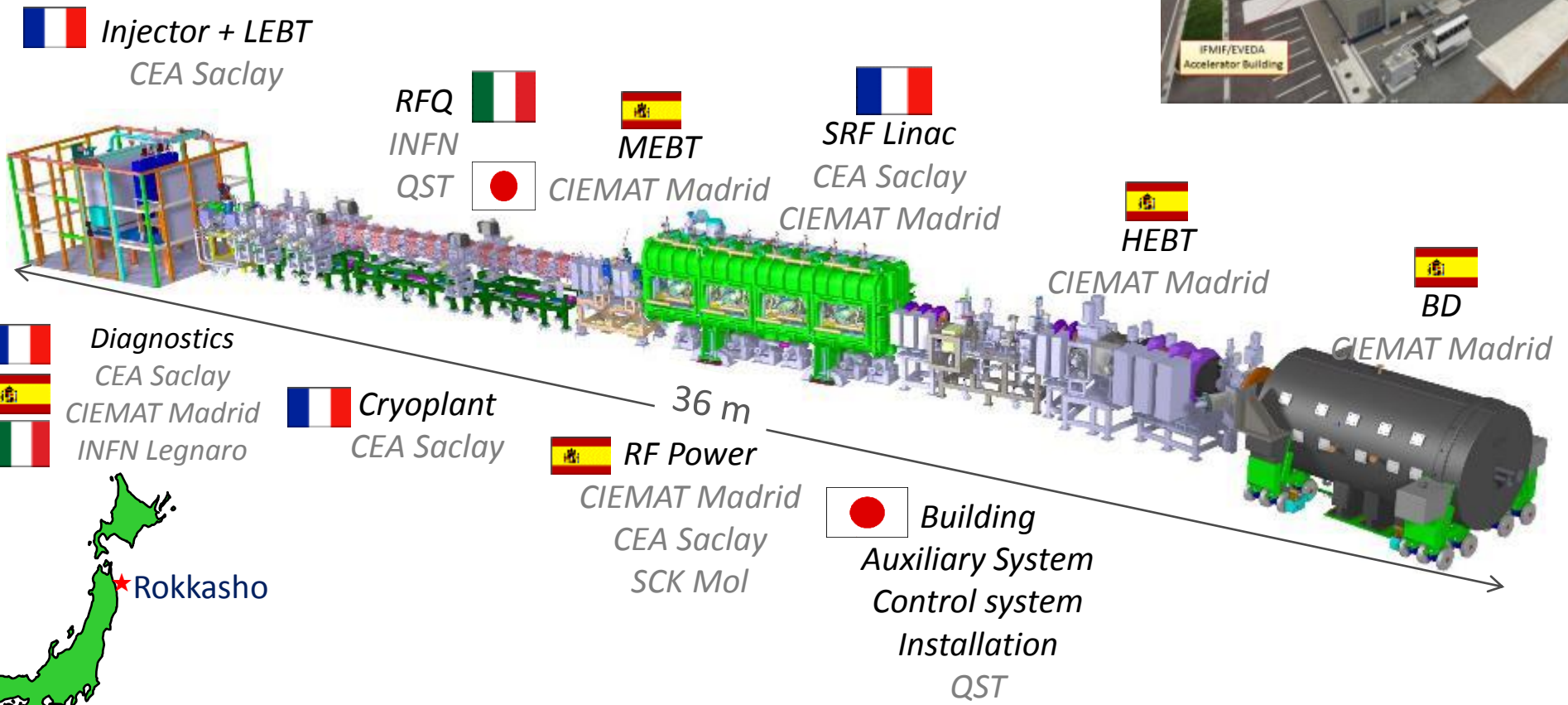
- Funded within the Broader Approach to Fusion: construction of a **9 MeV 125 mA cw deuteron accelerator** (LIPAc, Linear IFMIF Prototype Accelerator) to be built in Rokkasho, (Japan), based on a high power RFQ followed by a Half Wave Resonator superconducting



IFMIF EVEDA

Linear IFMIF Prototype Accelerator

Accelerator components from Europe
Beam tests in Japan



Status of LIPAc Phases (Rokkasho site)

Injector under commissioning



MEBT set up



Diagnostics Plate set up



RFQ assembled and tuned



RF power system under completion

INFN: the RFQ system organization

- Contact Person: A. Facco
- Responsible A. Pisent
 - Responsible for Padova: A. Pepato
 - Responsible for Torino: P. Mereu
 - Responsible for Bologna: A. Margotti

About **30** persons involved, **20** FTE, **10** dedicated contracts



- Responsible A. Pisent
- Module Mechanics design and construction **A. Pepato**
 - Quality assurance: A. Prevedello
 - Module production follow up M. Benettoni
 - Stainless steel components production A. Margotti
- High power tests and RFQ integration: **E. Fagotti**
 - Engineering integration **P. Mereu**
 - Physical design : M. Comunian
 - Radio frequency: A. Palmieri
 - Computer Controls: M. Giacchini
 - Vacuum system and technological processes C. Roncolato
 - Cooling system integration G. Girauddo

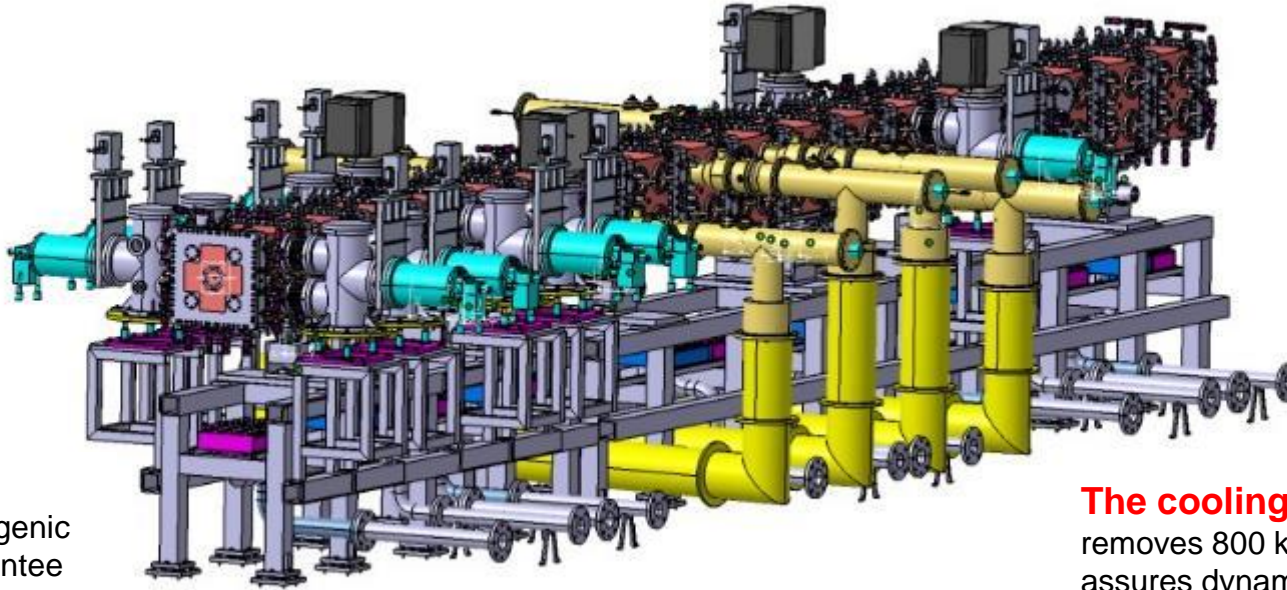
Components of the 9.8 m long RFQ

18 modules

each module approx.
550 mm and 600 kg.
Modules assembled
and aligned in 3
supermodules
(separately
transported to Japan)

Vacuum system

10 sets, based on cyogenic
pumps (in cyan) guarantee
 $5 \cdot 10^{-7}$ mbar with beam loss
gas load



Local Control system

PLC and EPICS, for
cooling and vacuum
systems, temperature
and RF probes.

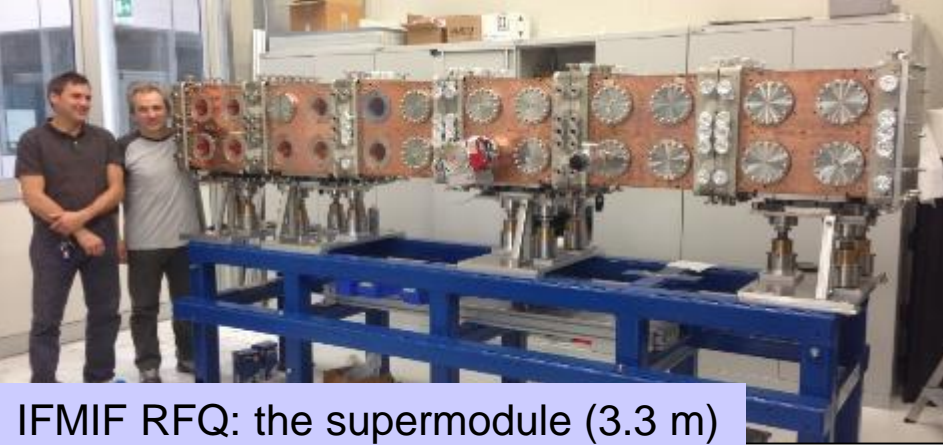
The cooling system

removes 800 kW and
assures dynamic RF
frequency tuning

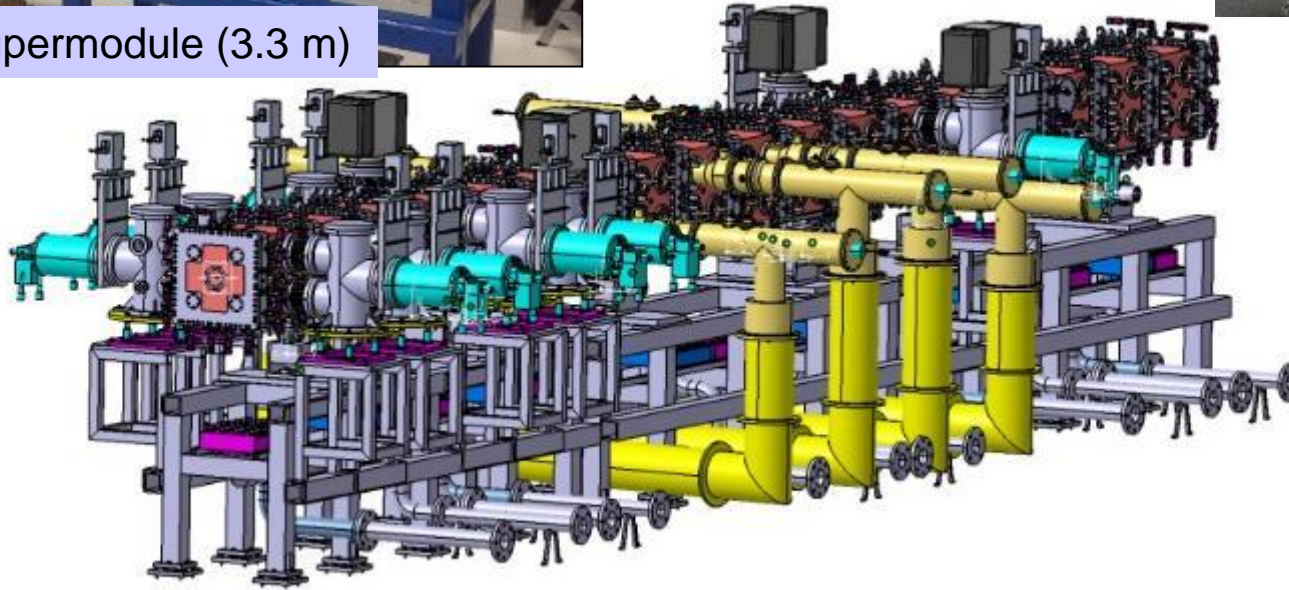
RF Power

8 RF systems and
power couplers, 200
kW each. (RF system
by Ciemat and final
couplers by JAEA)

Modules construction



IFMIF RFQ: the supermodule (3.3 m)



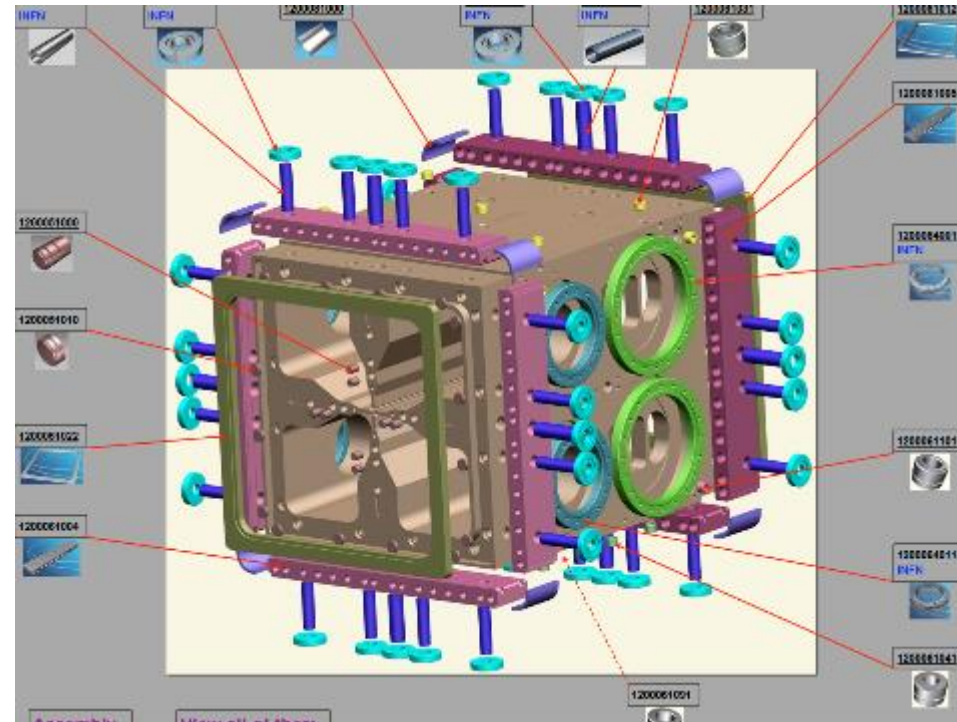
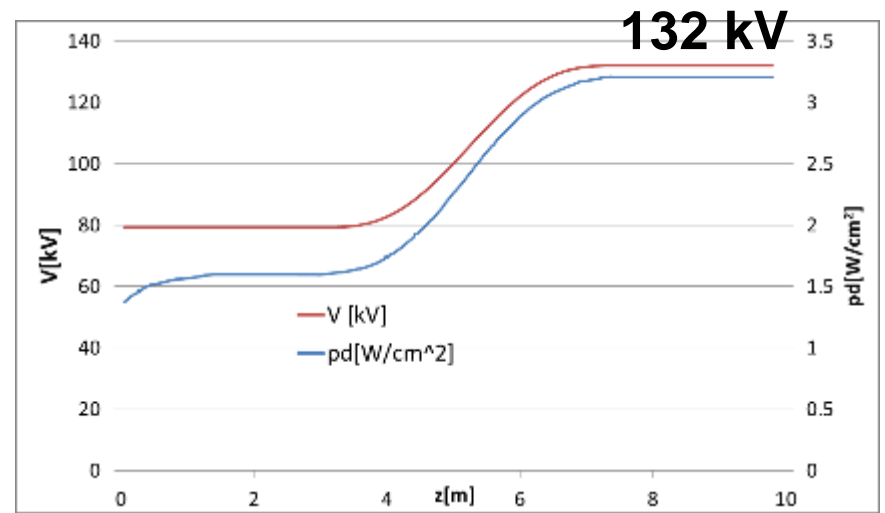
18 modules in three supermodules

- High energy SM built by Cinel, Padua (Italy),
- Intermediate energy built internally by INFN,
- Low energy attributed to RI Koln (Germany), concluded by INFN



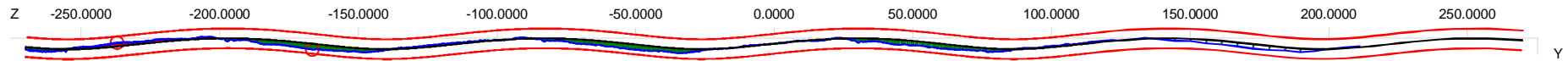
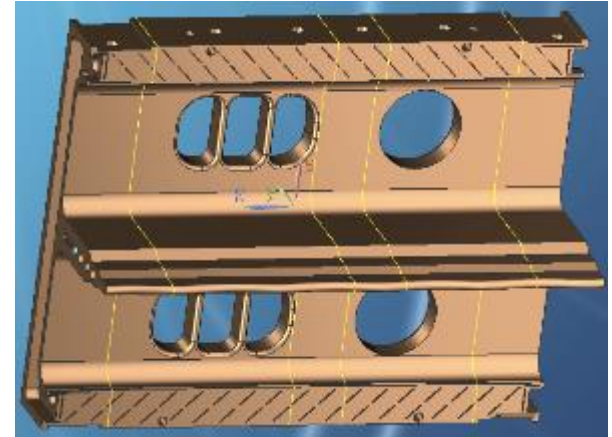
Design choices

- High beam current requires high focussing parameter B, and ramped high voltage
- The **four vane resonator** was the only possible solution for such high intervane voltage
- The **mechanical design** is based on a **brazed structure** and **metal sealing** to guarantee the necessary **high reliability**.
- These two choices determined many aspects of the design (for example 316LN stainless steel for most of the interface points).
- 550 mm long modules to increase the number of possible manufacturers



Geometrical tolerances

- The **electrode machining** can be very accurate and for this RFQ it was verified with continuous scanning **CMM** of each of the **72 electrodes** (**20 μm max error** in the modulation geometry of each module was achieved).



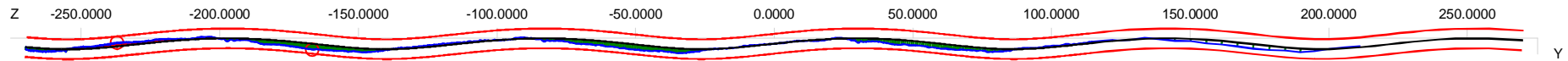
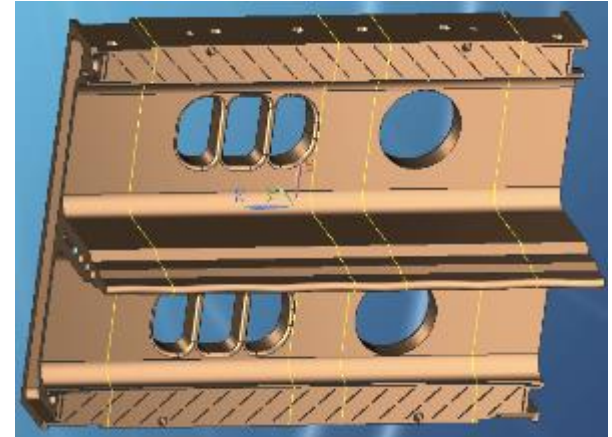
- The **beam axis accuracy** requires a precise alignment of the quadrupole center module after module (**better than 0.1 mm**).

Max Deviation: 10.5 μm

CMM machine at INFN Padova

Geometrical tolerances

- The **electrode machining** can be very accurate and for this RFQ it was verified with continuous scanning **CMM of each of the 72 electrodes** (**20 μm max error** in the modulation geometry of each module was achieved).



Max Deviation: 10.5 μm

CMM machine at INFN Padova

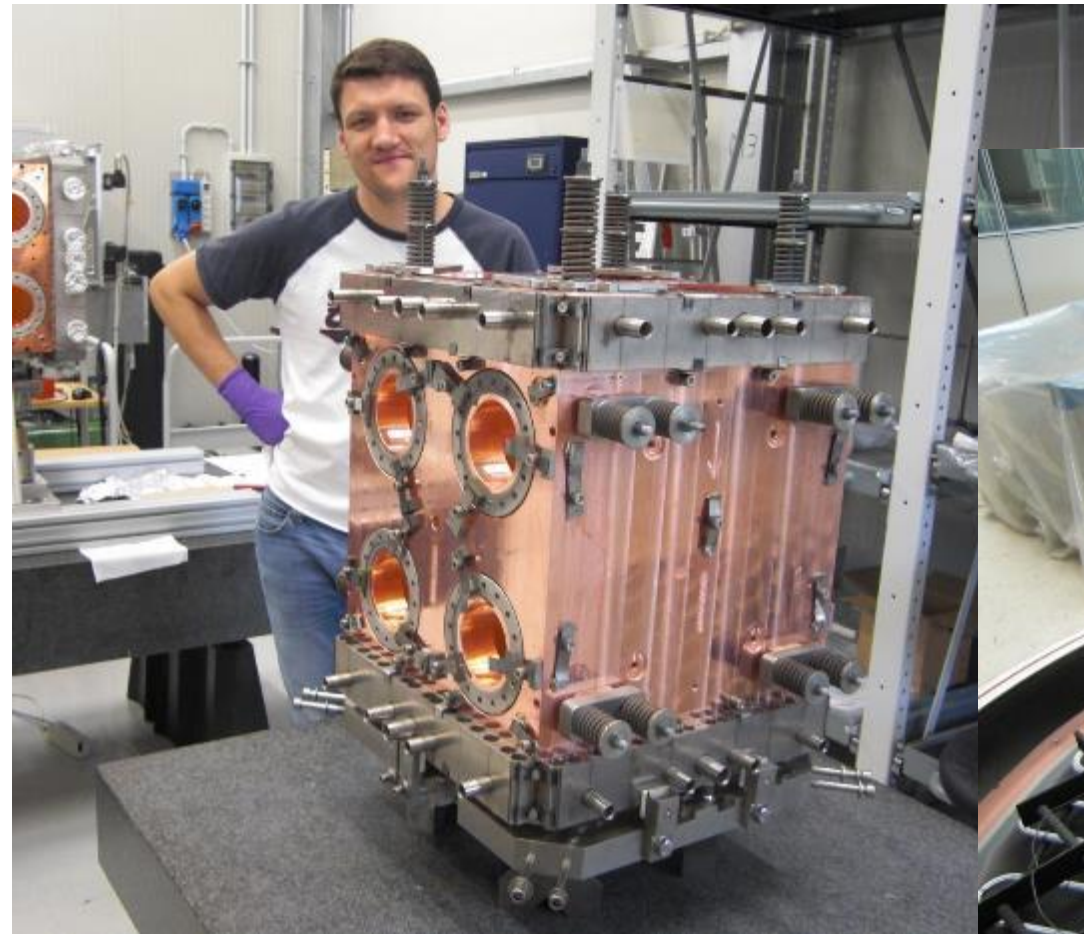
- The **beam axis accuracy** requires a precise alignment of the quadrupole center module after module (**better than 0.1 mm**).
- To keep the frequency within the tuning range and the **voltage law** along the 4.7λ structure requires guarantee electrode displacements below **50-100 μm** (depending on modulation amplitude).

INFN development for Brazing

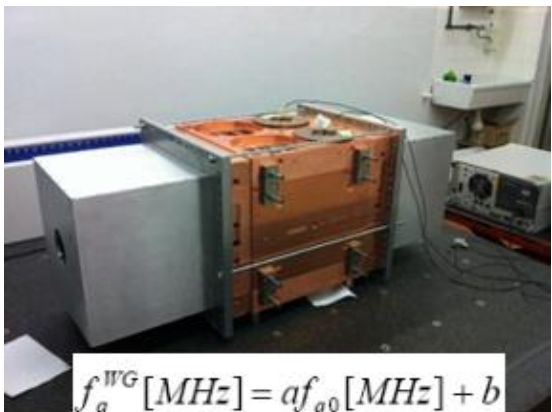
Large pieces with final tolerances of 50 μm in beam region

Vacuum oven in INFN LNL, metrology and precision machining at INFN Padova

Single step brazing procedure was developed and used for most of the modules.



QA of modules: Results of RF measurements before and after brazing

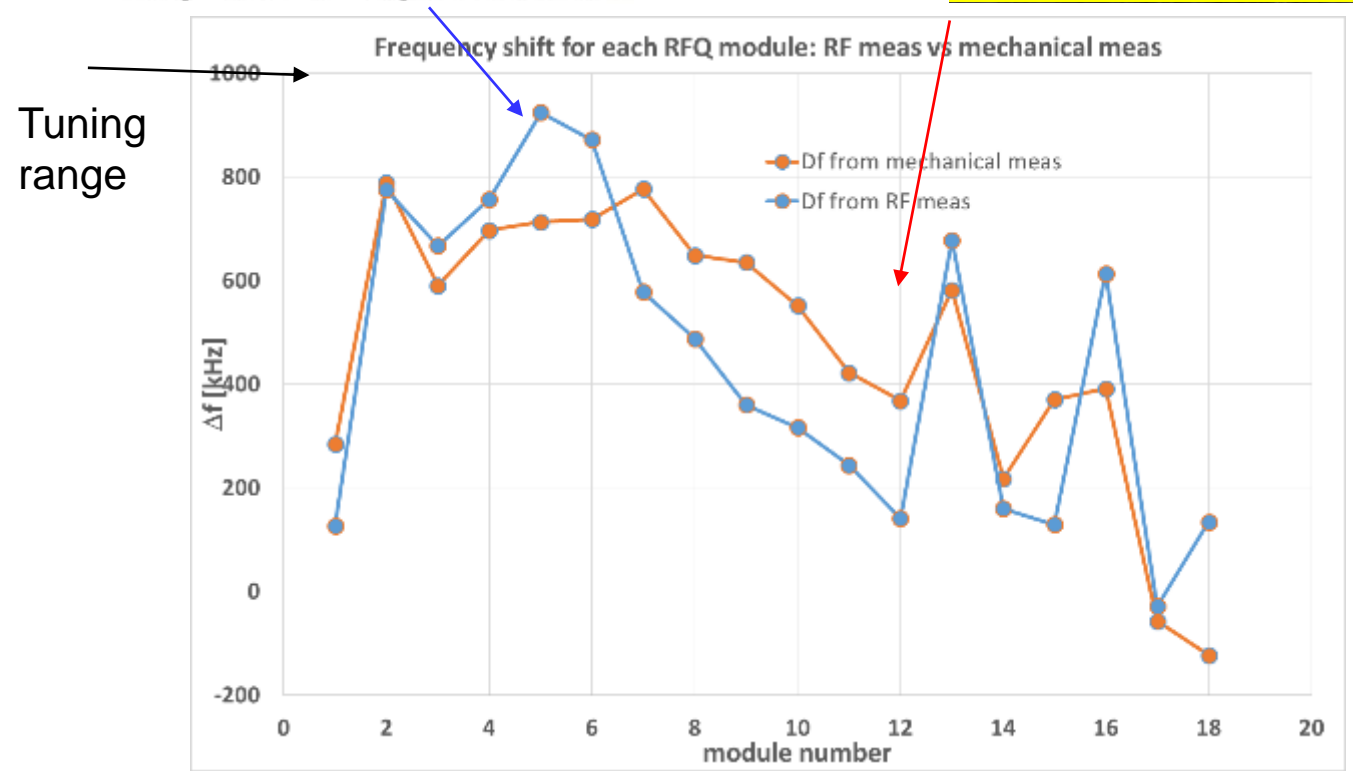


$$f_q^{WG} [MHz] = af_{q0} [MHz] + b$$



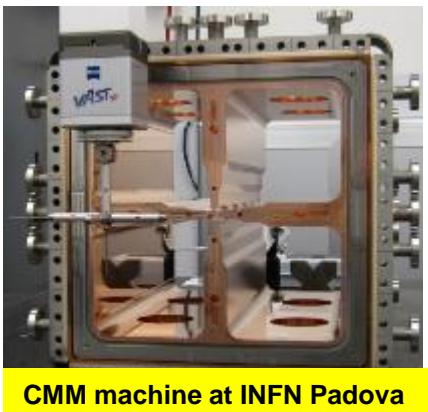
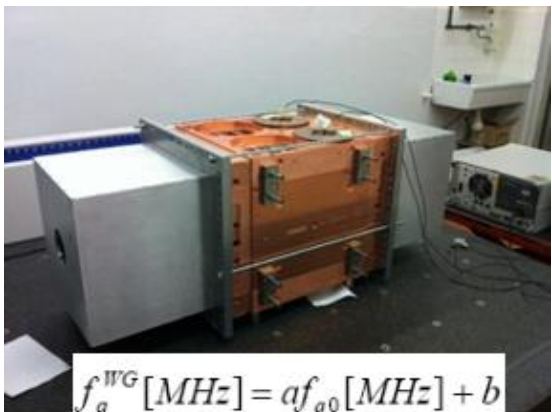
CMM machine at INFN Padova

All the measured values are such that $|\Delta R_0| < 100 \mu m$, with an average value on all the modules of **46 μm for the RF measured data and of 50 μm for the mechanical measurement data.**



IFMIF RFQ MODULE CHARACTERIZATION VIA MECHANICAL AND RF MEASUREMENTS
L. Ferrari et al THPLR050

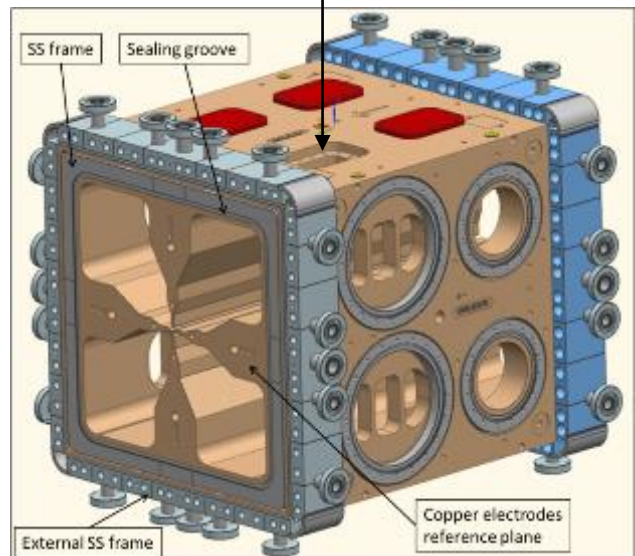
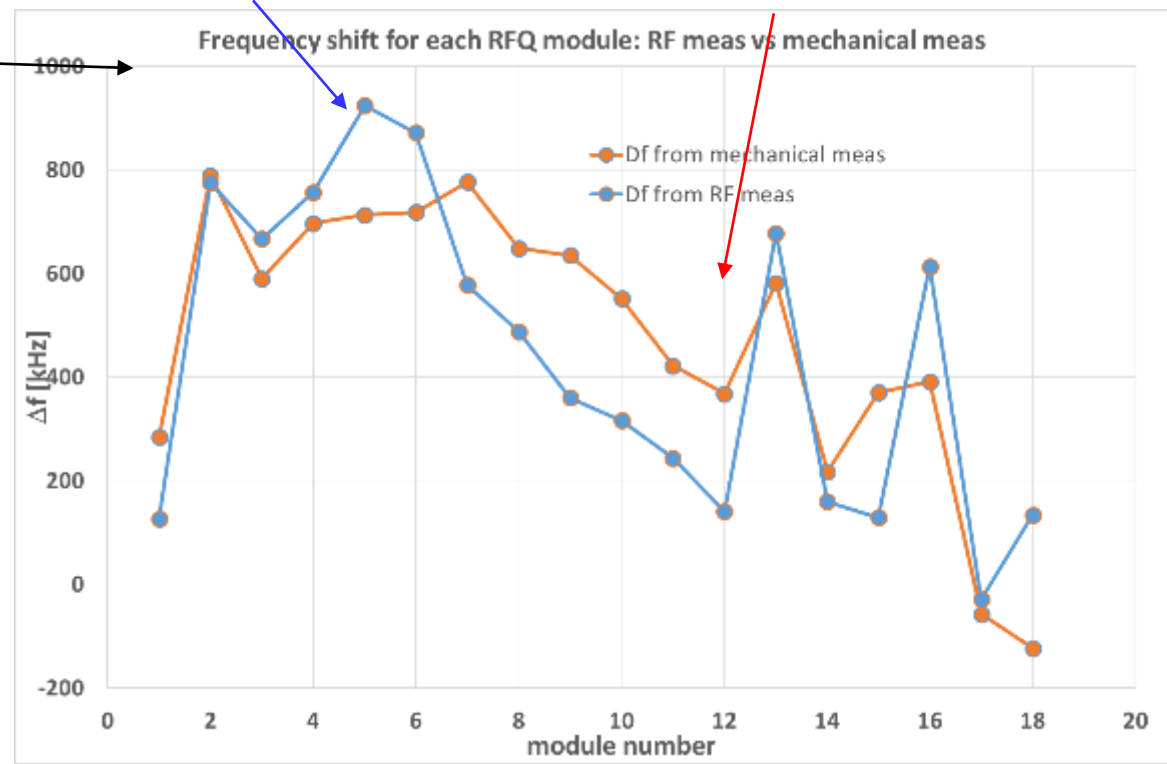
QA of modules: Results of RF measurements before and after brazing



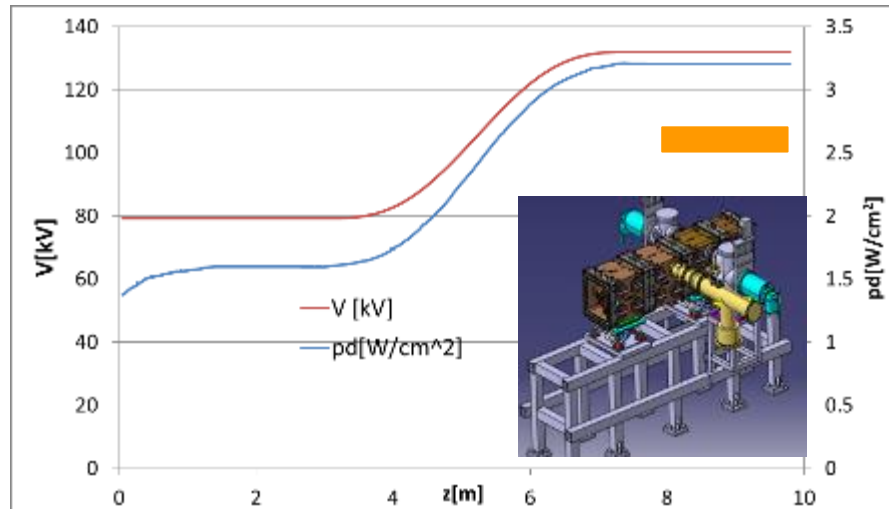
All the measured values are such that $|\Delta R_0| < 100 \mu m$, with an average value on all the modules of **46 μm for the RF measured data and of 50 μm for the mechanical measurement data.**

Additional opening for frequency correction

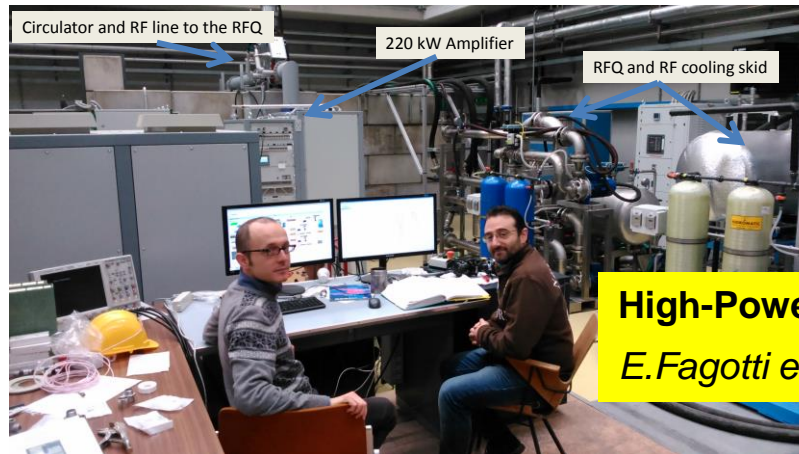
Tuning range



High power tests at Legnaro (1/5 of the structure)



- A 500 kW test stand able to test 4 RFQ modules, to test at full power density the structure (**200 kW RF power**)
- The test was necessary to validate the design during the module construction
- **Max field (1.8 Ekp and max power density 90 kW/m) have been demonstrated**



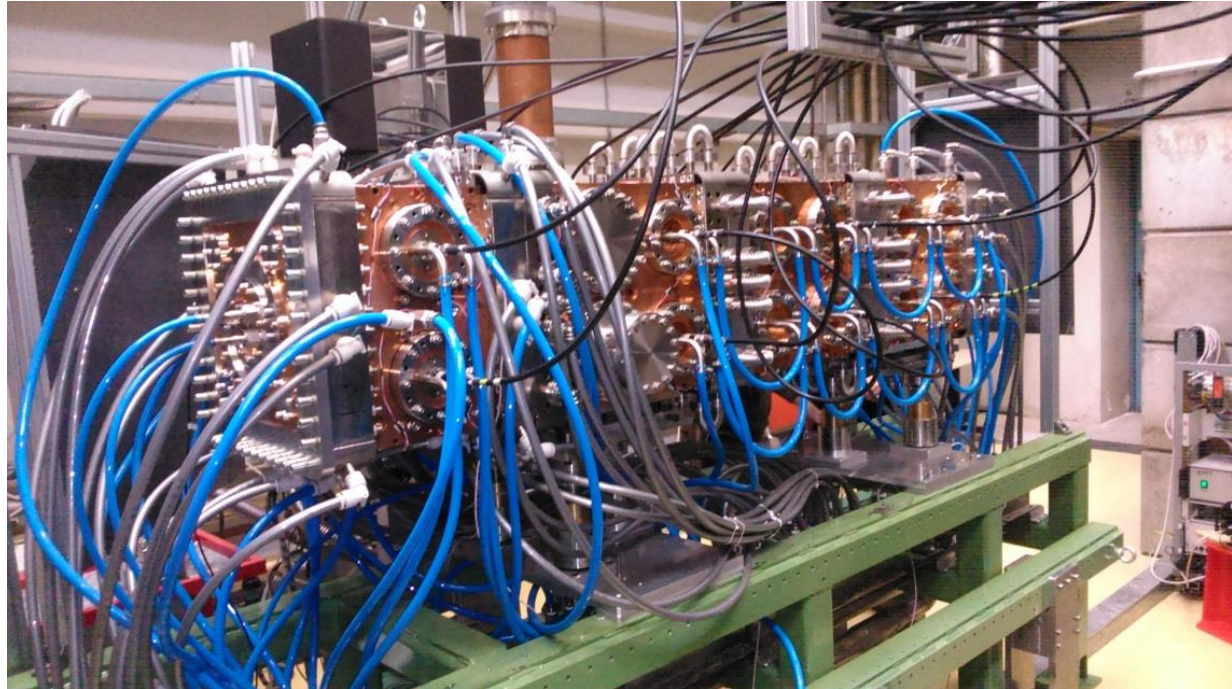
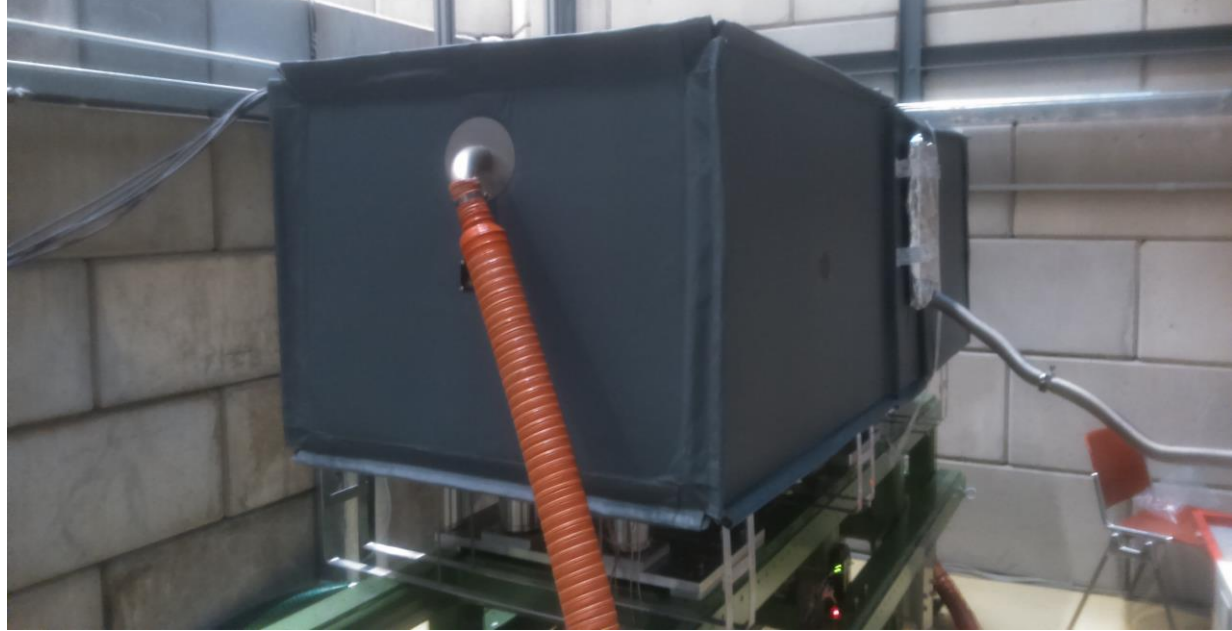
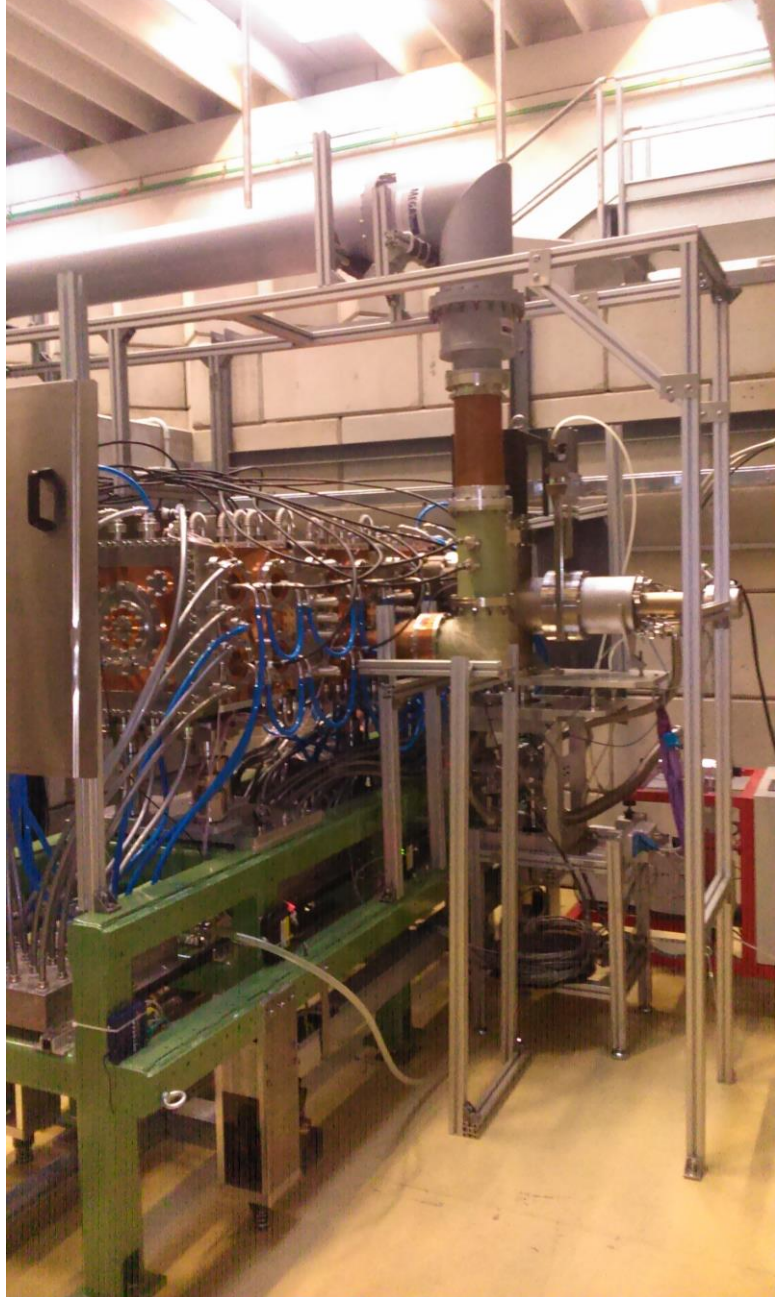
High-Power RF Test of IFMIF-EVEDA RFQ at INFN-LNL
E.Fagotti et al THPLR051

The INFN couplers (200 kW cw)

- Developed by INFN for the power test
- They will be used at Rokkasho for the first RFQ operation.

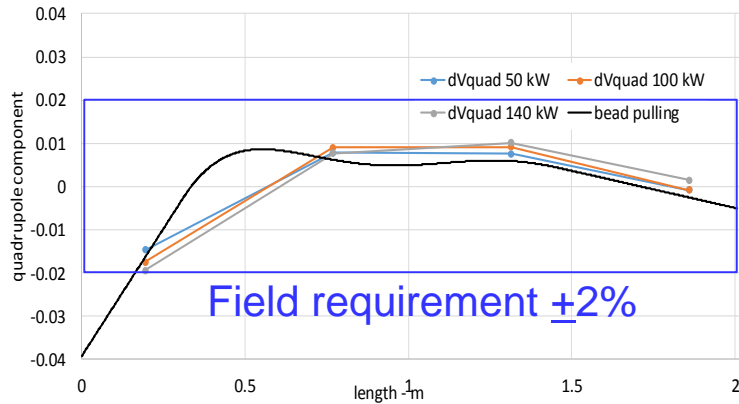


E. Fagotti et al. "The Couplers for the IFMIF-EVEDA RFQ High Power Test Stand at LNL: Design, Construction and Operation" LINAC2014, Geneva (Switzerland) p. 643

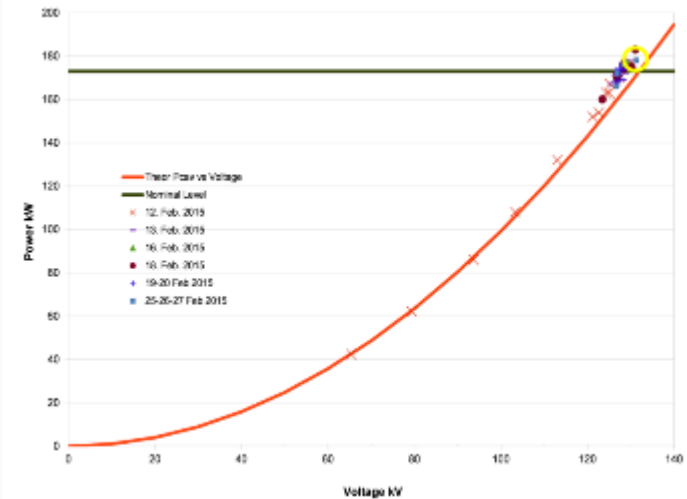


Results: nominal performances demonstrated

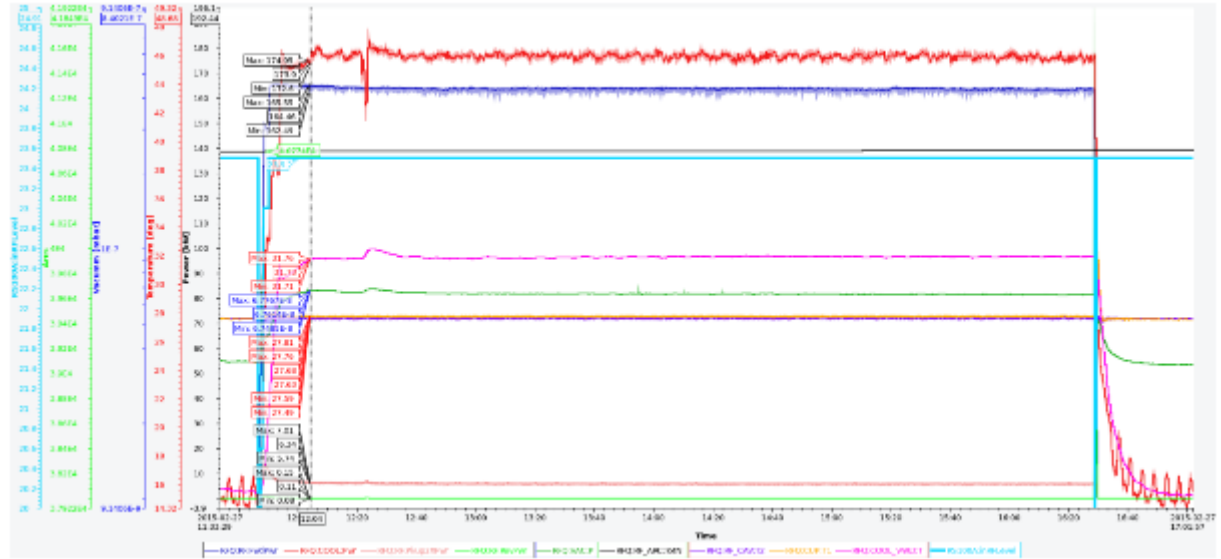
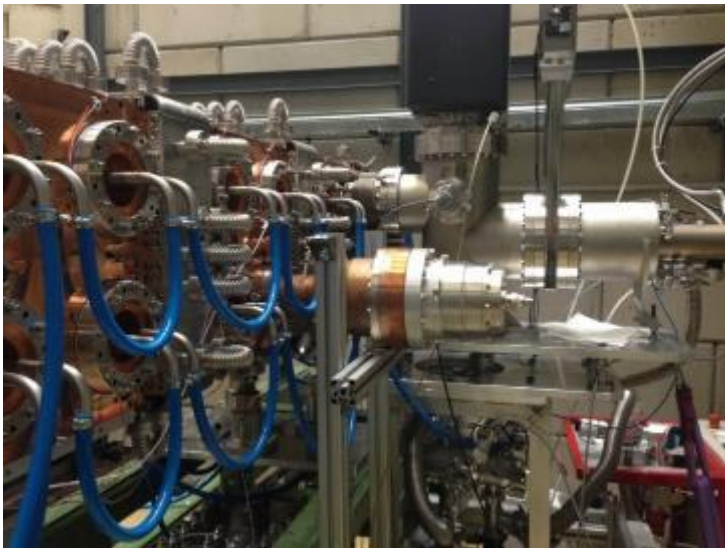
173 kW (90 kW/m)



Field configuration (pick up reading) at different RF level

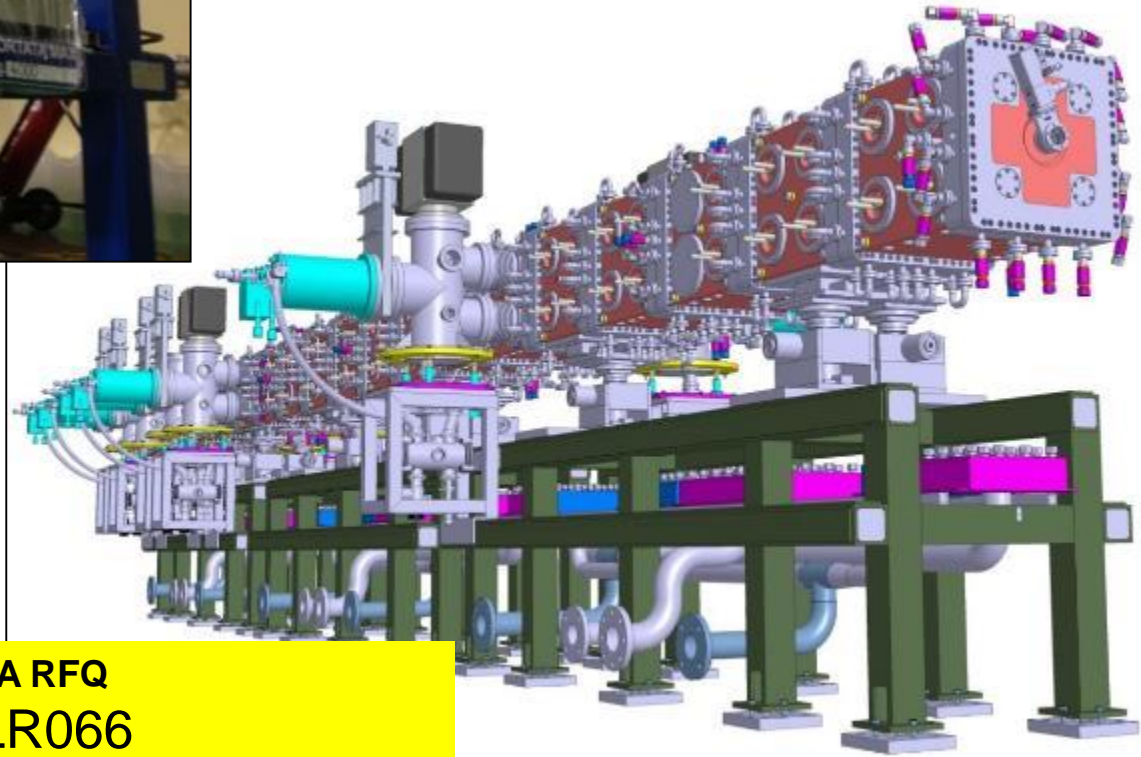


Cavity power (calorimetric measurements) vs. cavity voltage. The yellow circled dot corresponds to the nominal voltage level. $Q_0=12500$, i.e. 173 kW vs. 132 kV



On 27 February '15 the RFQ remained 5 hours at nominal field level. It corresponds to the yellow circle in fig above.

The 9.8 m RFQ assembly

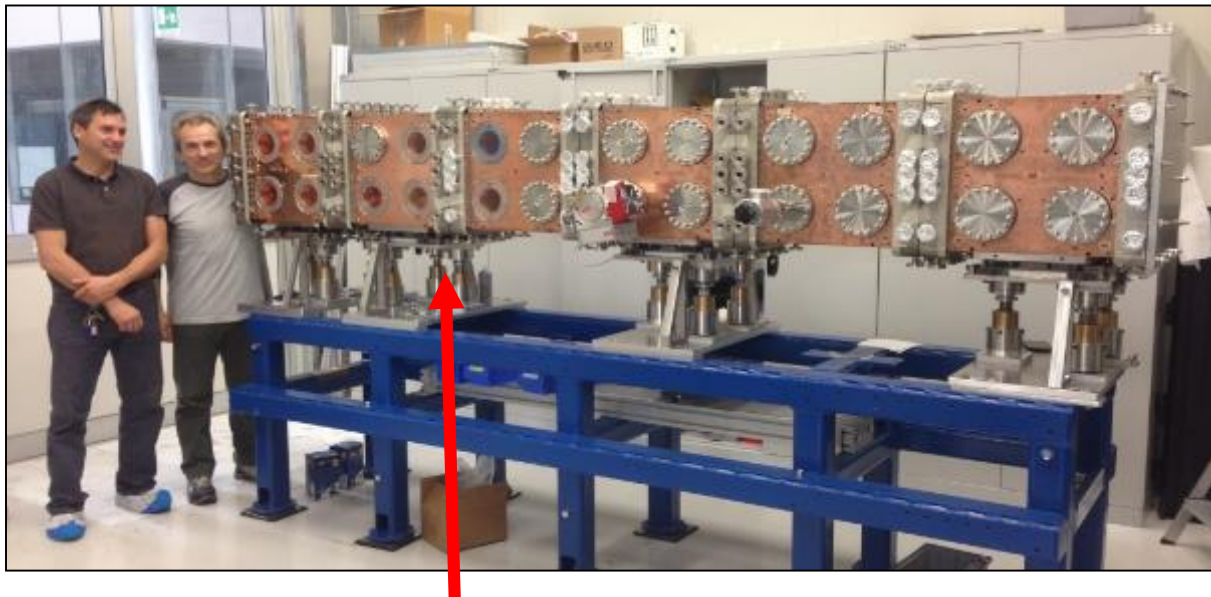


**PREPARATION AND INSTALLATION OF IFMIF-EVEDA RFQ
AT ROKKASHO SITE**

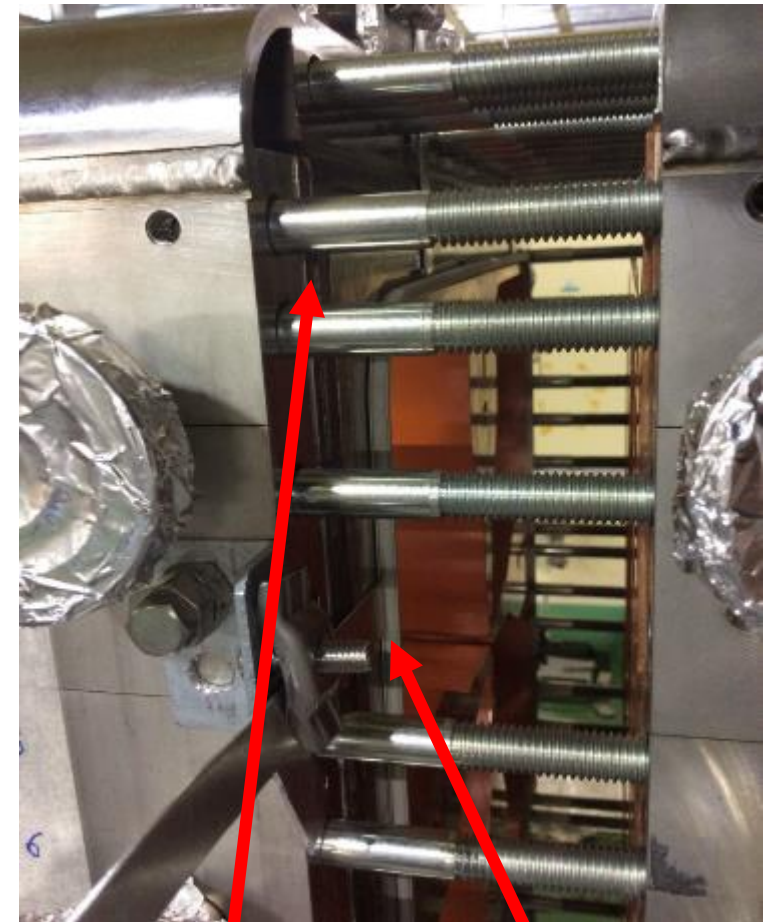
E.Fagotti et al THPLR066

SUPERMODULE ASSEMBLY AT LNL

- All alignments determined by FARO Ion Laser Tracker using interferometric option.
- it was possible to reach a module transverse misalignment of 0.03 mm and longitudinal one of 0.04 mm (calibrated spacers).
- End of January 2016 the three supermodules were ready for transportation to Japan



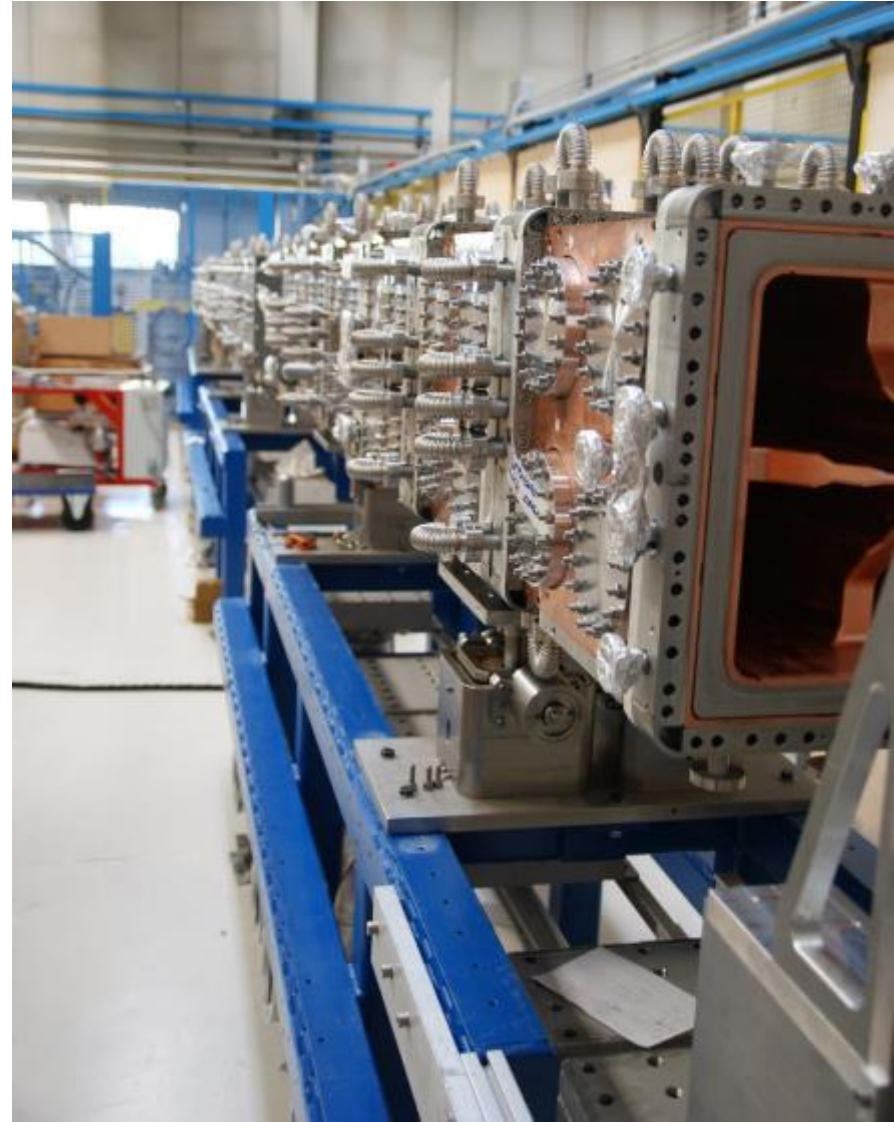
Temporary module support (6 degree of freedom regulation, sliding allowed)



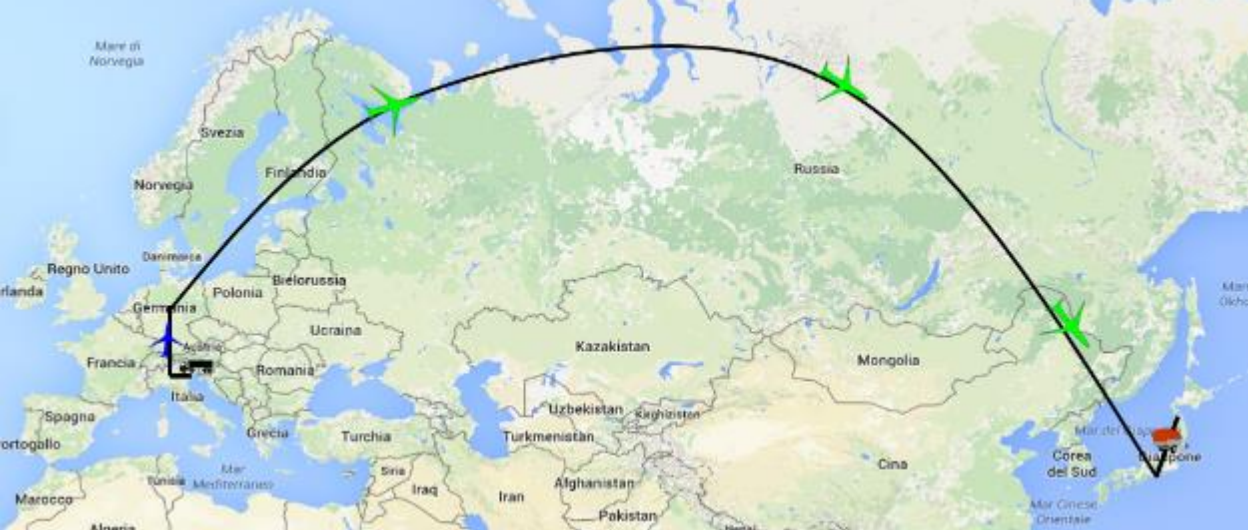
Calibrated spacers

Metallic gasket

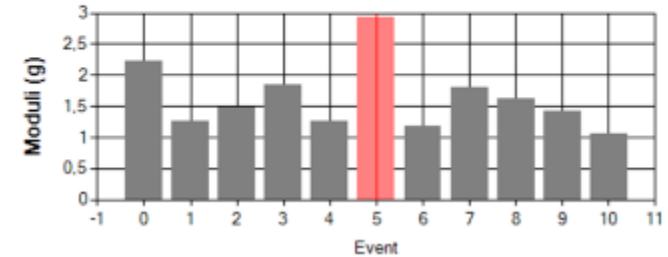
Assembled at LNL from 10/2015 to 01/2016



SUPERMODULE SHIPMENT



	Event	Axis	Date/Time	Modulus (g)	Temp (°C)
First Alarm	0	Z	17/02/2016 05:24:09	2.23	14.20
First Warning	1	Z	17/02/2016 22:52:28	1.27	13.50
Most Severe	5	Z	07/04/2016 00:38:52	2.93	17.20
Event Summary	11 Events (6 Warnings, 5 Alarms)				



Data extrapolated from the shock recorder mounted on SM2.

- The three SMs were completely assembled at LNL, filled with nitrogen
- Rubber spacers and wood supports were used between to damp vibrations in the box
- Shock recorders, Shocklog 298, were screwed on the top of each SMs.



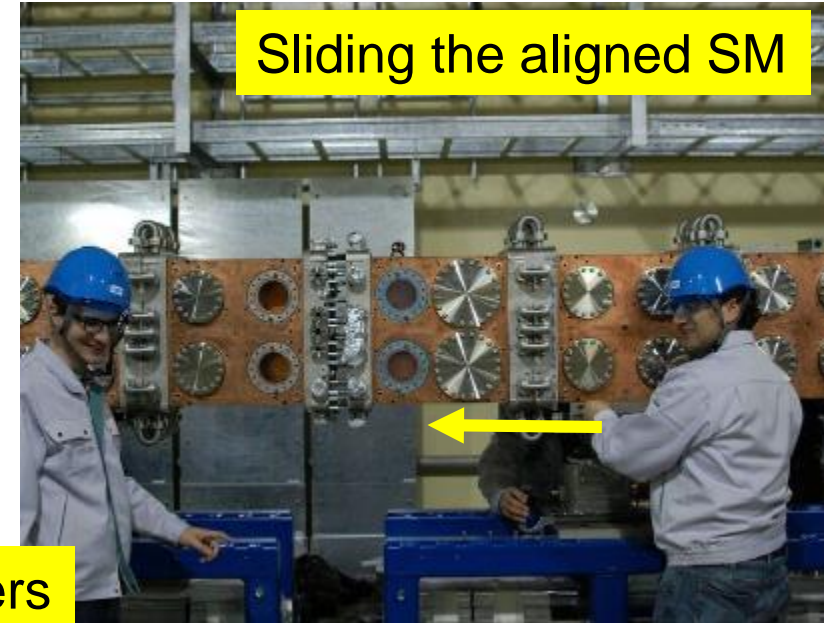
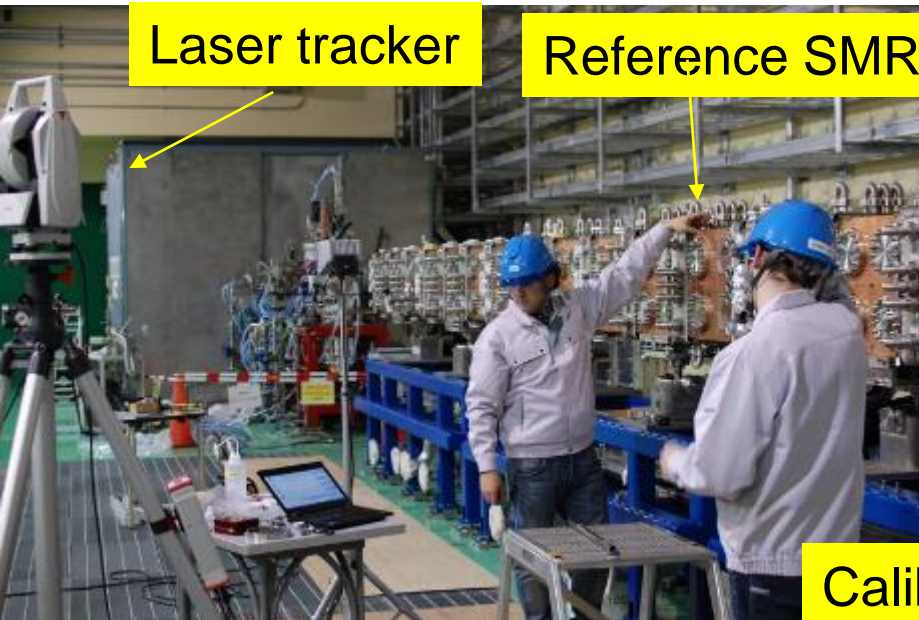
Rokkasho accelerator hall:

SM1-SM2-SM3 vacuum leak test

Vacuum leak $< 2 \cdot 10^{-10}$ mbar-l/s per module

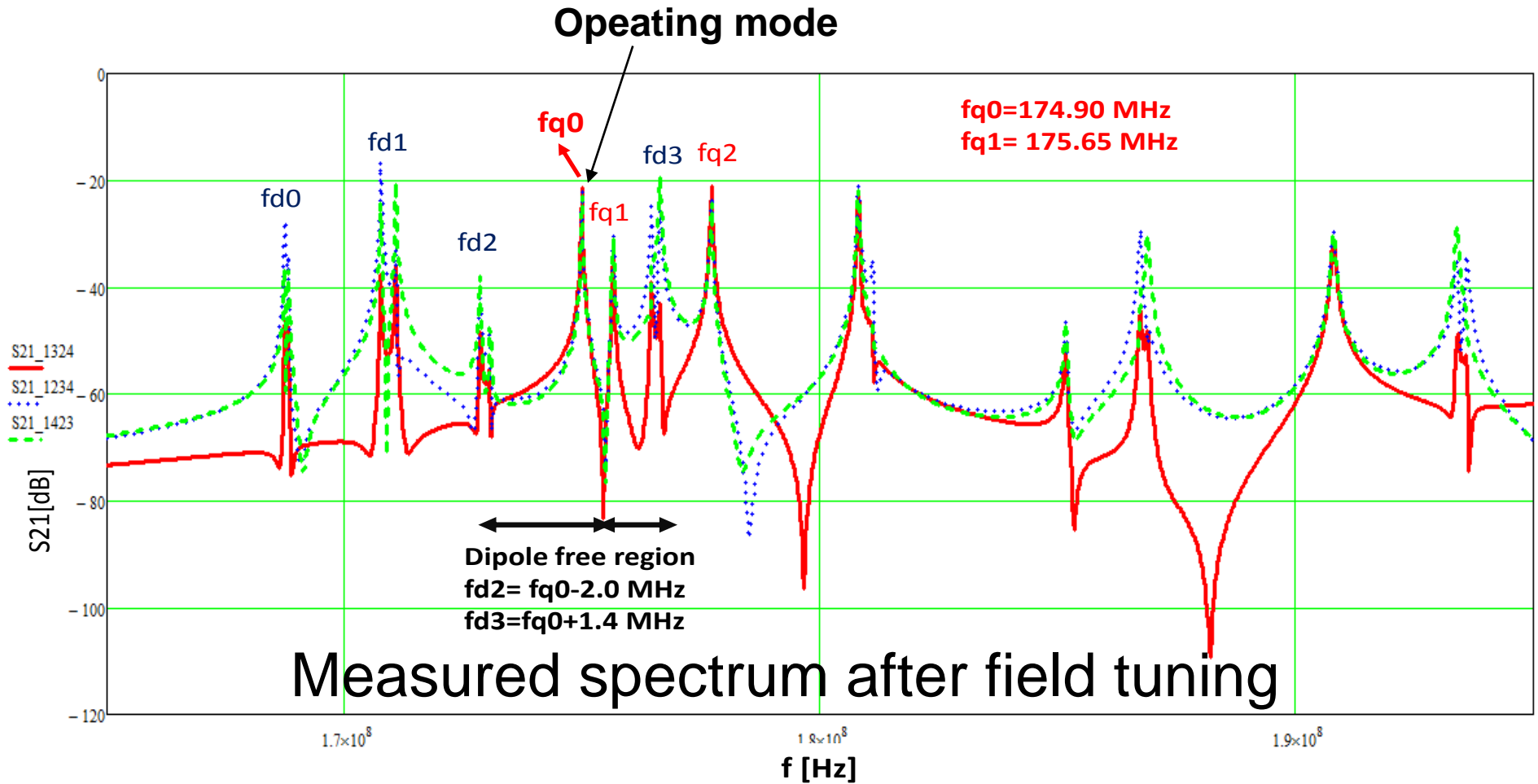


RFQ mechanical installation



- In particular we achieved 0.03 mm maximum misalignment between SM (± 0.1 mm beam dyn. requ.),
- RFQ axis moves down respect to nominal beam axis up to -0.2 mm at the level of coupling between SM1 and SM2 (acceptable).

Tuning of a long RFQ



108 tuners to be set

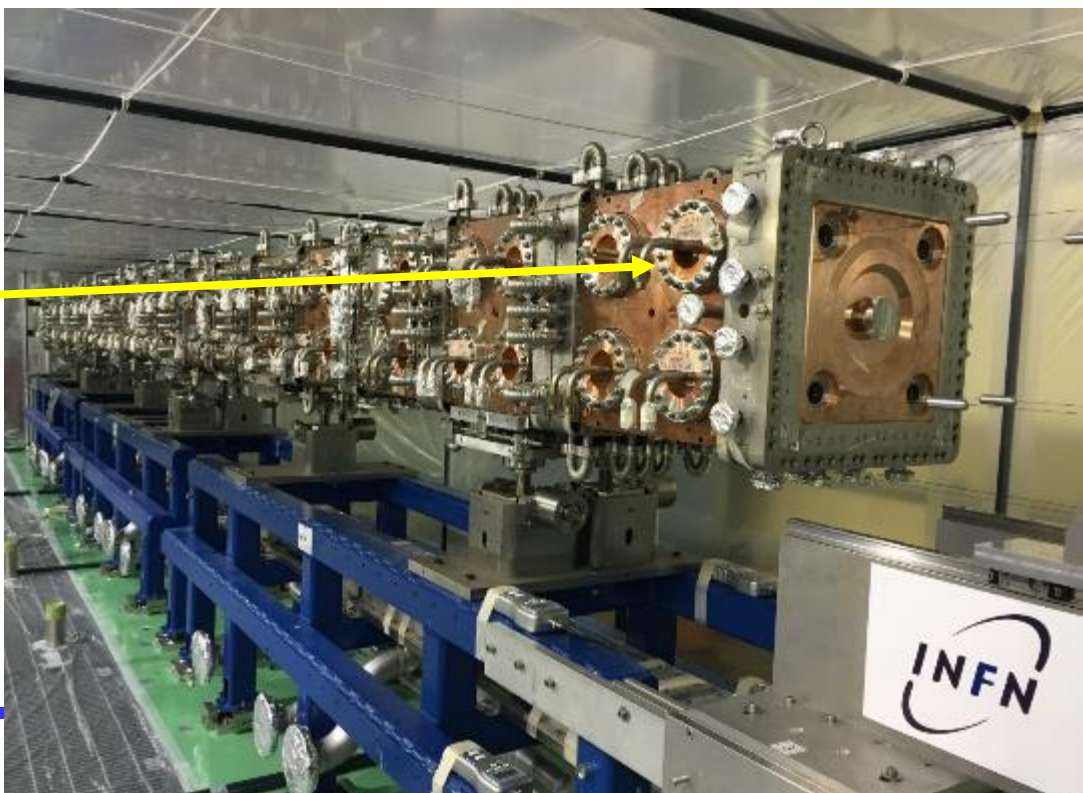
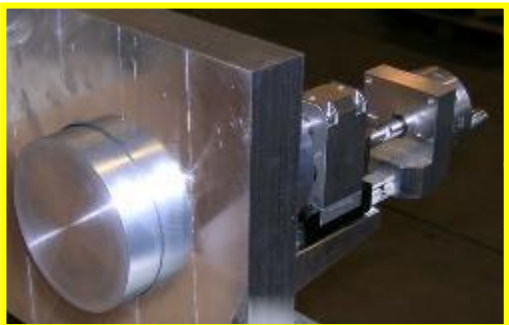
TUNING THE IFMIF 5MEV RFQ ACCELERATOR

A. Palmieri *et al* THPLR049

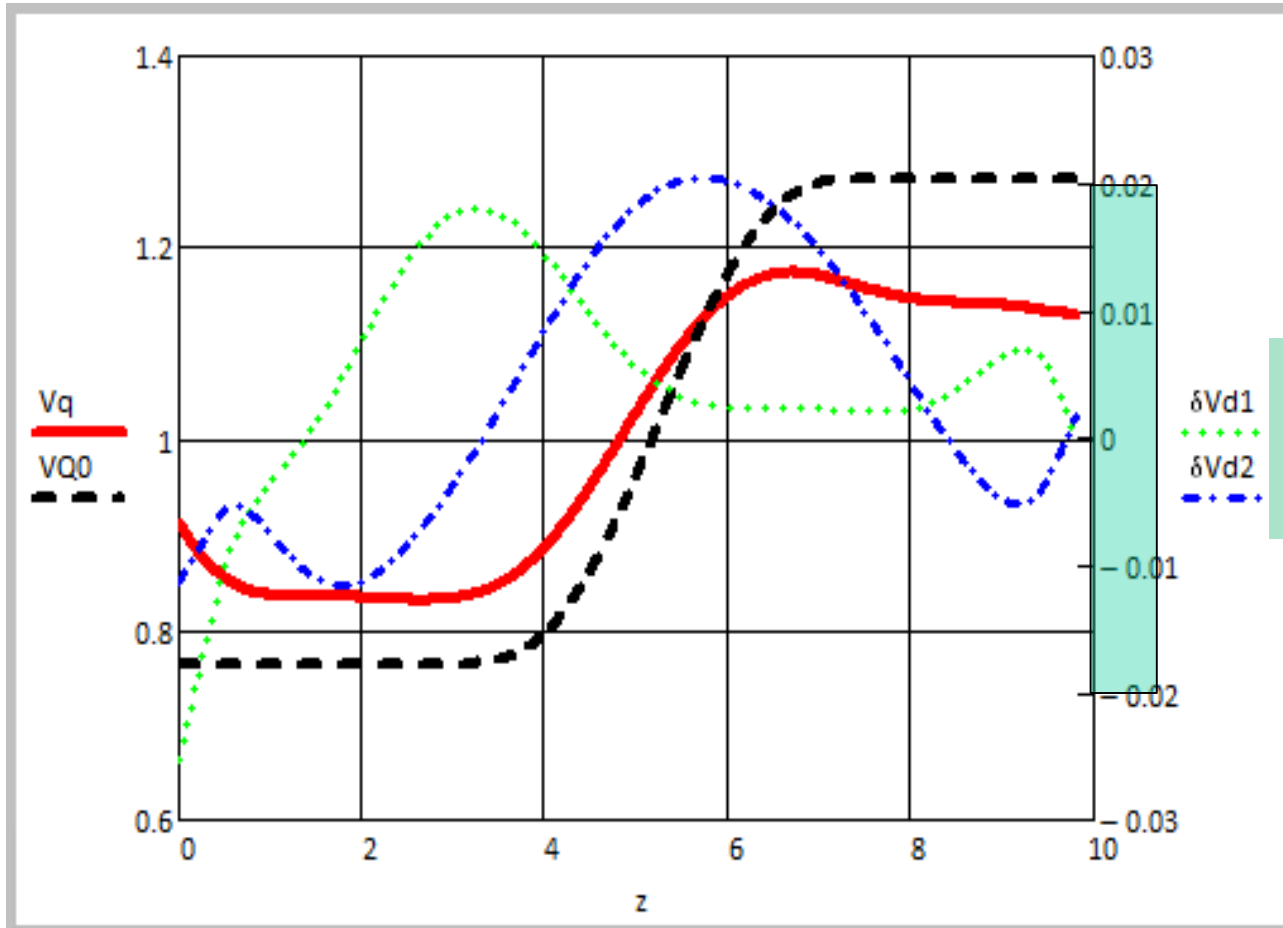
- $\pm 10 \mu\text{m}$ modulation tolerances
- $\pm 60 \mu\text{m}$ tolerance R_0 final (incl brazing) equiv to $\pm 1 \text{ MHz}$.
- 108 dummy tuners ($\pm 15 \text{ mm}$ equiv $\pm 1 \text{ MHz}$), field correction
- Active (water temperature, 10 deg approx $\pm 0.1 \text{ MHz}$)



From dummy to final tuners



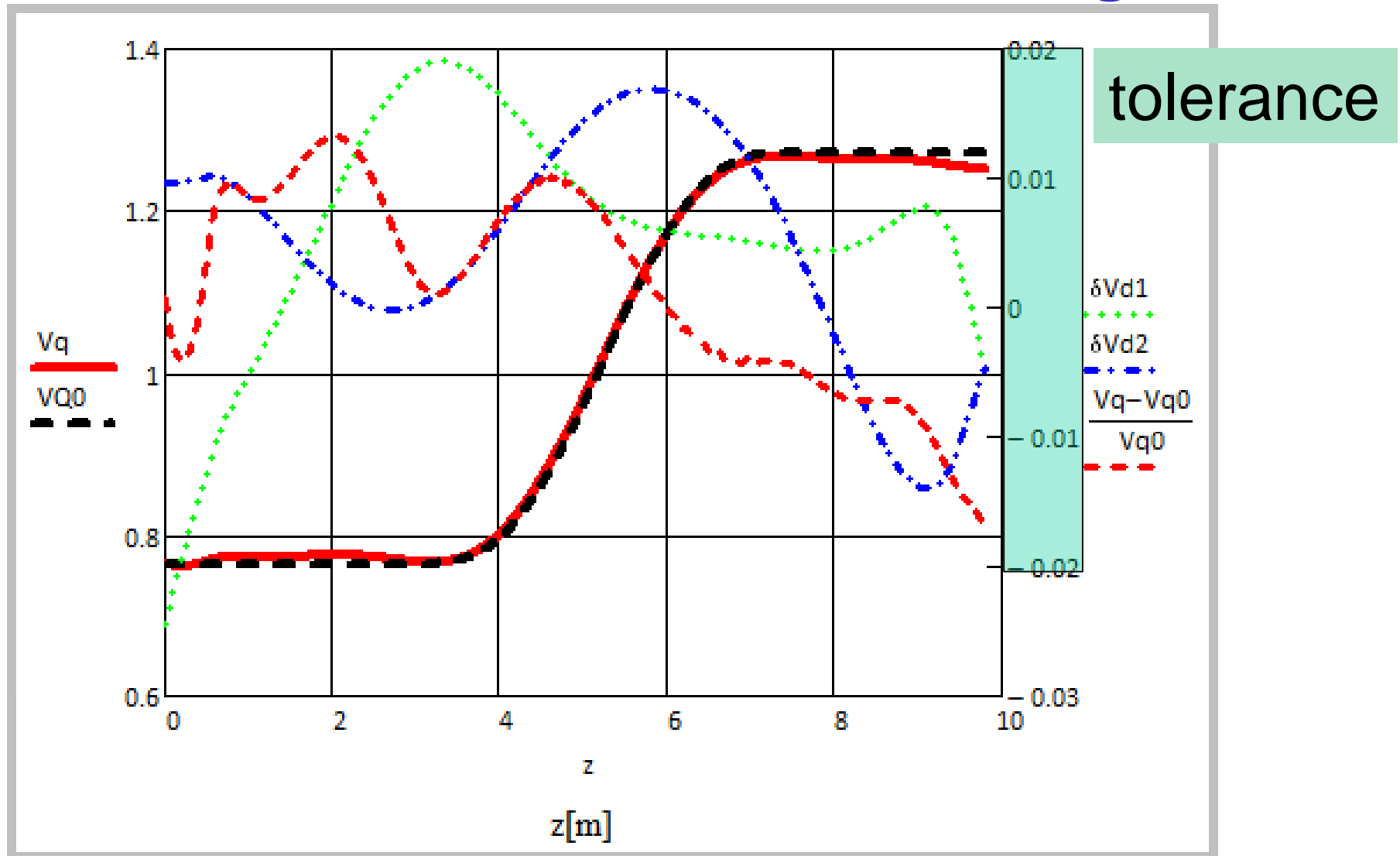
Field distribution before tuning



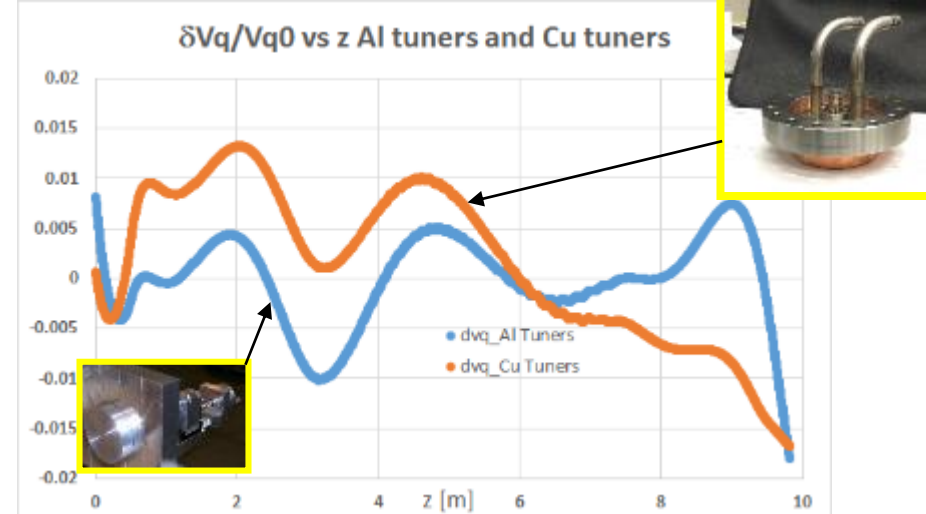
Dipole component
Tolerance

Flush tuners

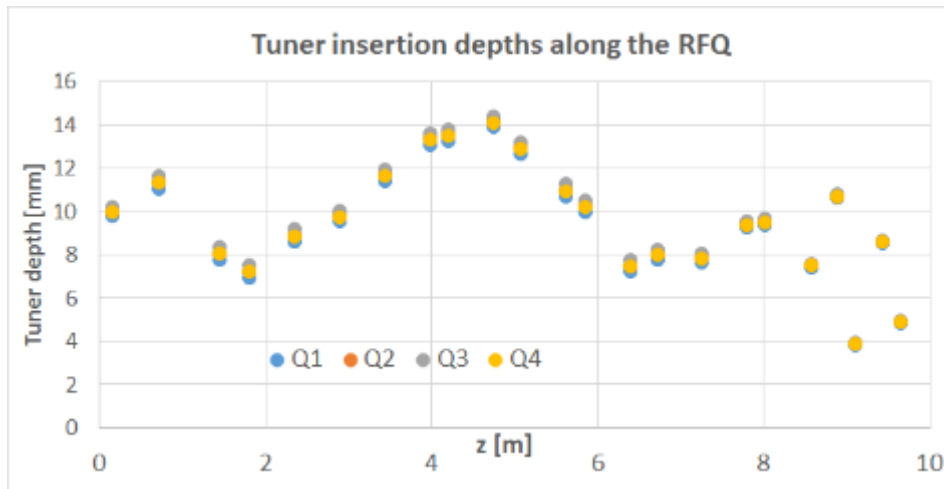
Field distribution after tuning



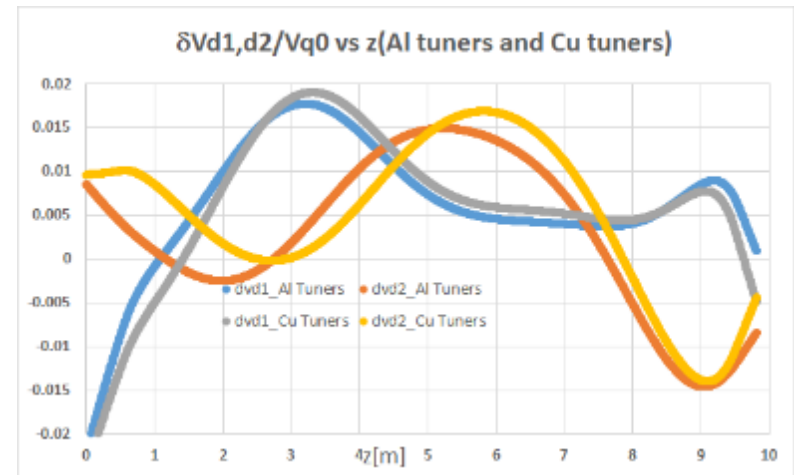
Quadrupole and dipoles with dummy (Al) and final (Cu) tuners



dV_q/V_{q0} vs z for dummy tuners (Al, blue curve) and final tuners (Cu, red curve)



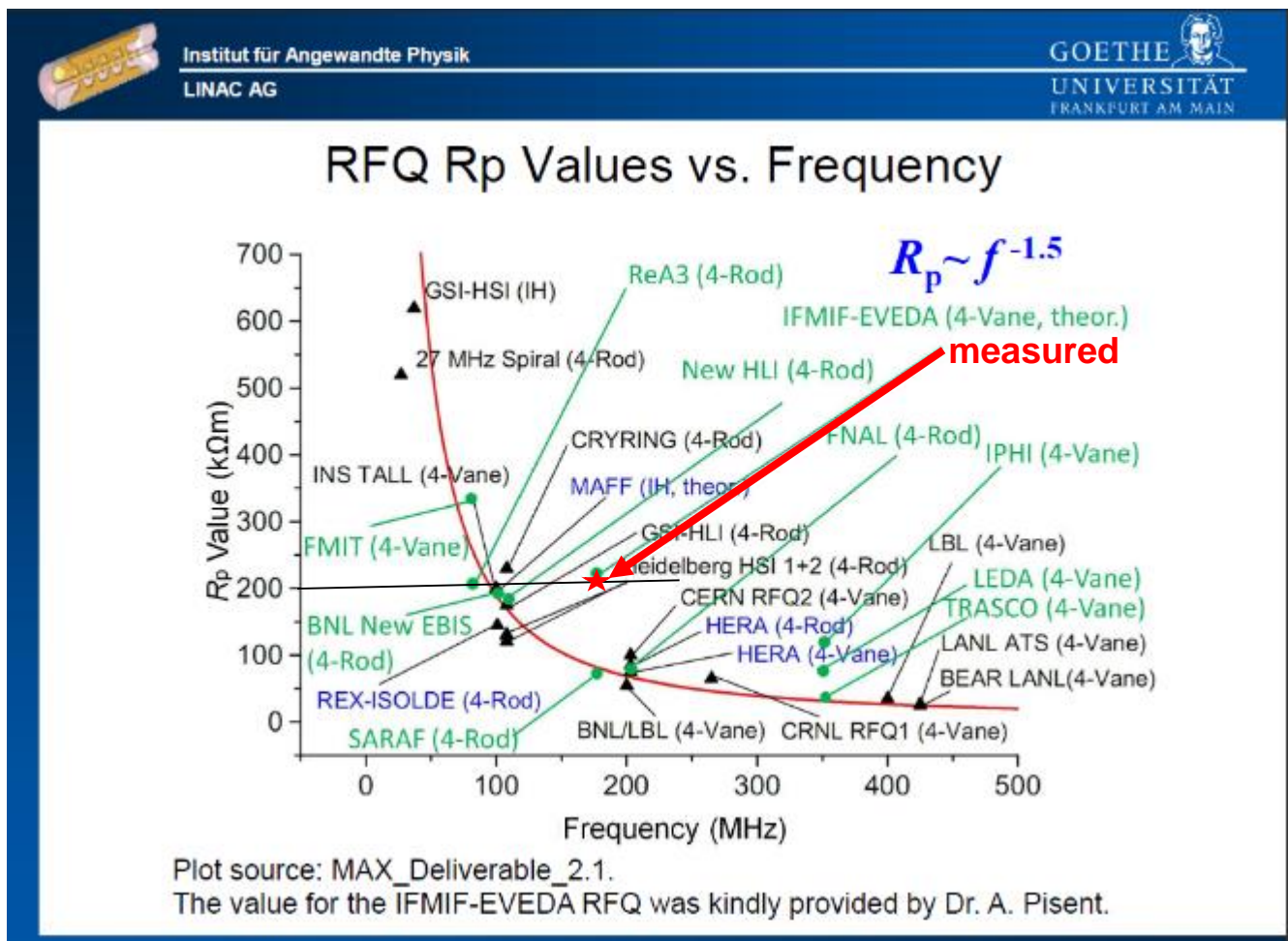
Tuning range -10 +30 mm



dV_{qd1}/V_{q0} vs z for dummy tuners (Al, blue curve) and final tuners (Cu, red curve)

Eigen frequency and shunt impedance achieved

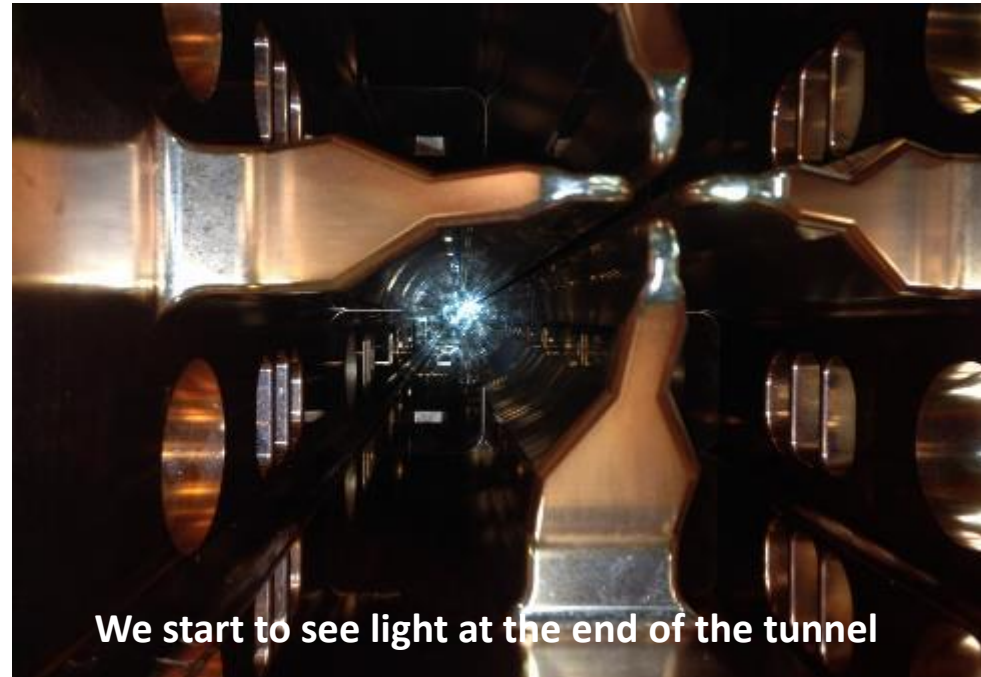
- The final measured frequency was equal to 174.989 MHz, equivalent to **175.014 MHz**, if one takes into account the rescaling to nominal 20°C temperature and the effects of vacuum and beam loading. Such value corresponds to -1°C water temperature regulation for the vessel.
- **$Q_0 = 13'200 \pm 200$**
- (82% of SUPERFISH value), low tuner losses
- **$R_{sh} = 201 \text{ k}\Omega \cdot \text{m}$**



Original transparency by prof. H. Klein

Conclusions

- The RFQ construction is concluded (18/18 module accepted, RF and CMM tests ok).
- The cw RF performances (maximum field, power density, water temperature frequency control loop) have been achieved in the high power test in Italy.
- The air-transportation in three supermodules and the assembly in Japan was successful. The RF field have been tuned to the nominal shape with specified accuracy (2%).
- The excellent shunt impedance of the design has been achieved ($Q=13\ 200$).

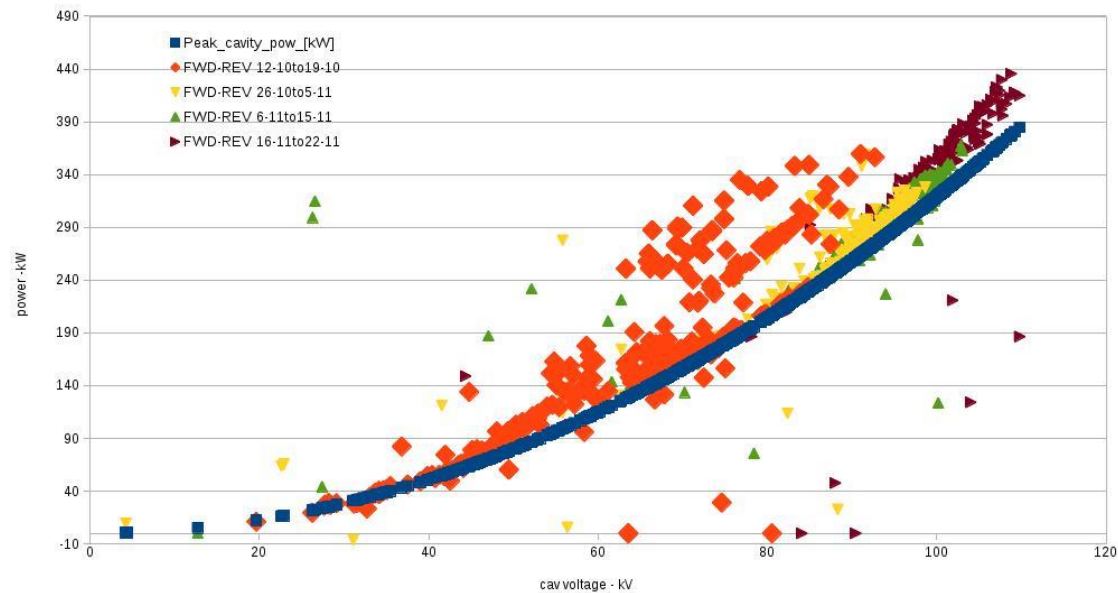


*Components of INFN RFQ team (LNL, Padova, Torino, Bologna):
A. Pisent (coordinator), E. Fagotti (integration and high power tests), A. Pepato (module production), P. Mereu (engineering integration), L. Antoniazzi, D. Agugliaro, A. Baldo, L. Bellan, P. Bottin, A. Conte, M. Comunian, D. Dattola, R. Dima, J. Esposito, L. Ferrari, M. Giacchini, G. Giraudo, F. Grespan, A. Macri, A. Margotti, M. Montis, A. Palmieri, M. Poggi, A. Prevedello, L. Ramina, M. Romanato C. Roncolato*

Thanks to our colleagues from QST (ex JAEA), F4E, Project team, CEA and Ciemat for constant support

Last update

- The RFQ is in final position, fully installed (vacuum, RF, water cooling).
- The conditioning started in September and is proceeding with pulsed RF (about 60us).
- Beam tests foreseen for next March
- will start March 2018.



MUNES

MULTIdisciplinary Neutron Source

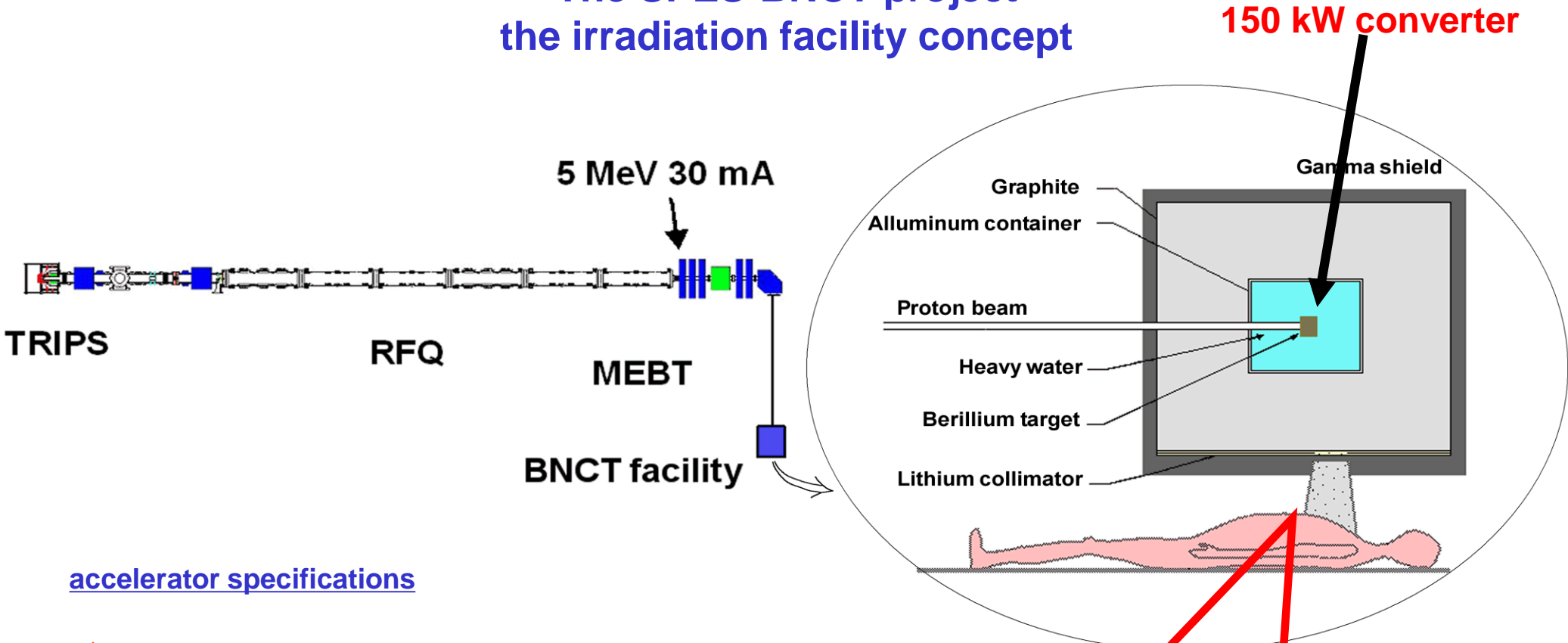
A. Pisent, P. Colautti, E. Fagotti

- First ideas with **SPES-BNCT**, based on TRASCO RFQ, almost abandoned with the choice of the cyclotron for SPES project at LNL.
- In **2011** trilateral agreement **INFN**, **University of Pavia** and **SOGIN** (public company for nuclear sites decommissioning) for the study of a neutron source based on INFN **high intensity linear accelerator** to be installed in Pavia.
- **2012** MUNES Granted as «progetto premiale» by Italian Ministry for research (5 M€, previous INFN investments in TRASCO RFQ and BNCT for about 10 M€)



Andrea Salvini

The SPES-BNCT project the irradiation facility concept



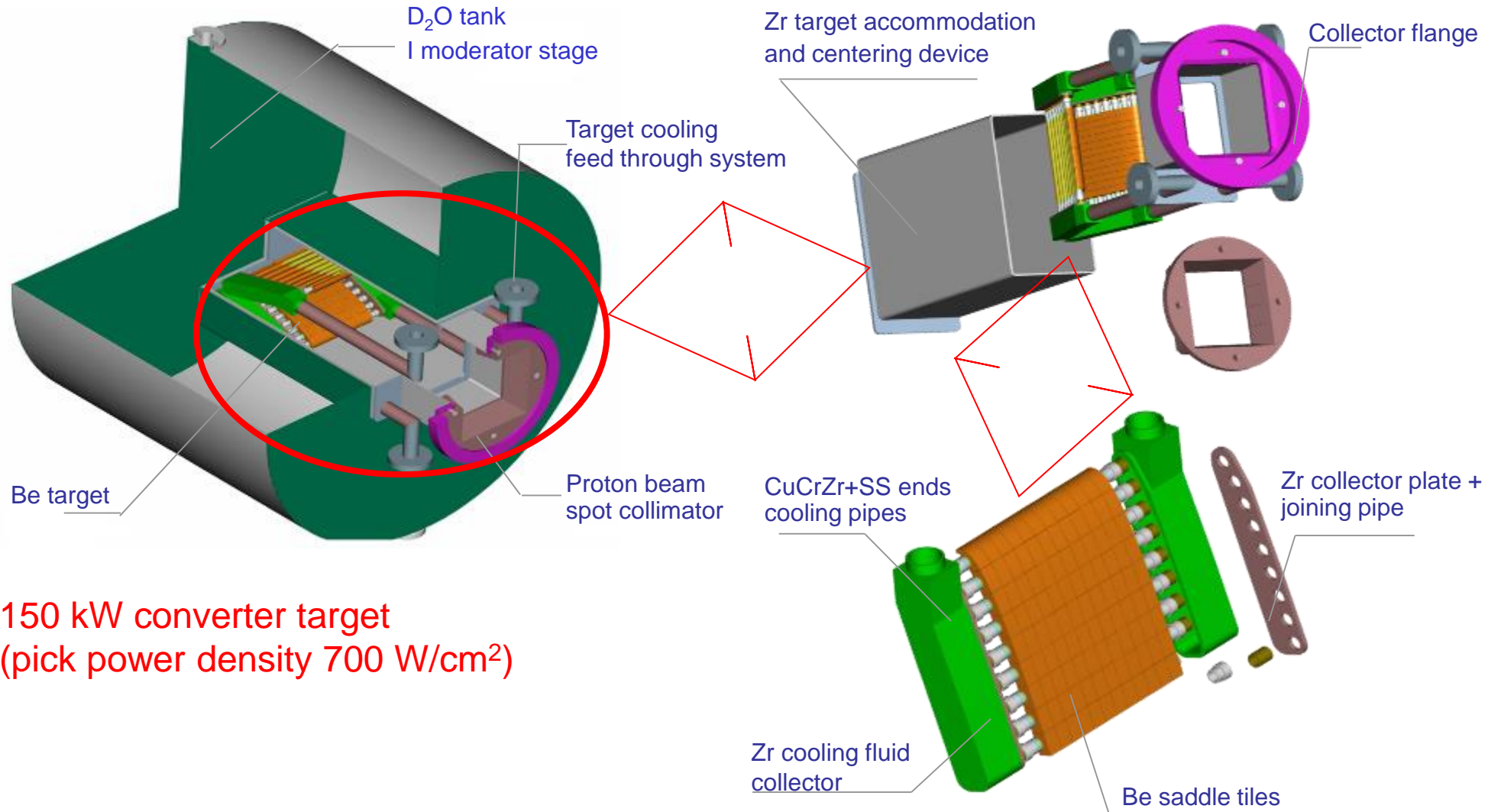
accelerator specifications

- ✓ beam particle: proton
- ✓ beam energy: 5 MeV
- ✓ beam current: 30 mA
- ✓ beam power: 150 kW

neutron beam requirements	
$\phi_{n\ th\ (\leq 0.4\ eV)}$	$\geq 10^9\ [cm^{-2}\ s^{-1}]$
$\phi_{n\ th} / \phi_{n\ total}$	≥ 0.9
$D_{n\ epi+fast} / \phi_{n\ th}$	$\leq 2 \cdot 10^{-13}\ [Gy\ cm^{-2}]$
$D_{\gamma} / \phi_{n\ th}$	$\leq 2 \cdot 10^{-13}\ [Gy\ cm^{-2}]$

The LNL-BNCT project

Efremov Step II neutron converter prototype design



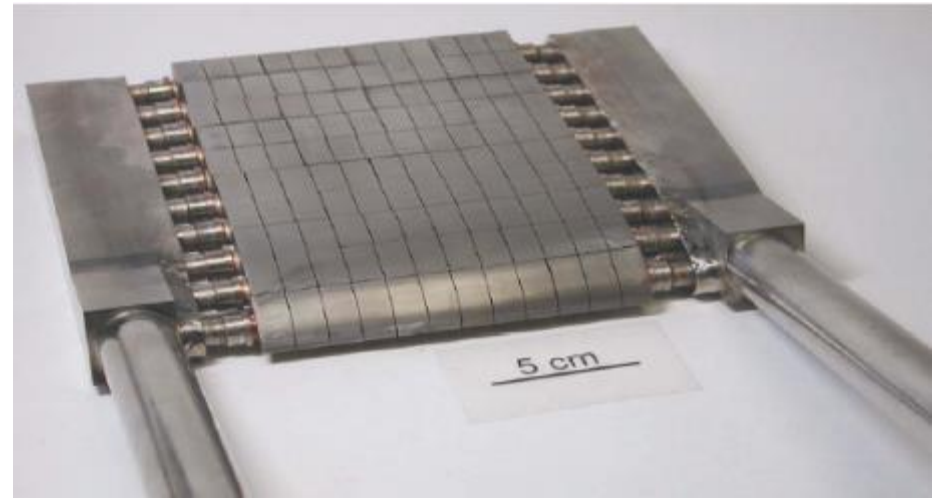
150 kW converter target
(pick power density 700 W/cm^2)

The LNL-BNCT project

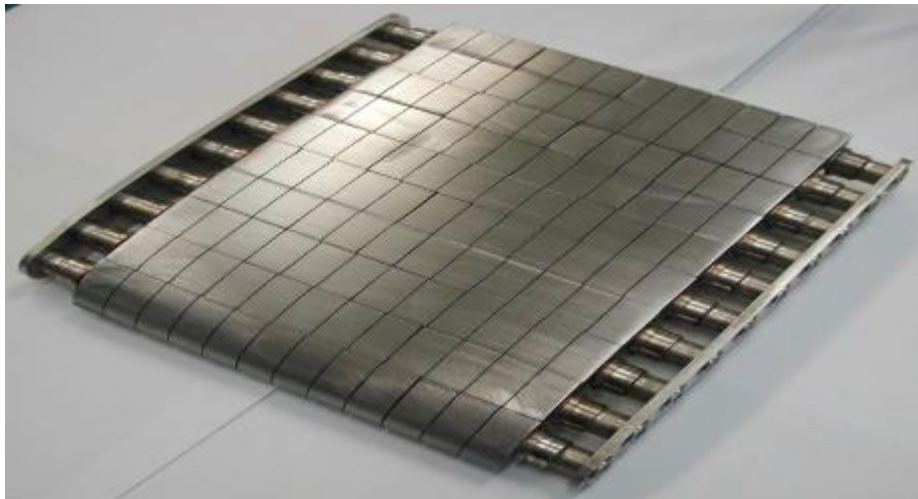
neutron converter prototype assembling and first full beam power test



1. Be tile brazed cooling pipes



3. Final target assembling



2. collector plates welding & EDM manufacturing process

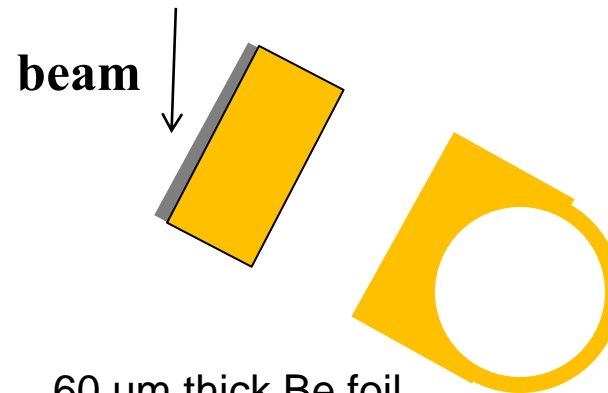
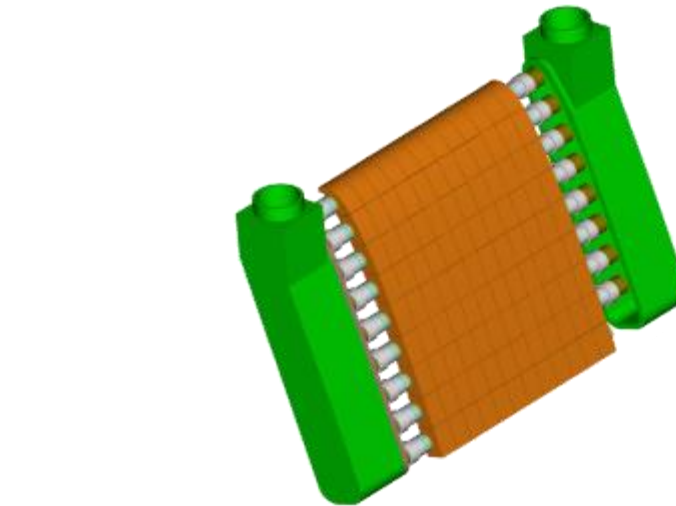


700 Wcm⁻² pick power density
60 kW total power (e-beam)

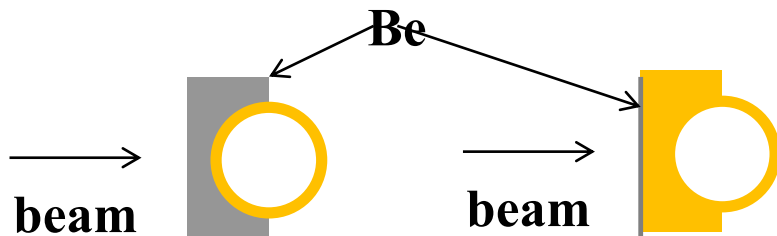
4. Visual inspections after e-beam full power test

Test of target damage by protons

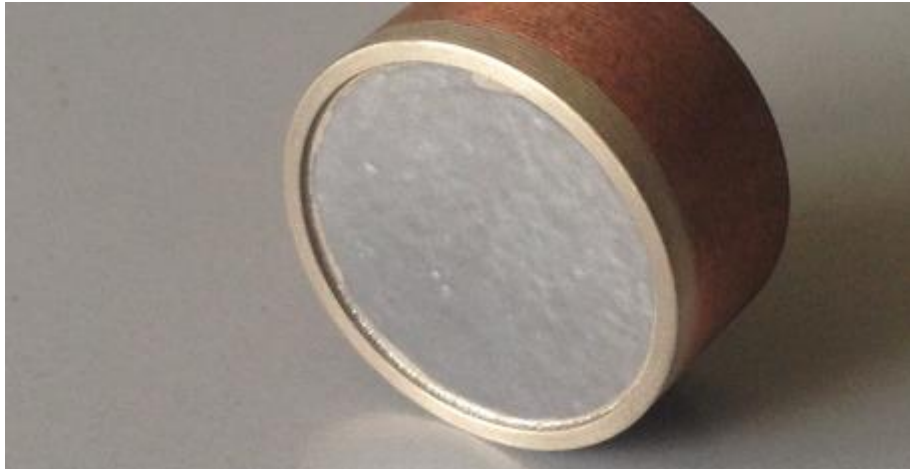
- **Assesment of target duration** (Be has high melting point 1278 degC and high heat conductivity, but gas permeability if extremely low (9 order lower than average materils). H bubbles can be trapped in bulk beryllium and couse fractures.
- Proton radiation damage effects on Be surface were planned in 2008, measurements at the State Polytechnic Institute (SPbSPU), St. Petersburg (Russia) (interrupted for funds problem, contract now under preparation)
- New target design to be tested based on a very thin Be foil brazed on Cu alloy tube



60 um thick Be foil
Brazed to copper substrate in specialized company
Construction of the target in Cu and 316L substrate
Possible at LNL



New target and moderator development



Moderator, low power@CN accelerator at INFN

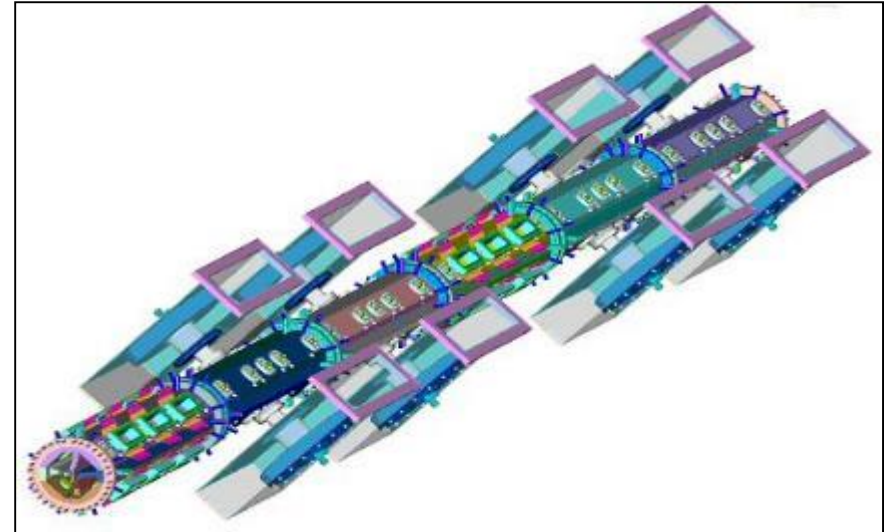
60 um beryllium target brazed on Cu substrate



Target, holder and beam collimator (low power)

Eight independent 125 kW amplifiers (one per RF coupler) are coming (5 ordered amplifiers).

Each amplifier needs 5 racks as in the following scheme (including power supply)



Advantages respect to a klystron

- *Lower operating costs (cost and duration of components)*
- *Availability e reliability (no stop operation in case of components failure)*
- *Absence of high voltages very important for the operation in a hospital*

Has been successfully tested at LNL

(140 kW cw to allow the substitution on line of one module)



Key technologies for a high power p or d linac (5-90 MeV) (well developed in INFN)

- ECR sources (high intensity, high reliability continuous beam)
- RFQ acceleration with high transmission (about 90%) of a continuous beam and preparation of time structure for RF acceleration.
- DTL with permanent magnets (high duty pulsed beam).
- Superconducting cavities for cw linac operation (HWR or QWR derived from heavy ion linacs like ALPI)
- Solid state RF amplifiers for reliable cw operation (10-150 kW)
- High power targets (solid beryllium or carbon, liquid lithium). SPES BNCT and SPIRAL2 prototypes
- Dosimetry to characterize the neutron field

